

https://dspace.org/

The discharge capacity and design of curb inlets with and without clogging

Dube, Ntombikayise

2019

https://hdl.handle.net/10539/29359

Dube, Ntombikayise, (2019) The discharge capacity and design of curb inlets with and without clogging, University of the Witwatersrand, https://hdl.handle.net/10539/29359

Downloaded from a DSpace repository. https://dspace.org/

THE DISCHARGE CAPACITY AND DESIGN OF CURB INLETS WITH AND WITHOUT CLOGGING

Ntombikayise Dube

A dissertation submitted to the Faculty of Engineering and the Built Environment, University of Witwatersrand, Johannesburg, in fulfilment of the requirements for the degree of Master of Science in Engineering.

Johannesburg, 2019

DECLARATION

I, Ntombikayise Dube, declare that this thesis is my original unaided and has not been submitted before for any degree or examination in any other university. It is being submitted to the Degree of Master of Science to the University of Witwatersrand, Johannesburg, South Africa.

……
……

(Signature of Candidate)

…….. day of …… month ……. year
……

ABSTRACT

Prolonged surface runoff on streets contributes to flooding, thus compromising the structural integrity of roads, increasing the probability of accidents and traffic stagnation, and as such drainage structures such as the Pretoria type curb inlet are integrated into the road infrastructure to facilitate conveyance of surface runoff into conduits. The Pretoria type inlet is popular in South Africa, but there is limited literature on its hydraulic performance. Therefore, this research is aimed at expanding the existing literature by assessing the behavior of the Pretoria type curb inlet and, developing design tools.

Various configurations of the model of the Pretoria type curb inlet were fabricated in the Hydraulics laboratory of the School of Civil and Environmental Engineering at Witwatersrand University, and tests were carried out in a flume that simulated flow on the roadway with model a curb inlet that intercepted a portion of the flow. The tests were carried out on three longitudinal slopes of 0.25%, 0.5% and 0.75%, two cross-section slopes of 2% and 3%, with an undepressed and depressed gutter, and the mouth of the inlet free from any clog material and with clog material. To confirm the uniqueness of the Pretoria type curb inlet, we found that the Hydraulic Engineering Circular No. 22 (HEC-22) and Izzard methods did not give good prediction of the discharge capacity of the Pretoria type curb inlet. In contrast to previous work on the Pretoria type curb inlet which was restricted to 80% and 100% interception, this study explores a wider a range of interception efficiencies which make it more useful for design. Further, this work is the first known research investigation in South Africa that examines the influence of clogging on the performance of the Pretoria type curb inlet. We found that the discharge capacity of the curb inlet increases with the length of the opening, and an upstream transition section improves its efficiency. The efficiency of the inlet favors steep cross-sectional slopes and gentle longitudinal slopes; depression of the gutter enhances the interception efficiency and this supports why the Pretoria type curb inlet is now synonymous with the depressed gutter. The reduced performance of the inlet due to

clogging calls for concerted efforts at better solid waste management in South Africa.

ACKNOWLEDGEMENTS

It would have been impossible to complete my thesis without the guidance and support of my supervisor, laboratory technicians, friends and my family. I would like to express my gratitude and appreciation to the following people;

My supervisor, Professor A. Taigbenu, for his guidance, sharing his knowledge, being patient and supportive especially during the model construction period. I would also like to express my gratitude to the hydraulics senior laboratory technician, Mr. W. Costopoulos for his great and enthusiastic assistance and guidance in constructing the model. My mother, Nomsa Dube, brother and close friends have been my backbone from the beginning of the research project and I'm grateful for their support. Finally, I would love to thank GOD my Father, who has been my constant strength and guide.

TABLE OF CONTENTS

DECLARATION i

ABSTRACT ii

ACKNOWLEDGEMENTS iv

LIST OF SYMBOLS xii

ABBREVIATIONS xiv

1 INTRODUCTION 1

1.1 Problem Statement 2

1.2 Aims and Objectives 3

1.3 The Scope 4

1.4 Thesis Outline 5

2 LITERATURE REVIEW 6

2.1 Factors Affecting Discharge Capacity and Efficiency of Curb Inlets on Grade 8

2.2 Clogging of Curb Inlets 9

2.3 Previous Research on the Discharge Capacity and Clogging of Curb Inlets 14

3 HYDRAULIC MODELLING AND EXPERIMENTAL METHODS 27

3.1 Description of Prototype 28

3.2 Model Scaling 28

3.3 Model Road Surface Roughness 30

3.4 Model Layout 31

3.5 Measurements 36

3.6 Model Construction 37

3.7 Tests Carried Out 38

3.7.1 Combination of curb inlets 38

3.7.2 Test procedure 39

4 DISCUSSION OF TEST RESULTS 41

4.1 Comparison between Experimental Results and Literature Based Results 41

4.1.1 Experimental Results vs. The Izzard Method vs. The HEC-22 Method 41

4.1.2 Efficiency from The Grobler Method 47

4.2 Influence of Upstream Transition Section on Inlet Efficiency 48

4.3 Influence of Inlet Opening on Inlet Efficiency 52

4.4 Influence of Depressed Gutter on Inlet Efficiency 54

4.5 Influence of Clogging on Inlet Efficiency 57

4.5 Design Curves 63

4.5.1 Derivation of Design Curves 64

4.5.2 Froude Number Sensitivity Analysis 66

4.5.3 Predicted vs. observed efficiency for inlets on SL=0.25% from the empirical equations 66

4.5.4 Demonstration of Use of Design Curves to Estimate Curb Inlet Length 69

5 CONCLUSION AND RECOMENDATIONS 72

5.1 Conclusions 72

5.2 Recommendations 75

6 REFERENCES 76

7 APPENDICES 80

7.1 Appendix A – Detailed Drawings of The Pretoria Type Curb Inlet 80

7.2 Appendix B - Model Schematics 81

7.3 Appendix C - Regression Analysis Statistics 83

7.4 Appendix D – Predicted Vs. Experimental Efficiency (S_L=0.25%) 84

LIST OF FIGURES

Page

Figure 2.1 Two roads of opposing gradients. The curb is located in the middle (City of Lubbock Texas Storm Water Management, 1997) 7
Figure 2.2 A road on a constant grade (City of Lubbock Texas Storm Water Management, 1997) 8
Figure 2.3 Portable gravel sediment trap (The Southern Sydney Regional Organisation of Councils and the Natural Heritage Trust, 2010) 12
Figure 2.4 Gravel sediment trap (The Southern Sydney Regional Organization of Councils and the Natural Heritage Trust, 2010) 12
Figure 2.5 Temporary sediment trap (The Southern Sydney Regional Organization of Councils and the Natural Heritage Trust, 2010) 12
Figure 2.6 Side entry pit trap installed in a catch pit with trapped solid waste (Government of Western Australia-Department of Water, 2011) 13
Figure 2.7 Water surface profile for supercritical flow (Uyumaz, 1992), where, Q_w, Q_s, and y are the interception capacity of curb inlets, the flow-rate of street flow and the water depth at the curb respectively 14
Figure 2.8 Water surface profile for subcritical flow (Uyumaz, 1992) 15
Figure 2.9 Gutter / road cross-section where S_x is the cross-sectional slope, y is the depth of water and T is the spread of water 15
Figure 2.10 β values against λ values for varying S_{x1} (road cross-sectional slope) and varying S_{x2} (gutter cross-sectional slope) (Uyumaz, 1992) 16
Figure 2.11 The Pretoria-type / Tshwane-type curb inlet (Johannesburg Roads Agency, 2015) 18
Figure 2.12 Grobler's Design Curves (SANRAL, 2007) 20
Figure 2.13 Curb inlet on-grade test data (Comport et al., 2009) 22
Figure 2.14 Predicted vs. observed curb inlet efficiency from Equations 2.5 and 2.7 (Comport et al., 2009) 23
Figure 2.15 Predicted vs. observed efficiency from the modified UDFCD equation (Comport et al., 2009) 24

Figure 2.16 Observed vs. Predicted efficiency values from the empirical Equation 2.11 (Comport et al., 2009) 25
Figure 3.1 Schematic drawing of the Hydraulics Laboratory water supply system 32
Figure 3.2 Inside the overhead tank 32
Figure 3.3 Upstream section of the constructed street model 33
Figure 3.4 Flooded street model with clogged curb inlet 33
Figure 3.5 Yellow flume terminating at a 90^{o} V-notch weir (a tape measure glued to the wall of the flume was used to measure the depth of water) 35
Figure 3.6 Tail-box terminating at a 90^{o} V-notch weir (a tape measure glued to the wall of the tail-box was used to measure the depth of water) 35
Figure 3.7 Rating curve for the V-notch weir in the side channel that conveys the flow intercepted by the curb inlet 37
Figure 4.1 Q_{pi} *vs* Q_{pt} for undepressed curb inlet A on S_x= 2% 42
Figure 4.4.2 Q_{pi} *vs* Q_{pt} for undepressed curb inlet A on S_x= 3% 42
Figure 4.3 Q_{pi} *vs* Q_{pt} for depressed curb inlet A on S_x= 2% 44
Figure 4.4 Q_{pi} *vs* Q_{pt} for depressed curb inlet A on S_x= 3% 44
Figure 4.5 Differences in interception efficiency between the observed and Izzard and HEC-22 methods: (a) S_x=2% and (b) S_x=3% for depressed inlet A 46
Figure 4.6 Assessment of upstream transition lengths with average efficiencies of undepressed inlets A, B and D without clog material 48
Figure 4.7 Assessment of upstream transition lengths with average efficiencies of depressed inlets A, B and D without clog material 49
Figure 4.8 Photo of curb inlet showing damming effect from downstream transition section 50
Figure 4.9 Influence of inlet opening on average interception efficiencies of undepressed inlets A, C and F without clog material 52
Figure 4.10 Influence of inlet opening on average interception efficiencies of depressed inlets A, C and F without without clog material 53
Figure 4.11 Influence of depressed gutter on average efficiencies of inlets A, B, C, D, E and F on S_x=2% without clog material 54

Figure 4.12 Influence of depressed gutter on average efficiencies of inlets A, B, C, D, E and F on S_x=3% without clog material 55
Figure 4.13 Influence of clogging on average efficiencies of undepressed inlets A, B and D on S_x=2% 57
Figure 4.14 Influence of clogging on average efficiencies of undepressed inlets A, B and D on S_x=3% 58
Figure 4.15 Photo of street flow when a curb inlet is clogged 59
Figure 4.16 Influence of clogging on average efficiencies of depressed inlets A, B and D on S_x=2% 60
Figure 4.17 Influence of clogging on average efficiencies of depressed inlets A, B and D on S_x=3% 60
Figure 4.18 Comparison between inlet E empirical equation and experimental results 67
Figure 4.19 Comparison between inlet F empirical equation and experimental results 67
Figure 4.20 Comparison between inlet C empirical equation and experimental results 68
Figure 4.21 Comparison between inlet E empirical equation and experimental results 69
Figure 4.22 Design curves for depressed curb inlet A on S_x= 2% 70
Figure 7.1 Pretoria type curb inlet isometric view and cross-sections (City of Tshwane Roads and Transport Department, 2013) 81
Figure 7.2 Side view of a curb inlet with an undepresed gutter 81
Figure 7.3 Side view of a curb inlet with a depressed gutter 81
Figure 7.4 Plan view of the model set-up in the flume 82
Figure 7.5 Honeycomb used to stabilise the flow-rate 83
Figure 7.6 Predicted vs. Experimental Efficiency for inlet A on S_x=2% and S_L=0.25%. 84
Figure 7.7 Predicted vs. Experimental Efficiency for inlet B on S_x=2% and S_L=0.25%. 85
Figure 7.8 Predicted vs. Experimental Efficiency for inlet C on S_x=2% and S_L=0.25%. 85

Figure 7.9 Predicted vs. Experimental Efficiency for inlet D on S_x=2% and S_L=0.25%. 86
Figure 7.10 Predicted vs. Experimental Efficiency for inlet A on S_x=3% and S_L=0.25%. 86
Figure 7.11 Predicted vs. Experimental Efficiency for inlet B on S_x=3% and S_L=0.25%. 87
Figure 7.12 Predicted vs. Experimental Efficiency for inlet D on S_x=3% and S_L=0.25%. 87
Figure 7.13 Predicted vs. Experimental Efficiency for inlet E on S_x=3% And S_L=0.25%. 88

LIST OF TABLES

Page

Table 2.1 Clogging coefficient (UDFCD, 2016) 10
Table 3.1 Summary of scale ratios 30
Table 3.2 Prototype and model properties 30
Table 3.3 Dimensions of each of the 9 sacks 34
Table 3.4 Combinations of model curb inlet dimensions 39
Table 3.5 Combination of conditions tested on each curb inlet 40
Table 4.1 Difference between the observed and predicted average *E* (the negative values indicate underestimation while positive ones indicate overestimation) 43
Table 4.2 Difference between observed and predicted average *E* (the negative values indicate underestimation while positive ones indicate overestimation) 45
Table 4.3 Differences between Grobler's Pretoria type curb inlet and the Pretoria type curb inlet studied in this research 47
Table 4.4 The influence of the longitudinal slope on average interception efficiencies of inlets A, B and D on S_x=2% and S_x=3% 51
Table 4.5 Influence of cross-sectional slope on undepressed and depressed curb inlets when the cross-sectional slope is increased by 1% 51

Table 4.6 Increment of efficiency of inlets A, B, D, C, E and F when the gutter is depressed on S_x=2% 56
Table 4.7 Increment of efficiency of inlets A, B, D, C, E and F when the gutter is depressed on S_x=3% 56
Table 4.8 The average reduction in efficiency of undepressed curb inlets A, B and D with C_L=14.3%, C_L=32.1% and C_L=50% 61
Table 4.9 Single unit clogging factors for each inlet under varying conditions 63
Table 4.10 Empirical equations for depressed curb inlets on S_x=2% and S_x=3% 65
Table 7.1 Regression analysis statistics for depressed curb inlets on S_x=2% 83
Table 7.2 Regression analysis statistics for depressed curb inlets on S_x=3% 84

LIST OF SYMBOLS

a	Gutter depression
A	Flow area
A_r	Area scale ratio
b	Width of the weir
C	Multiple-unit clogging factor for an inlet with multiple units
C_d	Discharge coefficient
C_L	Clog material height as a percentage of the height of a curb
C_o	Single unit clogging factor
d	Approaching head at point gauge in a weir
d_{50}	Median grain size
e	Decay ratio less than 1, which is 0.25 for curb inlets
E	Efficiency ratio of intercepted flow to the total gutter flow/ street flow
E_e	Efficiency of clogged inlet
E_o	Ratio of flow in the depressed section of the gutter to the total gutter flow
F_r	Froude Number
$(F_r)_r$	Froude Number Ratio
g	Gravitational acceleration
g_r	Acceleration due to gravity scale ratio
h	Vertical opening of the curb opening
K	Clogging coefficient
L	Length of curb opening inlet
L_e	Effective unclogged length of curb inlets
L_m	Width of the flume (width of the model street section)
L_p	Width of the street section of the prototype
L_r	Length scale ratio
L_T	Curb opening inlet length that is required to capture 100% of the gutter flow
m	Depth of flow in a gutter
n	Manning's roughness coefficient
N	Number of curb opening inlets

n_r	Manning's roughness coefficient ratio
N_r	Coefficient of regression
p	Height of the weir crest relative to the canal flow
Q_b	By-passed flow
$Q_{i(e)}$	Intercepted flow of clogged curb inlet
Q_i	Intercepted flow
Q_r	Flow rate scale ratio
Q_t	Total flow rate/total gutter flow
Q_{pi}	Intercepted flow of prototype
Q_{pt}	Total flow rate/total gutter flow (prototype)
R^2	Coefficient of determination for regression analysis
R_r	Hydraulic radius scale ratio
S_L *(or* S_o*)*	Longitudinal slope
S_r	Slope scale ratio
S_x	Street cross-sectional slope or transverse slope
T	Spread of water of water over the road
v	Average velocity of street flow
v_r	Velocity scale ratio
W	Depressed gutter section width
Y_o	Depth of water in a curb inlet
y	Flow depth against the curb

ABBREVIATIONS

FHWA	Federal Highway Administration
HEC-22	Hydraulic Engineering Circular No.22
JRA	Johannesburg Roads Agency
SANRAL	The South African National Roads Agency Limited
UDFCD	Urban Drainage and Flood Control District

1 INTRODUCTION

Stormwater drainage systems constitute a part of the road infrastructure which plays a very important role of reducing or eliminating surface runoff on roads. Inefficient storm drainage structures prolong the presence of surface runoff on roads and also contribute to flooding of not only the road infrastructure but also adjoining areas during intense storm events (Butler and Davis, 2004). Pools of water on roads lead to loss of traction between the vehicle wheels and the road and cause splash and spray which reduces the visibility of motorists thereby increasing the probability of traffic stagnation and road accidents with consequent fatalities in some instances (Urban Drainage and Flood Control District [UDFCD], 2016). Furthermore, the structural integrity of roads is threatened when surface runoff is not efficiently drained. In South Africa, there has been an increase of short-lived intense storm events due to climate change, which have resulted in frequent flash floods (Piketh et al., 2014). Current stormwater drainage structures have been unsuccessful at intercepting runoff brought about by these short-lived intense storms. Although there is no available data in South Africa on the consequences of the inefficient inlet drainage on the road infrastructure and road users, it could run into millions of Rands annually for the road infrastructure in the country (The South African National Roads Agency Limited [SANRAL], 2011).

Areas that are most vulnerable to flash floods in Johannesburg are townships such as Alexandra and Diepsloot as they have inadequate storm drainage infrastructure. Additionally, the storm drainage structures tend to be frequently clogged by solid waste rendering them inefficient. Currently, it is difficult for the City Council to adequately manage solid waste disposal due to sporadic and unplanned establishment of settlements. Due to financial constraints and restricted space in townships, the City Council is unable to construct additional stormwater drainage structures that have the capacity to accommodate increased runoff due to land-use densification and solid waste ingress.

Townships have been part of Johannesburg since the apartheid era, yet the few storm inlet drainage structures that have been successfully constructed are similar

to those found in the more affluent areas of Johannesburg where there are more effective waste disposal systems. This indicates that city engineers have not yet found a sustainable way to modify storm drainage structures to suit the needs of townships and its residents.

There are various types of inlet drainage structures, which include: curb inlets, grate inlets, slotted drain inlets and combination inlets (a combination of a curb inlet and a grate inlet). In Johannesburg, the most common and favoured inlet drainage structure is the curb inlet as it is the least likely to be clogged (SANRAL, 2007) and does not interfere with the traffic but it performs poorly on steep longitudinal slopes (UDFCD, 2016).

A curb inlet is a rectangular opening in a road curb and intercepts gutter flow, directing it into stormwater catch-pits and conveyance channels. Its design depends on the intended site location, type of highway, available funds, gradient of the site location and the intensity as well as frequency of storm events. A curb inlet is modelled and analyzed as a side weir on a continuous grade or longitudinal slope and as a transverse weir or an orifice on a sump location (Brown, et al., 2009).

A few drainage manuals and research papers mention the influence of clogging on curb inlets. The UDFCD (2016) accounted for clogging by proposing that the curb inlet opening length be increased by 10%. Australia has developed methods and put in place systems to remove or prevent material such as debris and solid waste from clogging inlets. These methods have been found to be effective but require high maintenance (Allison, et al., 1998) and will not be economically sustainable in South Africa where indiscriminate disposal of solid waste is still common, particularly around informal settlements and townships. Accounting for clogging of curb inlets in design should be carried out to reflect local conditions in order to ensure that they perform efficiently when implemented.

1.1 Problem Statement

Since the 1940s, a substantial amount of research has been conducted on the hydraulic performance of curb inlets, but there is little research covering the clogging of curb inlets. Technical papers such as the HEC-22 have adopted design

strategies from researchers such as Izzard (1950) and are widely used in the USA. Unfortunately, the curb inlets used in the USA are considered to be outdated and are being phased out in the province of Gauteng, South Africa. Currently, Gauteng is installing curb inlets with transition sections known as the Pretoria type curb inlets. The Pretoria type curb inlet has transition sections upstream and downstream of the inlet (see Figure 2.11).

A handful of South African authors such as Zwarmbon (1966) and Grobler (1994) have studied the hydraulic performance of this type of curb inlet. Grobler (1994), whose research findings from experimental investigations have been incorporated into the SANRAL (2007), produced design curves which allow engineers to design curb inlets for a variety of longitudinal slopes without repeatedly carrying out experiments when a new curb inlet is required.

However, these design curves are restricted to curb inlets with 80% and 100% interception efficiencies (which were the only efficiencies investigated in his experimental set up) and are subject to limited inlet dimensions, road slopes and do not account for the influence of clogging on the efficiency of curb inlets. These limitations are the grounds on which the following aims and objectives have been established.

1.2 Aims and Objectives

The research project aimed to obtain more refined equations and design curves that cater for various configurations of the Pretoria-type curb inlet that is widely used in the Gauteng region of South Africa. These equations were applicable to 2% and 3% cross-sectional slopes, and various longitudinal slopes. As in the UDFCD drainage manual, this project intended to obtain more accurate clogging factors that can be used in designing curb inlets by evaluating the influences of various levels of clogging on their performance. The results on clogging impact on inlets obtained from this investigation will be more applicable to local conditions. This thesis, therefore, serves to bring awareness to city engineers and city residents on the negative impacts of improper solid waste disposal on stormwater drainage structures.

The objectives of this project was to compare the results of the experimental investigations carried out on the Pretoria-type curb inlet in a flume with the empirical equations developed by the HEC-22 drainage manual and Izzard (1950). The analysis of the experimental data collected was used to establish various relationships between the efficiency of curb inlets and the road gradient, gutter depression, cross sectional slope and curb inlet clogging.

1.3 The Scope

Inefficient curb inlets lead to prolonged surface runoff which negatively impacts motorists and rapidly degrades and reduces the life span of roadways, with the consequence of considerable loss of financial and human resources. This research, therefore, is aimed at the development of tools that can be used to design efficient and economically viable curb inlets.

The literature that is currently available is very limited on the performance of curb inlets at various levels of clogging, and the few available research works from developed countries are inappropriate for South Africa. Therefore, this study will augment the existing literature on the influences of clogged curb inlets on stormwater drainage system. To accomplish this, the scope of the research has been set below.

Six different models or curb inlet configurations were constructed, each with a unique combination of upstream and downstream transition sections and curb opening lengths. Each model was constructed to represent the Pretoria type curb inlet with the geometric ratio of the prototype relative to the model being 2.5:1. The gutter length, for curb inlets with both depressed and undepressed gutters, was kept equal to the total length of the curb opening length, the upstream and downstream transition lengths. The model curb inlet was tested under open flow conditions and the total channel flow rate (street flow) was varied for different cross-sectional slopes, longitudinal slopes and depths of clog material on depressed and undepressed curb inlets.

A few constraints and limitations that occurred during the experimental procedure are identified and listed below.

- The total time required to carry out all desired experiments was limited and this affected the number of discharge rates admitted into the flume and intercepted by the curb inlet model. Having a larger amount of data with smaller increments in discharge rates and wider range of longitudinal and cross sectional slopes would have allowed for the development of more accurate and comprehensive design curves.
- A prototype to model scale of 2.5:1 was used in the experimental investigation. The model was inserted into a 2 m wide and 12 m long flume. The scale was chosen so that the curb inlet model could be accommodated within the dimensions of the flume. With rigorous dimensional analysis effected on the data, scaling effects were inevitable and they present some of the limitations of the results presented in this research project.

1.4 Thesis Outline

The thesis is divided into six chapters;

The introduction (chapter 1), gives a general introduction to the thesis and a brief background study on current drainage systems.

The literature review (chapter 2), presents the background study with focus on curb inlets on grade or longitudinal slopes;

The hydraulic modelling and experimental results (chapter 3), presents the experimental methods used in conducting tests;

The discussion of test results (chapter 4), gives a detailed analysis of the test results;

The design curves (chapter 5), presents the design curves obtained from the test data and the methods employed in producing them; and,

The conclusion and recommendations (chapter 6), provides a summary of the major findings from chapter 4 and chapter 5 and recommendations for further studies.

2 LITERATURE REVIEW

Climate change has brought about extreme weather events in Southern Africa such as increased temperatures and more intense short-lived storms which at times suddenly produce flash floods in urban environments. Flash floods result in the destruction of property and, in some instances, have led to the loss of lives. Stormwater drainage structures such as curb inlets are usually designed to intercept a portion of storm runoff on grade (see Figure 2.2) and all of the runoff on sag (see Figure 2.1), and redirect the flow into open or closed drains, thereby prevent the occurrence of flooding within the roadway and adjoining areas. In South Africa, curb inlets are the most common and favored type of inlet over the grate inlet, combination inlet and slotted drains. Despite a curb inlet's low efficiency on steep grades, they are favored above other inlets because they are affordable, have low maintenance, safe for pedestrians and cyclists and remain operational to some extent when partially clogged by debris (Grobler, 1994).

A curb inlet may be simply described as a rectangular opening in a curb and can be made of either concrete cast-in-place or pre-cast concrete. In some instances, a curb inlet has additional components such as an upstream and downstream transition sections, a depressed bottom lip at the curb opening or a depressed gutter to improve its performance.

In South Africa, curb inlets are required to intercept excess runoff on streets, that is, runoff that is more than 6 mm in depth for a 1 in 5-year storm event (SANRAL, 2007). Once runoff is intercepted by a curb inlet, water is directed into a catch-pit located below a street walkway. It is then conveyed into a stormwater conveyance system (City of Lubbock Texas Storm Water Management, 1997).

A curb inlet prevents flooding or waterlogging which is a nuisance and dangerous to motorists as it slows down traffic and may cause accidents as a result of hydroplaning that produces loss of visibility from splash and spray (Federal Highway Administration [FHWA], 1984). Furthermore, street flooding can also damage property such as roads, construction sites, buildings and the environment (City of Lubbock Texas Storm Water Management, 1997). Water on the streets is also undesirable for pedestrians as it is seen as an inconvenience and a nuisance.

Streets are designed to have a cross-sectional slope greater than 0% (usually 2% or 3%). This allows for runoff to be collected at the edge of a road, that is, on the curb face or collected into a depressed street gutter which directs runoff into a curb inlet. A longitudinal slope of a road greater than 0% also prevents waterlogging by directing water downstream, allowing it to be intercepted by a downstream curb inlet.

A Curb inlet may be located at a low point (sag) or on a continuous grade (slope) as illustrated in Figure 2.1 and Figure 2.2 respectively. On a low point, a curb inlet behaves as a weir, orifice or mixed flow depending on the depth of the gutter flow or street flow (City of Lubbock Texas Storm Water Management, 1997). A curb inlet on a low point is usually placed at the edge of a gutter (FHWA, 1984) and is designed to intercept 100% of the runoff (City of Lubbock Texas Storm Water Management, 1997). If a curb inlet is depressed and has weir characteristic, the length of the weir is dependent on the width of the depression and the geometric properties of the curb opening. It is undesirable for a curb inlet at low points to behave as an orifice as this indicates waterlogging or flooding.

A curb inlet on a continuous grade is designed to capture a portion of the gutter or street flow as it is not always economic for it to capture 100% of street flow (UDFCD, 2016). If a curb inlet is designed to capture 100% of street flow, it may require that the curb opening length be excessively long. A curb inlet on grade has optimal performance when it is on low grades and its efficiency decreases as the street grade increases (UDFCD, 2016).

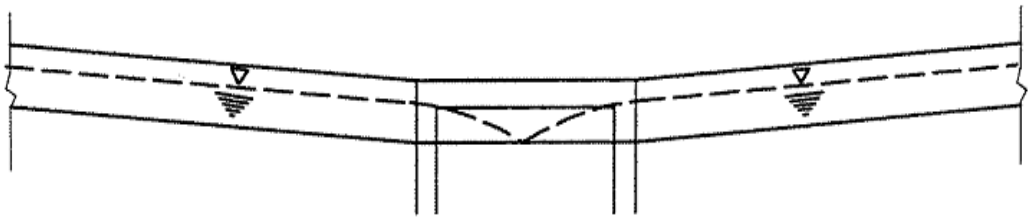


Figure 2.1 Two roads of opposing gradients. The curb is located in the middle (City of Lubbock Texas Storm Water Management, 1997)

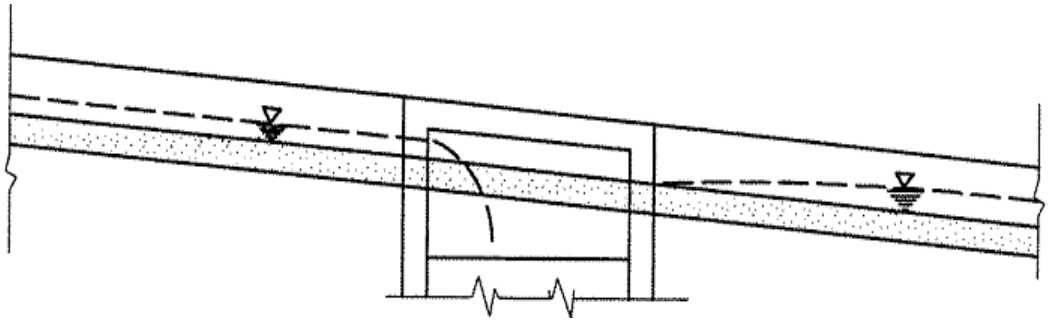


Figure 2.2 A road on a constant grade (City of Lubbock Texas Storm Water Management, 1997)

2.1 Factors Affecting Discharge Capacity and Efficiency of Curb Inlets on Grade

The performance of a curb inlet is measured by its efficiency, which is the intercepted runoff as a percentage of the total upstream street flow. In 1956, Li (1956) presented a research paper for the University of Johns Hopkins which included a study on factors that influence the efficiency of a curb inlet. The Johns Hopkins study concluded that:

- The geometric properties of a curb inlet, that is, the curb inlet length, height and shape directly influence its efficiency (Li, 1956).
- A steep longitudinal slope induces supercritical flow of high velocity and low water depth which diminishes a curb inlet's ability to intercept street flow, while a mild longitudinal slope induces subcritical flow of low velocity and high water depth thus improving its efficiency (Li, 1956).
- As the cross-sectional slope of a street and/or street gutter increases, the depth of the runoff at the curb also increases thus improving the ability of a curb inlet to intercept flow. However, a study by Zwamborn (1966) disagreed with the Johns Hopkins University study (Li, 1956) findings. Zwamborn (1966) stated that the cross-sectional slope does not influence the performance of a curb inlet.
- The depression and shape of a gutter are directly proportional to the magnitude of intercepted runoff. Zwamborn's research (1966) agreed with the Johns Hopkins University study (Li, 1956) and also established that the maximum depression of a gutter should be 61 mm for maximum efficiency.

- The presence of a downstream transition induces back-water or damming at the downstream transition which improves the discharge capacity of a curb inlet (Li, 1956).

2.2 Clogging of Curb Inlets

The presence of solids (such as plastics, paper, cans, and glass material) at the entrances to curb inlets is observed in some urban areas. In the townships and informal/semi-formal settlements of Johannesburg, these materials either partially or completely clog the curb inlets. These settlements tend to lack basic services such as proper solid waste disposal facilities, and where they exist they are usually not well managed. The absence of these facilities has encouraged illegal dumping on open land; consequently, during a storm, solid waste is transported by runoff to a curb inlet thus blocking and decreasing a curb inlet's ability to intercept the optimum amount of runoff. The consequences of clogging of curb inlets by solid waste have not been comprehensively studied therefore the design of curb inlets usually excludes countermeasures against clogging by solid waste.

Although curb inlets are susceptible to clogging, a few authors such as Guo and MacKenzie (2012) have only considered partial clogging and integrated it into their designs. Guo and MacKenzie (2012) applied a clogging factor of 10% to the length of a single curb inlet to account for clogging. However, the single unit clogging factor cannot be applied to each curb inlet in a street with multiple inlets because, based on his assumption, with the first flush of runoff the first curb inlet is most affected by debris and will experience the greatest clogging while the last inlet will be the least affected by clogging (Guo and MacKenzie, 2012). Applying the single-unit clogging factor on multiple inlets would result in the design of excessively long downstream inlets, therefore the clogging factor must decrease as the number of curb inlets increase.

Guo (2000) developed a relationship between the single-unit clogging factor (C_o), the decay ratio (e), the number of curb inlets and the multiple-unit clogging factor or decayed clogging factor (C) presented in Equation 2.1.

According to Guo (2017), the decay ratio is defined as "the incremental amount of debris captured by every single unit added to the inlet" or "the diminishing inlet capacity when adding an additional unit" (Guo, 2006), and it is less than 1. The definitions show that the decay ratio is related to the amount of debris in the streets and the length of each inlet or the number of inlets. From inlet clogging investigations performed in the past, researchers have recommended the debris decay ratio for curb inlets be 0.25 (Guo, 2006).

As seen in Equation 2.1 (UDFCD, 2016), for the first curb inlet, the single unit clogging factor is multiplied by the decay ratio raised to the power of zero, the second is multiplied by the decay coefficient to the power 1 and the third curb inlet is multiplied by the decay coefficient raised to the power 2. This pattern continues and is only applied to a maximum of eight curb inlets.

$$C = 1/N\,(C_o + eC_o + e^2C_o + \ldots + e^{N-1}C_o) = C = \sum_{i=1}^{i=N} e^{i-1}\,C_o/N = KC_o/N \qquad 2.1$$

Where

e is the decay ratio and it is less than 1. For curb inlets, it is 0.25; *K* is the clogging coefficient

Table 2.1 shows the clogging factors for *N* curb inlets. When there are 4 or more curb inlets, the clogging coefficient remains equal to 1.33.

Table 2.1 Clogging coefficient (UDFCD, 2016)

N	1	2	3	4 - 8
Clogging coefficient (*K*)	1	1.25	1.31	1.33

If there are more than 8 curb inlets or a single curb inlet with a very long length, then Equation 2.1 becomes Equation 2.2 (UDFCD, 2016).

$$C = C_o/N(1 - e) \qquad 2.2$$

Finally, the effective length (L_e) which is the expected unclogged length of a curb inlet on a continuous grade is:

$$L_e = (1 - C)L \quad \text{(UDFCD, 2016)} \qquad 2.3$$

In Australia, various countermeasures are employed to trap debris before it reaches the curb inlet. These traps are the portable gravel sediment trap, the gravel sediment trap and the temporary curb sediment trap (The Southern Sydney Regional Organization of Councils and the Natural Heritage Trust, 2010).

The portable gravel sediment trap, Figure 2.3, is a wire mesh rolled up with a geotextile filler fabric filled with gravel that is placed at the mouth of a curb inlet. A small space of approximately 50 mm between the trap and the top of the curb opening is left open to allow for overtopping (The Southern Sydney Regional Organization of Councils and the Natural Heritage Trust, 2010). The portable gravel sediment trap requires low maintenance as it can be easily removed and cleaned. The drawback of using this trap is that it is only able to trap small amounts of sediments (The Southern Sydney Regional Organization of Councils and the Natural Heritage Trust, 2010).

Unlike the portable gravel sediment trap, a wire mesh is placed over the street gutter and the sidewalk as shown in Figure 2.4. A large gravel filter is then placed on the upstream side of the curb inlet and partially over the wire mesh (The Southern Sydney Regional Organization of Councils and the Natural Heritage Trust, 2010). Sediments carried by runoff are trapped by the gravel filter and only allows sediment-free water to be captured by a curb inlet.

The Sandbag sediment trap is placed on the upstream end of the curb inlet as shown in Figure 2.5. The sediment trap is placed ahead of oncoming flow and traps any sediments or debris carried by runoff. A combination of two or three sandbags would be effective in ensuring that the sediments are trapped (The Southern Sydney Regional Organization of Councils and the Natural Heritage Trust, 2010).

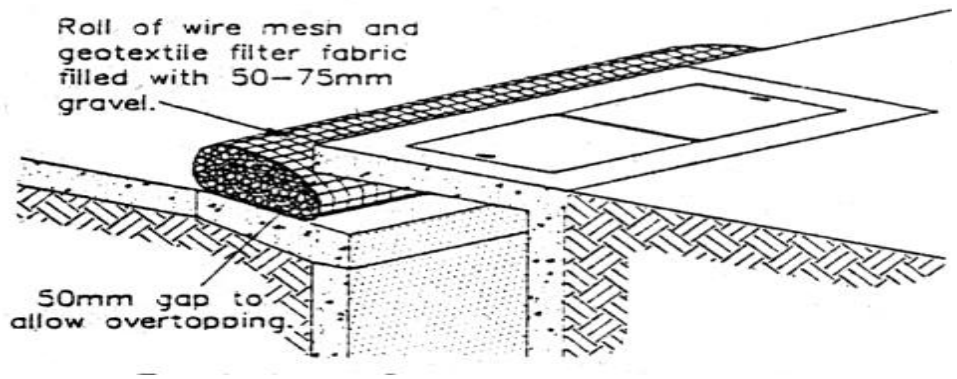


Figure 2.3 Portable gravel sediment trap (The Southern Sydney Regional Organisation of Councils and the Natural Heritage Trust, 2010)

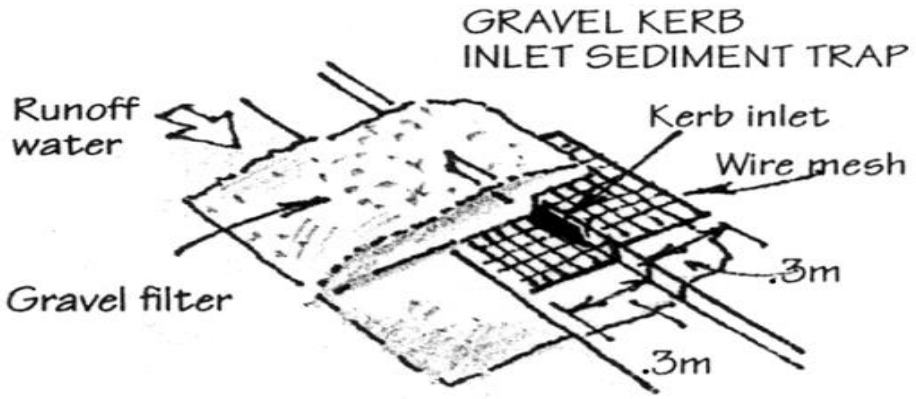


Figure 2.4 Gravel sediment trap (The Southern Sydney Regional Organization of Councils and the Natural Heritage Trust, 2010)

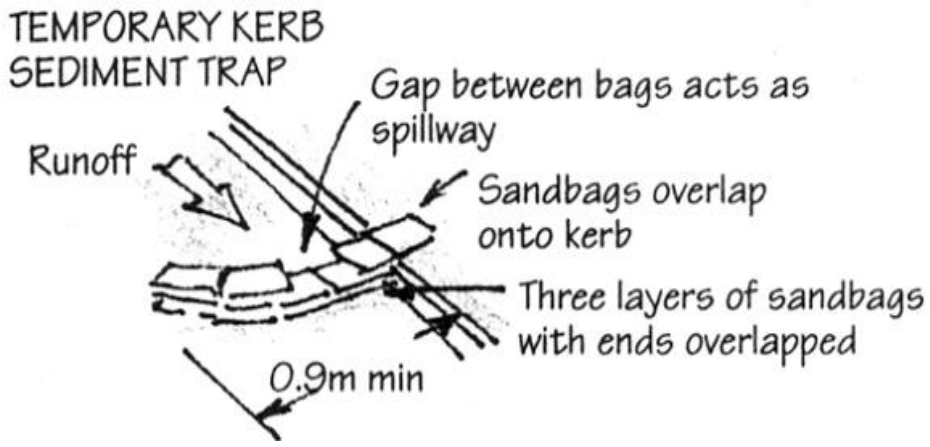


Figure 2.5 Temporary sediment trap (The Southern Sydney Regional Organization of Councils and the Natural Heritage Trust, 2010)

Gilau (2008) presented a research at the 11th International Conference on Urban Drainage in the United Kingdom in 2008 that addressed solid waste interception by curb inlets in rapidly growing informal settlements. Gilau (2008) suggested the use of entrance pit traps, shown in Figure 2.6, as a countermeasure against the clogging of catch pits and stormwater conveyance systems.

A side entry pit trap is a porous basket made of plastic or steel and is installed below the gutter invert in a catch pit to capture solid waste carried by intercepted runoff. Side entry traps are designed to be manually emptied every four to six weeks. This is to prevent side entry traps from excessively filling up which would cause blockage of curb inlets and overflow of solid waste into the catch pit.

According to Gilau (2008), side entry pit traps are effective for minor storm events or for supercritical street flow and when used in settlements with fairly regular solid waste disposal services (Gilau, 2008). Unfortunately, the use of side-entry pit traps requires costly maintenance (Allison et al., 1998) therefore many countries are reluctant to use them.

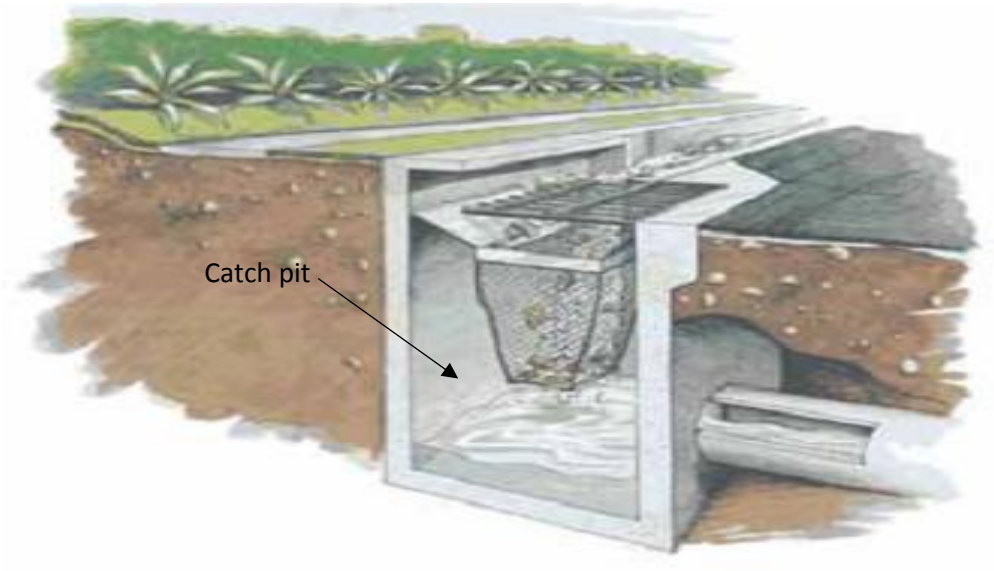


Figure 2.6 Side entry pit trap installed in a catch pit with trapped solid waste (Government of Western Australia-Department of Water, 2011)

2.3 Previous Research on the Discharge Capacity and Clogging of Curb Inlets

Uyumaz (1992) conducted experimental investigations on the hydraulic behavior of curb inlets. The investigation aimed to produce relationships between the discharge capacity of a curb inlet, the longitudinal and cross-sectional slopes of a street.

Tests were conducted on three depressed curb inlet models with lengths of 0.381 m, 0.762 m and 1.143 m. The prototype: model ratio was 25:1. The longitudinal slopes, cross-sectional slopes and the gutter cross-sectional slopes were altered from 0.00 to 0.06; 0.02 to 0.06, and 0.04 to 0.08 respectively.

The test results showed that for supercritical flow, the flow depth decreased along the curb inlets, shown in Figure 2.7, compared to the subcritical flow (Figure 2.8) which exhibited only a slight reduction of flow depth along the curb inlets in the direction of the street flow.

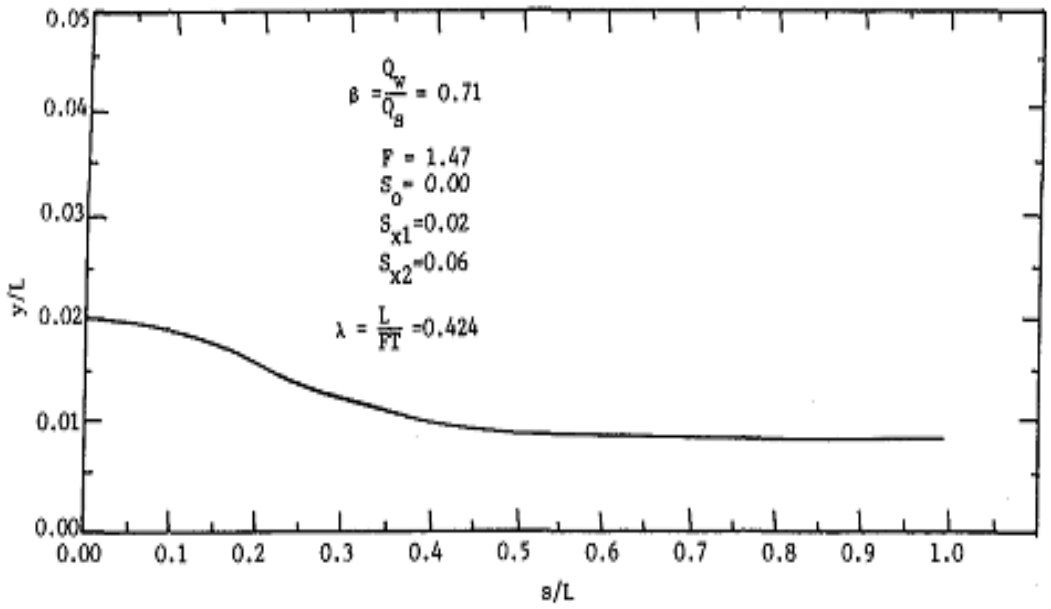


Figure 2.7 Water surface profile for supercritical flow (Uyumaz, 1992), where, Q_w, Q_s, and y are the interception capacity of curb inlets, the flow-rate of street flow and the water depth at the curb respectively

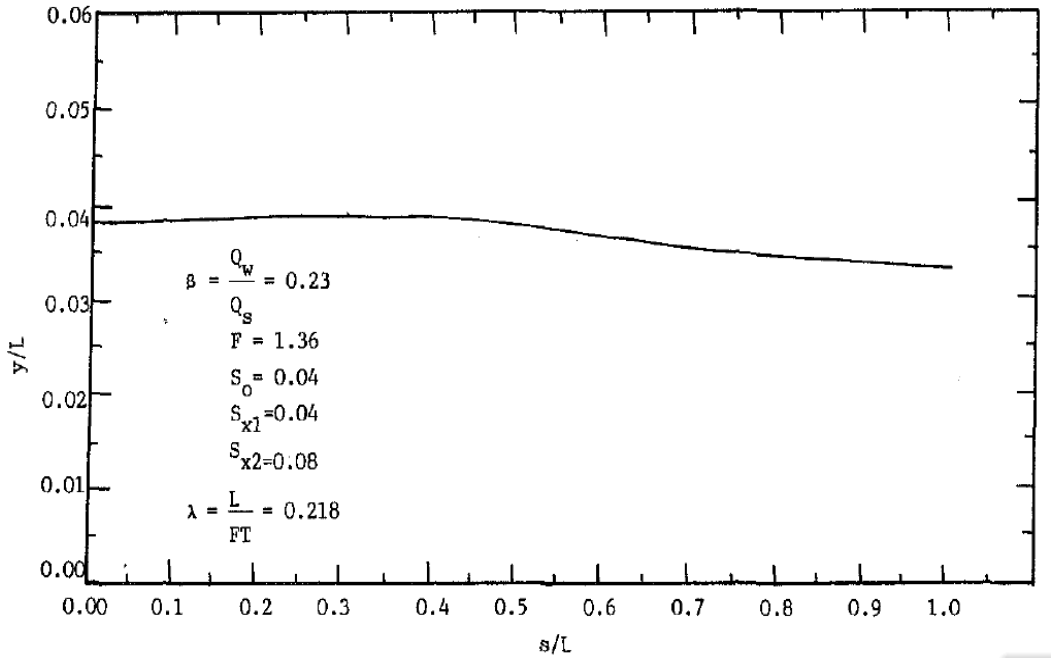


Figure 2.8 Water surface profile for subcritical flow (Uyumaz, 1992)

The parameters that influence the discharge capacity (Q_i) of a curb inlet are the length of the curb inlet (L), the height of a curb inlet (h), Froude number (F) and the spread (T) shown in Figure 2.9. Using these parameters, Uyumaz (1992) derived a dimensionless relationship presented in Equation 2.4, where β and λ are coefficients

$$Q_i = f\,[(L/h), \beta = (Q_i/Q), \lambda = (\,L/F_r T)] \qquad 2.4$$

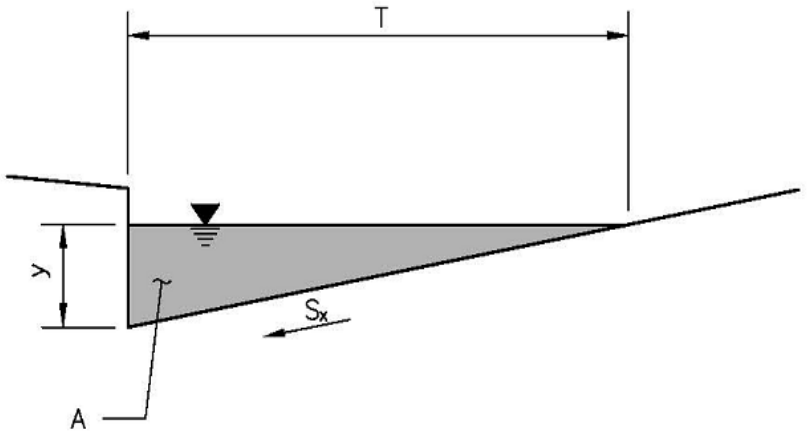


Figure 2.9 Gutter / road cross-section where S_x is the cross-sectional slope, y is the depth of water and T is the spread of water

Equation 2.4 was expressed in Figure 2.10 as curves with L/h=20 and S_L =0.04 using regression analysis. The graph shows an increase in β and λ as the gutter slope and the cross-sectional slope increases. This implies that the street and gutter cross-sectional slope improves the efficiency of a curb inlet, while, it was observed that increasing the longitudinal slope has an opposite effect on the performance of curb inlets.

Uyumaz observed that β and λ have a linear relationship when β is less than 0.6 and have a non-linear relationship when β is greater than 0.6.

The experimental results were compared to the curves presented in Figure 2.10 for varying street and gutter cross-sectional slopes. There is acceptable agreement between the curves and the experimental results with errors of less than 10% for a longitudinal slope of 0.04. This shows that the curves have satisfactory accuracy. The disadvantage of using Uyumaz's method is that, for each longitudinal slope, an equation corresponding to it has to be derived along with curves such as those in Figure 2.10.

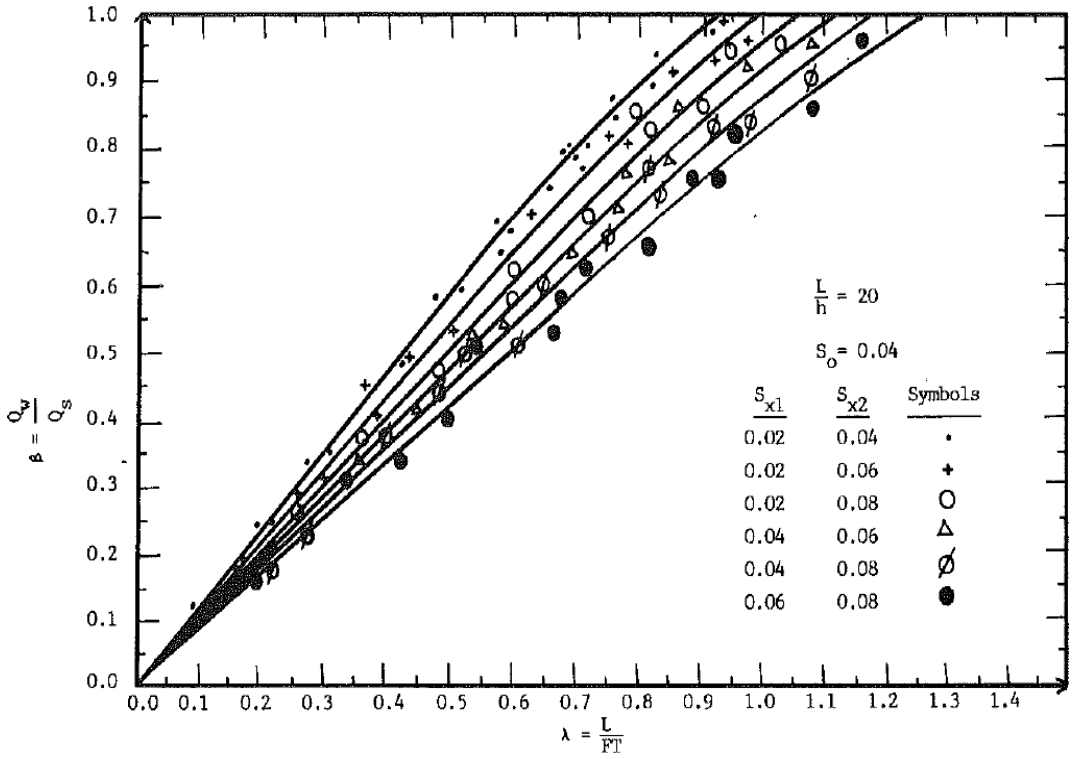


Figure 2.10 β values against λ values for varying S_{x1} (road cross-sectional slope) and varying S_{x2} (gutter cross-sectional slope) (Uyumaz, 1992)

In 1994, at the University of Stellenbosch in South Africa, **Grobler (1994)** conducted a study into the performance of the Pretoria type curb inlets and the development of design curves. The objectives of his work were to;

- Verify if the capacity of a curb inlet could be improved by adding a transition section;
- Assess the influence of a street cross-sectional slope on the discharge capacity of a curb inlet; and,
- Develop accurate and updated design curves.

Grobler conducted experiments on a full-scale Pretoria type curb inlet, shown in Figure 2.11, on City Council-owned land in Pretoria. The Pretoria type curb inlet was developed by Mr. Rodney Corin of the City Engineer's Department of Pretoria in the 1980s (Grobler, 1994).

The land had a street longitudinal slope of 4% and a cross-sectional slope initially set at 2.9% but was later adjusted to 2%. Two curb inlets, adjacent to each other, were used. The upstream curb inlet was designed to intercept approximately 80% of runoff, while the adjacent curb inlet intercepted the residual runoff.

Grobler set these two variables;

- curb opening lengths which varied from 1 m to 3 m, and,
- upstream transition shown in Figure 2.11 (see Appendix A, Figure 7.1 for detailed drawings) lengths were varied from 3 m to 6 m.

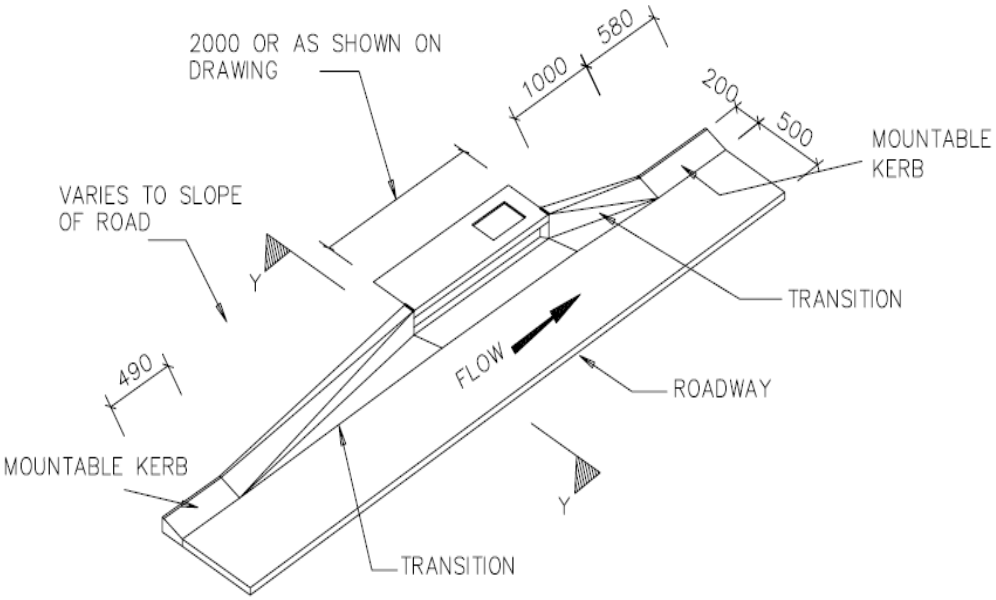


Figure 2.11 The Pretoria-type / Tshwane-type curb inlet (Johannesburg Roads Agency, 2015)

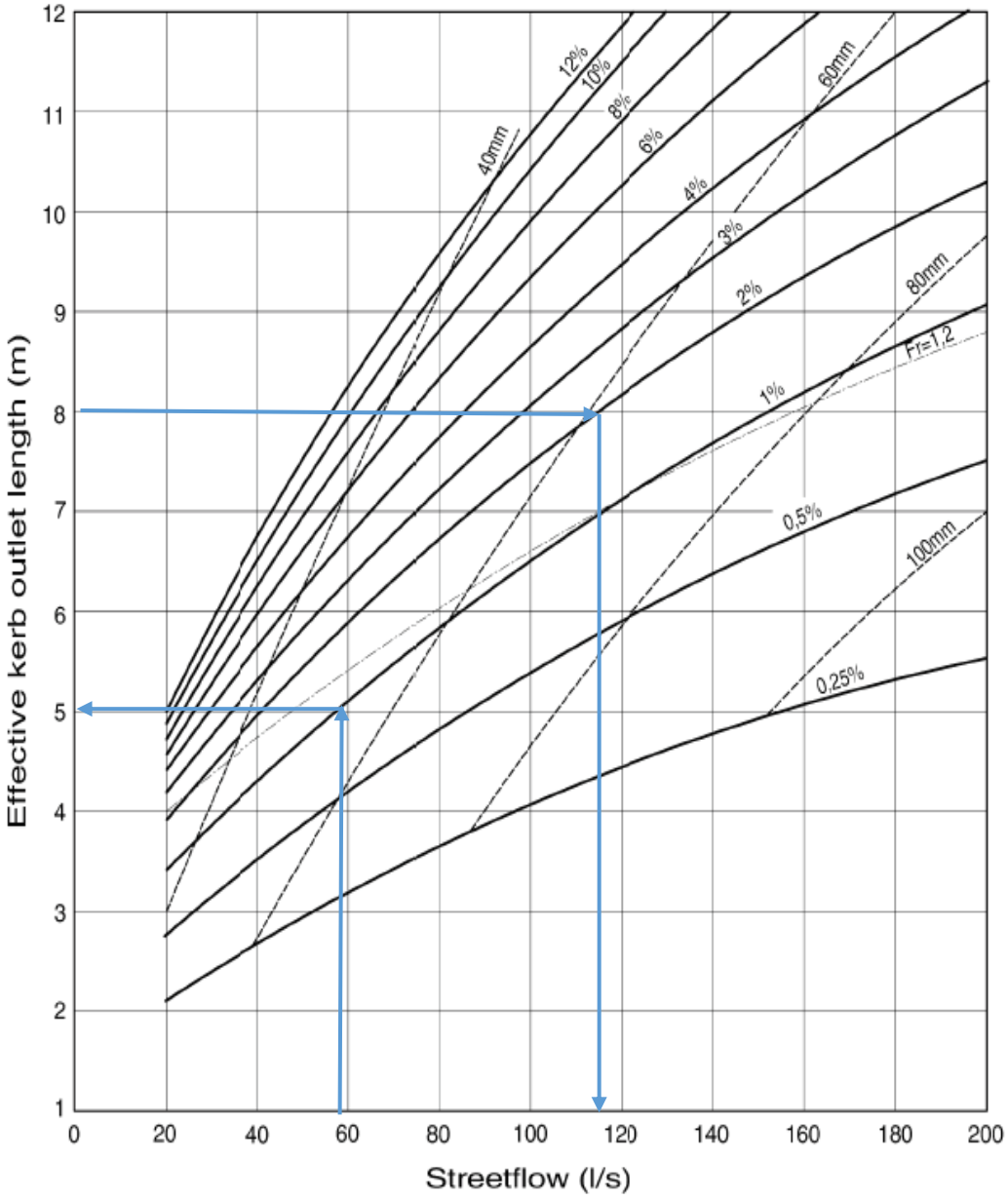
The downstream transition length was kept constant because Grobler assumed that it had an insignificant influence on the discharge capacity of a curb inlet. However, Grobler observed that approximately 50% of the downstream transition section had an impact on the performance of a curb inlet. Grobler also observed that the full length of the upstream transition section impacted on the discharge capacity of the curb inlet as well as the full length of the inlet opening. Subsequently, all the curb inlet components impact the discharge capacity of a Pretoria type curb inlet, therefore Grobler expressed the actual or effective length as the sum of upstream transition section, the inlet section and half of the downstream transition section.

The concept of effective length was incorporated into the experiments and assessed in relation to the discharge capacity of the curb inlet. Also, for each effective length, Grobler compared the discharge capacities of the curb inlets from his experimental investigation to those of previous design curves and equations. It is worth noting that those design curves were based on small-scale models in contrast to Grobler's work which was based on a full-scale model. The experimental discharge capacities from Grobler were significantly greater than those of previous design curves, except for the curb inlet with the 3 m upstream transition which had a defect. The

discrepancies were attributed to scale effects. Thereafter, Grobler modified the existing design curves to accommodate the scale effects by adjusting them upwards by 30%; nonetheless, the data generated from the adjusted design curves were still lower than Grobler's results.

Grobler produced design curves that are shown in Figure 2.12 that reflect the full-scale curb inlet model behavior. The curves produced were for varying longitudinal slopes (0.25% - 12%), curb flow depths (40 mm -100 mm) and a Froude number of 1.2. Grobler's design curves were compact, user-friendly and they accommodated most of the relevant variables that affect inlet performance. The curves, shown in Figure 2.12, are however limited to an inlet efficiency of 80%.

Grobler's observations and test results indicated that the discharge capacity of a curb inlet is improved by increasing the road cross-sectional slope (cross-fall), and the upstream transition section improves the discharge capacity of an inlet particularly for supercritical flow.



Legend:

Effective kerb outlet length at specified road gradient in %

Depth of flow at kerb (mm)

Froude number = 1,2

Curves depict 80% interception at specified streetflow

Flow definition and road gradient criteria			
Froude number	<1,2	>1,2	n/a
Road gradient (%)	n/a	<3	>3
Maximum ratio (Upstream transition length inlet section length)	2	2	6
Absolute maximum length of the transition	4	5	6

Figure 2.12 Grobler's Design Curves (SANRAL, 2007)

McEnroe et al. (1999) conducted an in-depth study into the performance of curb and gutter inlets at the University of Kansas. For the purposes of this literature review, only curb inlets on-grade locations were discussed. Tests were conducted on a street model, scaled down by a quarter. The street model incorporated three different concrete box structures of lengths of 1.5 m, 3 m, and 4.5 m with corresponding inlet opening lengths of 1.2 m, 2.7 m, and 4.3 m respectively. The model was designed to have adjustable longitudinal and cross-sectional slopes of 0.5% to 5%, and 1.6% to 3.1% respectively.

It is observed that there are fairly distinct variations in the intercepted flow with longitudinal slope for 1.5 m and 3 m curb inlets with cross-sectional slopes S_x of 1.6% and 3.1%, but these are more muted for inlet length of 4.5 m. McEnroe et al. (1999) concluded that the influence of the longitudinal slope diminishes as the curb opening increases. Also, curb inlets have higher performance at steep cross-sectional slopes and on mild longitudinal slopes.

A research team, **Comport et al.** (2009), at the Colorado State University presented a research study into the efficiency of grate and curb inlets. The research work is similar to the study done by McEnroe et al. (1999). The objective of this research was to quantitatively analyze the experimental results of three inlets (two grate inlets and one curb inlet) that are commonly used by the UDFCD manuals. Before this work, these inlets were designed by the design guidelines of the Federal Highway Administration (FHWA, 2009) that are titled, *Hydraulic Engineering Circular No. 22* (HEC-22). This research work underscores the importance of ensuring that the design equations employed are appropriate to the relevant curb inlet.

Tests were conducted on a model which was scaled down by a factor of one third. The variables in this investigation were;

- Longitudinal slope: 0.5% - 4%
- Cross-sectional slope: 1% - 2%
- Inlet length: 1.524 m, 2.743 m, 3.658 m and 4.572 m (5 ft., 9ft., 12 ft., and 15 ft. respectively)

- Flow depth: 0.101 m, 0.152 m and 0.30 5 m (0.33 ft, 0.5 ft and 1 ft respectively)

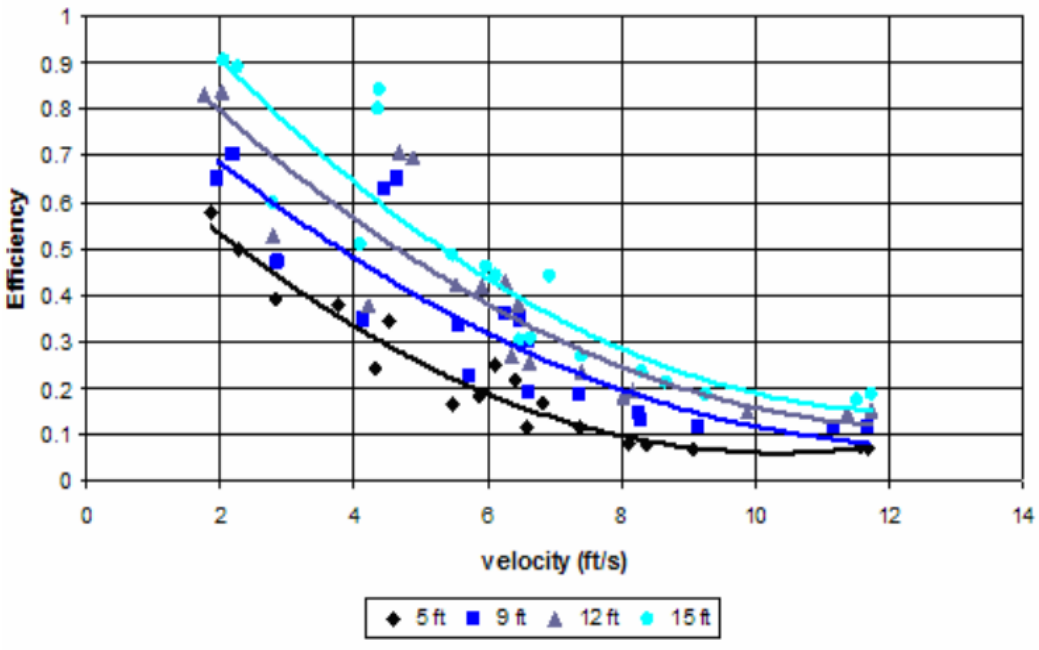


Figure 2.13 Curb inlet on-grade test data (Comport et al., 2009)

The trend lines through the experimental data for efficiency in relation to the velocity of flow on the road are reproduced in Figure 2.13. The trend lines exhibit exponential decay with low efficiencies associated with high velocities or high longitudinal slopes and higher efficiencies with longer inlets.

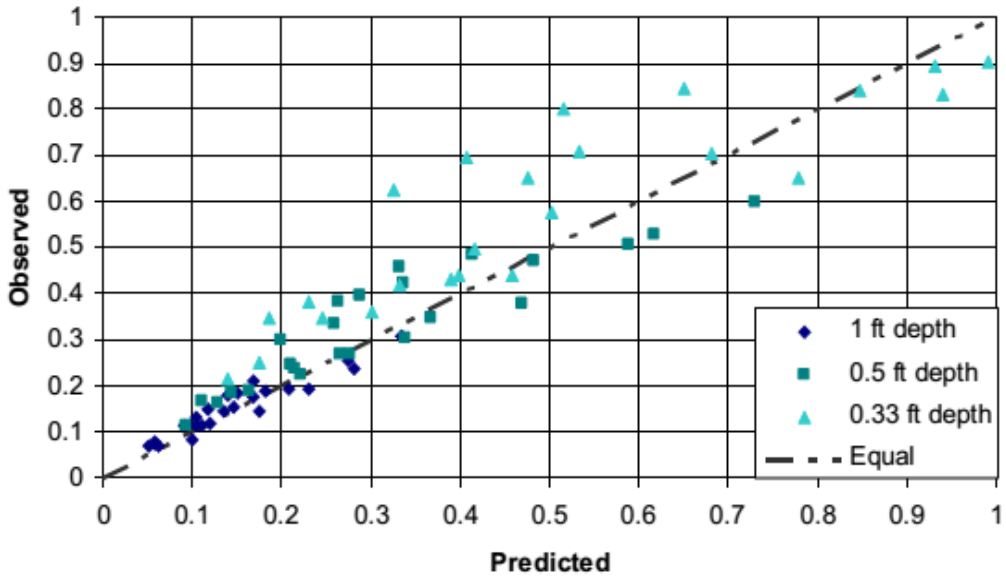
The efficiency (*E*,) and curb inlet length (L_T) required to intercept the entire street flow are computed by relationships given in the HEC-22 (FHWA, 2009) and reproduced in Equations 2.5 - 2.7 (UDFCD, 2008). These results were plotted against the experimental (observed) results and presented in Figure 2.13.

$$E = 1 - [1 - (L/L_T)]^{1.8} \quad 2.5$$

$$L_T = k \cdot Q^{0.42} \cdot {S_L}^{0.3} \cdot (1/(n \cdot S_e))^{0.6} \quad 2.6$$

Where *k* is 0.816 (S.I. Units) or 0.6 (Imperial Units)

$$S_e = S_x + (a/W)E_0 \quad 2.7$$



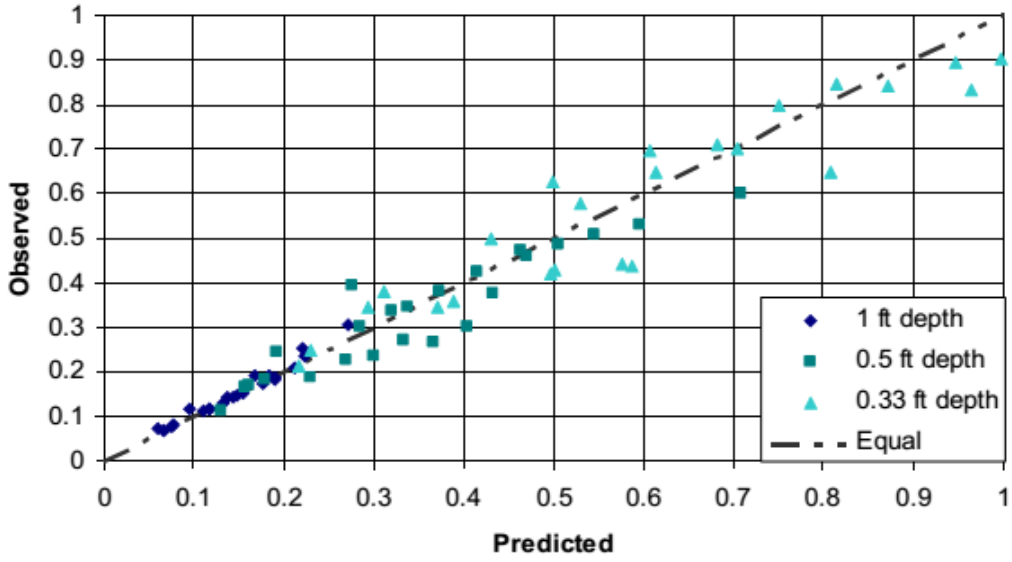
R^2	Average efficiency error (%)	Maximum efficiency error (%)
0.861	6.5	30.2

Figure 2.14 Predicted vs. observed curb inlet efficiency from Equations 2.5 and 2.7 (Comport et al., 2009)

The predicted and the experimental data are in agreement at low efficiencies, that is, below 0.2. The HEC-22 equations, mostly, underpredict the curb inlet's efficiency by an average error of 6.5% and a maximum error of 30.2% (Comport et al., 2009). The researchers proposed a revised Equation (2.8) in order to reduce the average and maximum errors in efficiency.

$$L_T = 0.38 \cdot Q^{0.51} \cdot {S_L}^{0.058} \cdot (1/(n \cdot S_e))^{0.46} \qquad 2.8$$

The modified equation was plotted against the experimental results in Figure 2.15 with reduced average and maximum efficiency errors of 3.8% and 15.7% respectively (Comport et al., 2009).



R^2	Average efficiency error (%)	Maximum efficiency error (%)
0.948	3.8	15.7

Figure 2.15 Predicted vs. observed efficiency from the modified UDFCD equation (Comport et al., 2009)

Comport et al. (2009) developed empirical equations for curb inlet efficiency using dimensional and regression analyses and validated with experimental data. The variables which influence the curb inlet efficiency are expressed by the relationship:

$$E=f\,[S_x, S_L, v, L_c, m, A, T] \qquad 2.9$$

Using the Buckingham Pi theorem produced these dimensionless variables.

$\pi_1 = m/L$, $\pi_2 = (V^2 \cdot T)/(gA)$, $\pi_3 = v^2/(gm)$, $\pi_4 = v^2/(gL)$, $\pi_5 = S_x$, $\pi_6 = S_L, \pi_7 = E$

These were combined to obtain the following general efficiency equation:

$$E = N_r((m^a/L_c) \cdot (v^2T^b/gA) \cdot (v^{2c}/gm) \cdot (v^{2d}/gL) \cdot {S_x}^e \cdot {S_L}^f) \qquad 2.10$$

Where

a, *b*, *c*, *d*, *e* and *f* are exponents determined by statistical analysis of experimental data that produced the relationship

$$E = 0.076 \frac{v^2}{gm}^{0.545} \cdot \frac{v^2}{gL_c}^{-0.879} \cdot S_x^{0.231} \qquad 2.11$$

The performance of Equation 2.11 on the experimental data is reproduced in Figure 2.16.

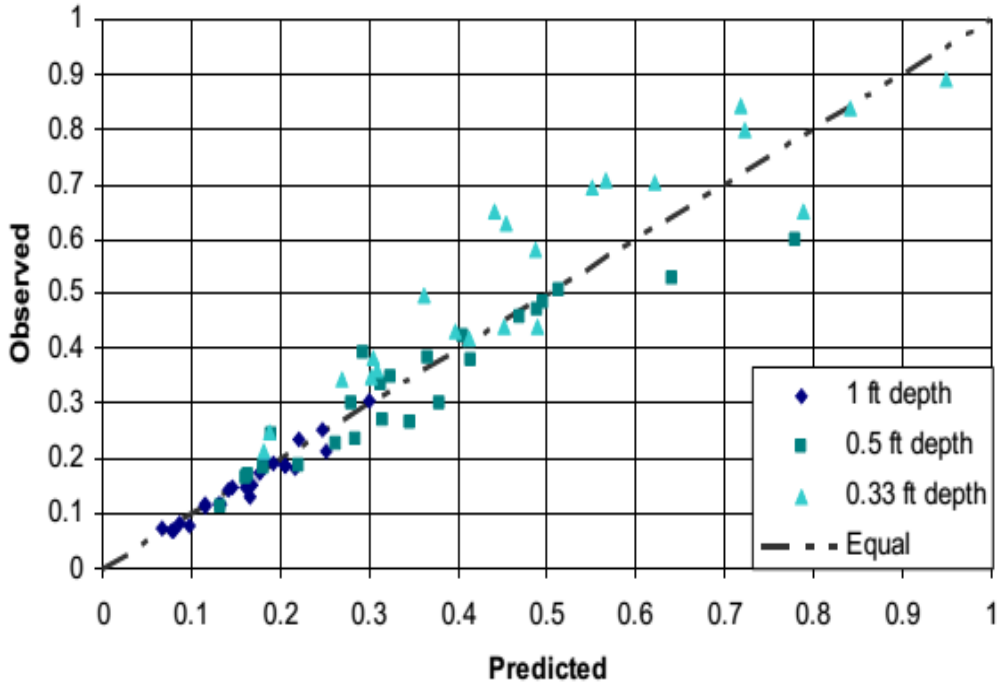


Figure 2.16 Observed vs. Predicted efficiency values from the empirical Equation 2.11 (Comport et al., 2009)

There is good agreement between the predicted and observed efficiencies, that is, below 0.2 in Figure 2.16. The average and maximum efficiency errors were found to be greater than the errors produced by the improved UDFCD equation, however, the empirical equation has greater accuracy than the original UDFCD (2008) equation. The average and maximum efficiency errors at R^2 of 0.89, were found to be 5.1% and 29.1% respectively. It is important to note that in Figures 2.14, 2.15 and 2.16, the predicted and observed data correlated better at high flow depths than at low flow depths. A sensitivity analysis was conducted to determine the impact of numerically adjusting each variable on the curb inlet efficiency. It was found that a 50% increase in the curb inlet length resulted in a 40% increase in its efficiency. The original UDFCD (2008) equations were found to be sensitive to changes in

velocity and flow depth and less sensitive to changes in street cross-sectional slope due to local inlet depression.

Izzard (1950) observed that highway stormwater drainage structures under-performed due to improperly specified spacing of the inlets and underperforming stormwater drains resulting in ponded roadways. The poorly designed street drainage system was a consequence of insufficient knowledge and understanding of the performance of inlets thus prompting Izzard (1950) to derive theoretical equations for the discharge capacity of curb inlets using basic hydraulic principles and mathematics.

In a roadway with an undepressed gutter, the relation between the street flow that is completely intercepted by a curb inlet and the length of the curb inlet *L* is given by;

$$Q_i = 0.39 \cdot L_T \cdot y^{1.5}[1 - L/L_T]^{2.5} \qquad 2.12$$

Where *y* is the flow depth upstream of the inlet. The theoretically derived equation by Izzard (1950) had a coefficient of 0.682 but was modified to 0.39 to achieve agreement with the experimental data of the University of Illinois. For an inlet in a depressed gutter, the relevant equation in SI Units is

$$Q_i = 0.39 \cdot L_T \cdot (a + y)^{1.5}[1 - L/L_T]^{2.5} \qquad 2.13$$

Where

a is the depressed gutter depth.

Izzard (1950) compared his theoretical equations with experimental data that was produced by authors from the Illinois University, North Carolina State College, and the U.S. Army Corps of Engineers. There was good agreement between the data obtained from the Illinois University and generated by Equation 2.13. Also, Izzard (1950) reported that Equation 2.13 was roughly in agreement with the North Carolina experimental data for a = 76 mm for inlet lengths that varied from 0.305 m to 2.134 m and longitudinal slopes that varied from 0.5 % to 10 %. For the limited data of the U.S. Army Corps of Engineers, only rough agreement was achieved with Izzard's theoretical results.

3 HYDRAULIC MODELLING AND EXPERIMENTAL METHODS

In fulfillment of the objectives of this research presented in Chapter 1, experiments were conducted on a small-scale street model. The street prototype was geometrically scaled down by 2.5:1. The model included a single one-lane road, a sidewalk, and an adjustable Pretoria type curb inlet shown in Figure 2.11 and a gutter section equal to the total length of the upstream and downstream transition sections and the curb inlet opening.

The test investigations took measurements of these variables: the flow depth upstream of the curb inlet, the flow rate of the street flow, and the flow rate of the intercepted flow. A total of 2880 tests were conducted on 6 depressed curb inlets and 6 undepressed curb inlets. All tests were conducted when the street was on-grade. The investigations took into account physical variables considered to influence the performance of a curb inlet. These variables are:

- Curb inlet length,
- Upstream transition length,
- Cross-sectional slope,
- Longitudinal slope,
- Clog height, and
- Flow rate.

During testing, the following street model components were kept constant for both depressed and undepressed curb inlets:

- Shape of gutter
- Inlet height
- Road surface roughness
- Gutter roughness
- Downstream transition length
- Gutter slope for depressed curb inlets
- Gutter length.

This chapter provides a detailed description of the construction and layout of the model, the testing facility, conditions tested and the experimental procedure.

3.1 Description of Prototype

Tests were performed on a street model similar to a residential street. According to the Johannesburg Roads Agency Roads and Stormwater Manual (2015), a residential street consists of a 3.5 m wide one-lane asphalt road with a Manning's roughness of 0.015-0.020, a 1.5 m sidewalk, a concrete gutter with a Manning's roughness of 0.012 and a curb inlet. The Pretoria type curb inlet (see Figure 2.11) was selected for this research. The inlet length and downstream transition sections are kept at 2 m and 1 m, respectively, while the upstream transition section depends on the longitudinal slope and varied from 1 m to 3 m.

3.2 Model Scaling

Several parameters such as the flow rate, velocity, longitudinal slope, pump characteristics, gravity head, street dimensions were wholly dependent on the existing laboratory infrastructure and equipment. Therefore, the laboratory infrastructure and equipment determined the scaling of the model.

The dimensions of the prototype and the flume are significantly different, and as such the prototype was geometrically scaled down to fit into the flume. Consequently, the flow rate, velocity, and Manning's roughness coefficient corresponding to the model were derived by using the principles of hydraulic similitude (PACE Advanced water engineering, 2011). The geometric similarity requires only the geometric properties of the model and the prototype to have a constant ratio. The ratio of the prototype length to the model length (or scale) was derived from Equation 3.1.

$$L_r = L_m/L_p \tag{3.1}$$

Where L_m is the model length and L_p is the prototype length. Hydraulic similitude is achieved with the flow in the prototype and the model having the same Froude number. This results from considering the inertia and gravity as the most important forces that influence the flow of water (PACE Advanced water engineering, 2011) on the road and in the flume. The Froude number is defined as:

$$Fr = v/\sqrt{gL} \tag{3.2}$$

Therefore the Froude number ratio is presented as:

$$(Fr)_r = (v_r/\sqrt{g_r L_r}) \quad 3.3$$

The Froude number and gravitational acceleration are equal for both the prototype and the model, hence Equation 3.3 becomes:

$$v_r = {L_r}^{0.5} \quad 3.4$$

The flow rate ratio relationship is as follows:

$$Q_r = A_r \cdot v_r \quad 3.5$$

$$Q_r = {L_r}^{2.5} \quad 3.6$$

Manning's roughness coefficient ratio for an open channel model with a fixed bed is derived from the Manning equation presented in Equation 3.7:

$$v_r = {R_r}^{2/3} {S_r}^{1/2} / n_r \quad 3.7$$

The condition for a fixed bed (that is an undistorted bed) is that the slope ratio is equal to 1 and the length ratio is equal to the hydraulic radius ratio, therefore Equation 3.7 becomes:

$$v_r = {L_r}^{2/3} / n_r \quad 3.8$$

By incorporating Equation 3.4 into Equation 3.8, the following equation is obtained.

$$n_r = {L_r}^{1/6} \quad 3.9$$

Table 3.1 summarizes the model scaling ratios discussed above. The scale ratios were utilized in model construction and experimental investigations. The cross-sectional and longitudinal slopes have a scale ratio of 1 as they are dimensionless. The scale ratio of fluid density is also 1 as the density of the fluid (water) was unchanged.

Table 3.1 Summary of scale ratios

	Scale Ratio
Length	L_r = 0.4
All slopes (cross-sectional and longitudinal)	S_r = 1.0
Velocity	v_r= 0.632
Flow rate	Q_r= 0.101
Fluid density	1.0
Manning's roughness coefficient	n_r = 0.858

Given the scale ratios presented in Table 3.1, the model and prototype geometric properties are computed and presented in Table 3.2.

Table 3.2 Prototype and model properties

Feature	**Prototype Properties**	**Model Properties**
Curb inlet length (m)	2 - 6	0.4 – 0.8
Upstream transition length (m)	1 - 3	0.2 – 0.6
Downstream transition length (m)	1	0.4
Roughness coefficient (road)	0.015 – 0.020	0.013 – 0.017
Roughness coefficient (gutter)	0.012	0.0103
Sidewalk (m)	1.5	0.6
Road (m)	3.5	1.4 m
Longitudinal slope (%)	0.25, 0.5 and 0.75	0.25, 0.5 and 0.75
Cross slope (%)	2 and 3	2 and 3

3.3 Model Road Surface Roughness

The Manning's roughness coefficient is a measure of resistance to flow in a channel due to surface roughness (Arcement and Schneider, 1989). For an asphalt road, the prototype Manning's roughness coefficient lies between 0.015 and 0.020. Manning's roughness coefficient for the model (n_m) is obtained by multiplying n_r (Table 3.1) with Manning's roughness coefficient of the prototype (n_p) giving a

value that lies between 0.013and 0.017. Recreating the road surface roughness required the use of sand grains with a grain size corresponding to the correct Manning's roughness coefficient. The relationship between Manning's roughness coefficient and the median sand grain size is expressed as:

$$n = 0.041 {d_{50}}^{1/6} \text{ (Henderson, 1966)} \qquad 3.10$$

Equation 3.10 and n_m of 0.0129 to 0.0172 gave a corresponding d_{50} of 0.97 mm to 5.45 mm. A sieve size of 1.18 mm was used as it was the closest to d_{50}=0.97 mm. A median sand grain size of 1.18 mm gives a Manning's roughness coefficient of 0.013.

On completion of the model, the Manning's roughness coefficient was verified by conducting 10 tests on the model. The longitudinal and cross-sectional slopes were set at 0.2% and 2% respectively and the flow rate was varied from 3 l/s to 12 l/s. By applying the Manning's equation (3.11), the average Manning's roughness coefficient of the road model was found to be 0.015 which is slightly higher than the expected n_m=0.013. However, it lies within the range stated above.

$$n = A \cdot R^{2/3} \cdot {S_o}^{1/2} / Q \qquad 3.11$$

3.4 Model Layout

Before conducting tests, water was pumped at 80 L/s from a sump tank to an elevated overhead tank (see Figure 3.1). The overhead tank consists of nine concrete broad-crested weirs, shown in Figure 3.2, which directed water to a pipe leading back to the sump tank. From the sump tank, water was pumped back to the overhead tank. This flow rotation was repeated for 5 minutes before water was channeled to the flume using a propeller digital flowmeter (see Figure 3.1). The digital flowmeter controlled the flow of water to the flume while the residual flow was recirculated. The gravity head between the flume and overhead tank was limited to 3 m due to the existing laboratory infrastructure. At the end of each test, water from the flume was collected in the tail-box (see Appendix B, Figure 7.4) and channeled through sluice gates into the sump tank.

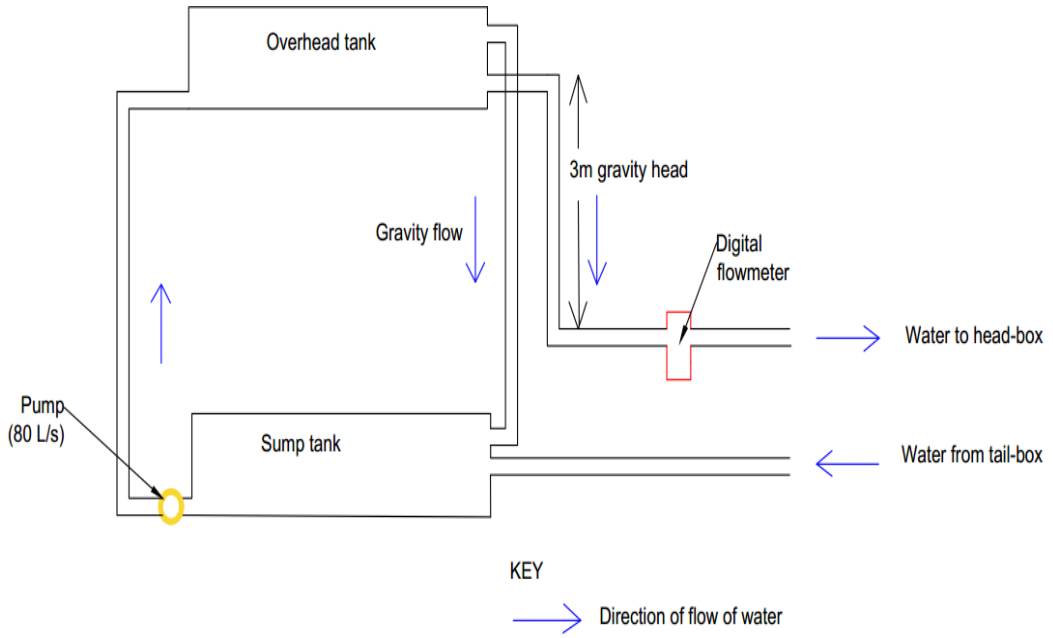


Figure 3.1 Schematic drawing of the Hydraulics Laboratory water supply system



Figure 3.2 Inside the overhead tank

A flume was required to effectively simulate and control street flow conditions. The largest available flume in the Hydraulics Laboratory of the School of Civil and Environmental Engineering, University of Witwatersrand is 2 m wide and 12 m long. It consists of a head-box at the upstream end of the flume which supplies water from the overhead tank to the flume and a tail-box on the opposite end designed to capture the total flow from the flume (see Figure 3.3, and Appendix B, Figure 7.4). The longitudinal slope of the flume was electronically adjustable from 0% to 0.9% while the cross-sectional slope of the road was manually adjusted from 2% to 3%.

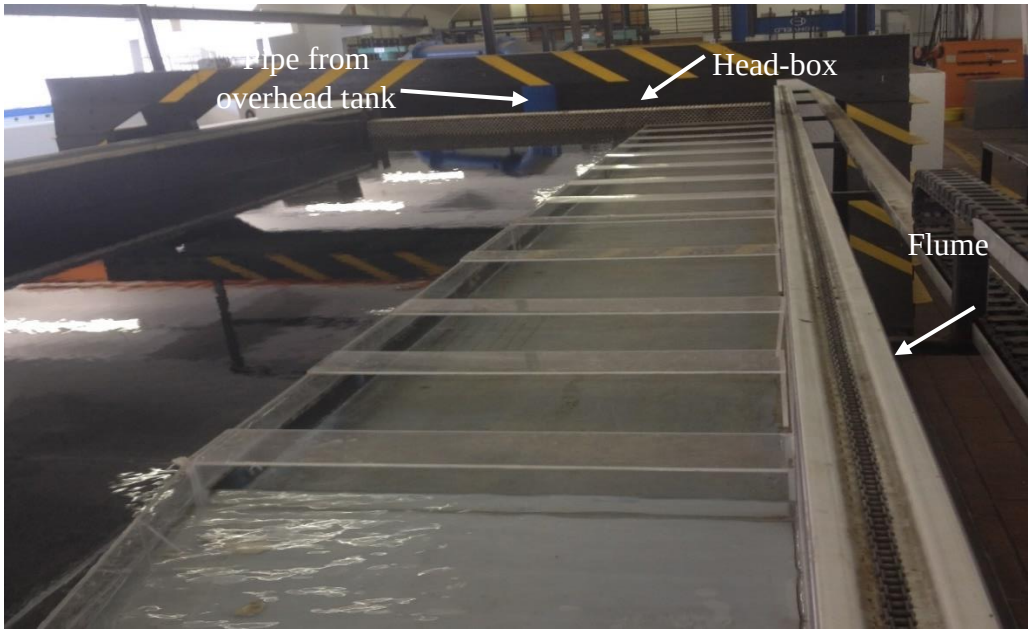


Figure 3.3 Upstream section of the constructed street model

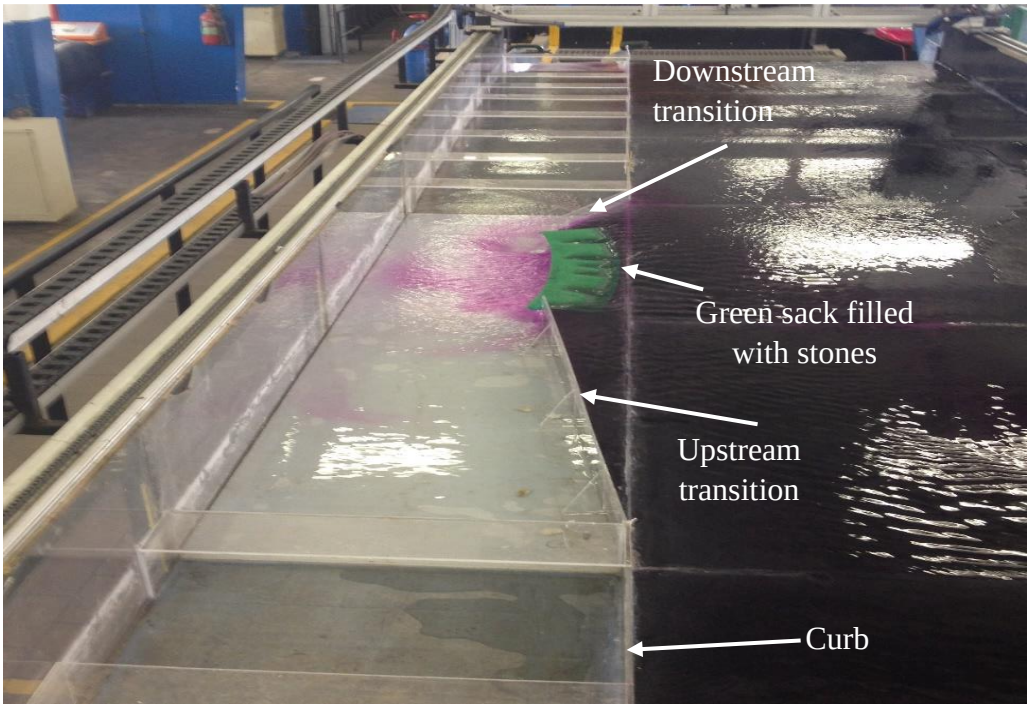


Figure 3.4 Flooded street model with clogged curb inlet

The road, made up of a series of fiber cement boards, had a width and length of 1.4 m and 12 m respectively. Each board was supported by short PVC pipes placed vertically underneath the boards. The shortest PVC pipes were placed near the curb while the longer PVC pipes were next to the flume walls creating a gentle road

cross-sectional slope. The cross-sectional slope of the flume could not be altered, and as such manual adjustments of the boards were done to effect the 2% and 3% cross-sectional slopes. The adjustment of the longitudinal slope was effected by the tilting device on the flume. Throughout testing, the gutter slope for depressed curb inlets remained uniform and likewise for undepressed curb inlets.

A curb inlet with an adjustable inlet opening length and upstream transition length was installed at approximately the middle of the length of the flume. The intercepted flow was conveyed into a yellow flume terminating at a 90^{o} V-notch weir shown in Figure 3.5. The carry-over flow and the intercepted flow were captured in a tail-box that also terminated at a 90^{o} V-notch weir shown in Figure 3.6.

Clogging of curb inlets was accomplished by placing green sacks of different geometric properties (see Table 3.3) at the mouth of the curb inlet, shown in Figure 3.4. It was essential for the stones to be retained in the sacks to prevent them from being individually washed away by street flow at high velocities. Nine sacks were created for the tests and each sack was filled with similar-sized stones.

Clogging simulations were not conducted as they fell out of the scope of the research.

Table 3.3 Dimensions of each of the 9 sacks

Sack	**Height (mm)**	**Length (m)**
1	8	0.8
2	18	
3	28	
4	8	1.2
5	18	
6	28	
7	8	1.6

8	18	
9	2	

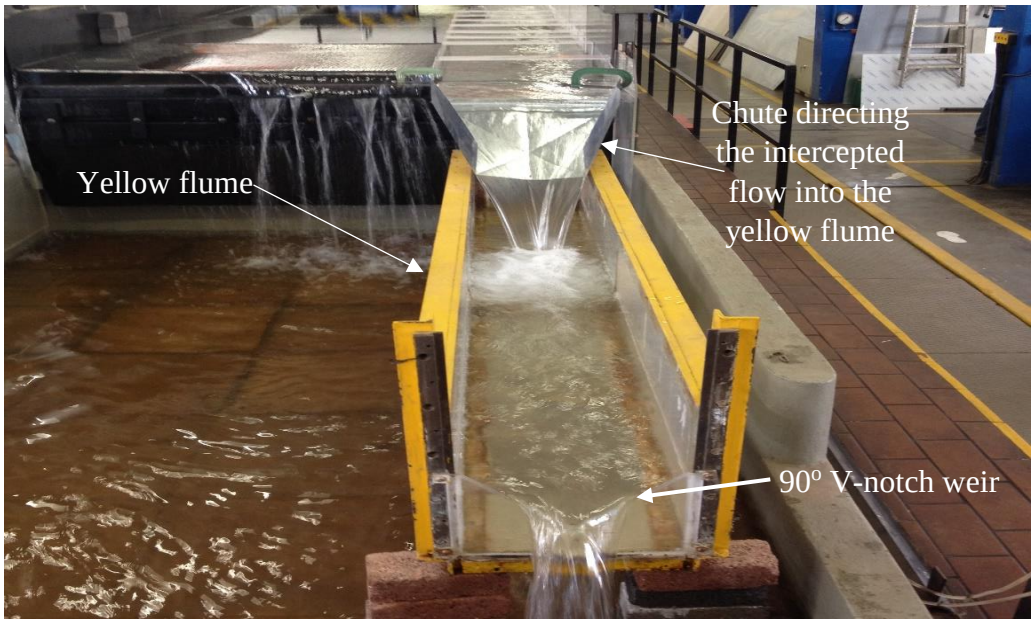


Figure 3.5 Yellow flume terminating at a 90° V-notch weir (a tape measure glued to the wall of the flume was used to measure the depth of water)



Figure 3.6 Tail-box terminating at a 90° V-notch weir (a tape measure glued to the wall of the tail-box was used to measure the depth of water)

3.5 Measurements

During testing, as earlier described, a program for data collection was put in place to obtain the following:

1. The flow-rate of the intercepted flow was measured by determining the depth of water in a side-channel (yellow flume) which terminates at a 90^o V-notch weir,
2. The total street flow was measured by measuring the depth of water in the tail-box, which also terminated at a 90^o V-notch weir , and
3. The depth of the street flow upstream of the curb inlet was measured by a digital Vernier height gauge.

Initially, only the tail-box V-notch weir had been calibrated. The calibration of the V-notch weir (of the yellow flume) was done using the rating equation (see Equation 3.7) from which the discharge coefficient C_d value and the exponent on the upstream head were determined. The rating equation, which is given by Equation 3.12, is used to calculate the flow-rate of water passing over a weir. The coefficient C is unique to each weir type and in this case, C for a V-notch weir is presented as Equation 3.13.

$$Q=Ch^b \quad \text{(Chadwick at al., 2004)} \qquad 3.12$$

Where*:*

$$C = C_d \cdot \frac{8}{15} \cdot tan(\frac{\theta}{2}) \cdot \sqrt{2g} \quad \text{(Chadwick et al., 2004)} \qquad 3.13$$

b is the exponent on the head h above the notch of the weir,

C_d is the discharge coefficient, and

h is the head over the weir (m).

In the laboratory, a computer was directly linked to the digital flow-meter and the flume. Installed in the computer was a software, “Water” published by Moog in 2012 that allowed a user to electronically control the longitudinal slope of the flume and to incrementally increase the flow rate of water into the flume.

For each flow-rate, the water depth upstream of the weir (of the yellow flume) was measured by a digital height gauge and the time taken to fill a 3.5-liter bucket was measured by a stopwatch. The location of the digital height gauge in the yellow flume was chosen to be where the drawdown to the weir and turbulence from the incoming flow was minimal. This location was found to be about mid-length along the side flume. The measurements for both water depth and time were repeated three times for each flow-rate and averaged. This procedure was carried out for 10 different flow rates. In Figure 3.7, the rating curve was obtained from the plotted data with an exponent of 2.472 (that is, *b* in Equation 3.12) and the coefficient, *C*, which corresponds to 1.188, gave a value for C_d, using Equation 3.13, of approximately 0.5.

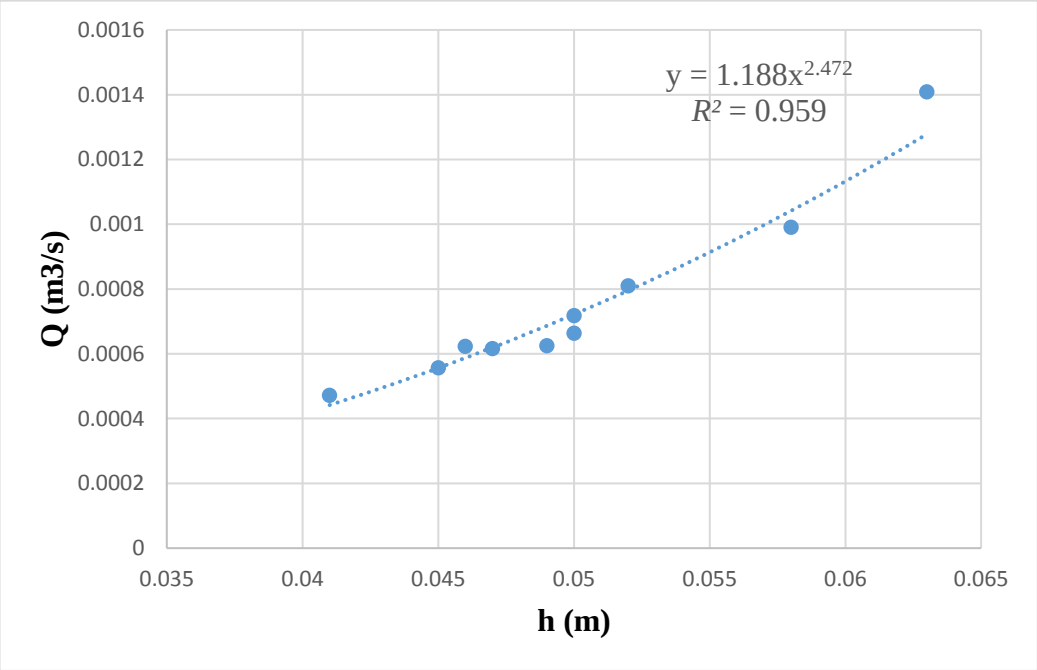


Figure 3.7 Rating curve for the V-notch weir in the side channel that conveys the flow intercepted by the curb inlet

3.6 Model Construction

The street model was constructed in the Hydraulics laboratory in the School of Civil and Environmental Engineering. Fiber cement boards were used in the construction of a single one-lane road of a width of 1.4 m. The boards were smoothened in preparation for the application of fiberglass resin, which is a strong adhesive.

Immediately after the application of fiberglass resin, sand of particle size of 1.18 mm was evenly spread over all boards creating a uniform surface roughness. When the fiberglass resin was dry, the boards were painted black.

Clear Perspex was used to construct a sidewalk with a width of 0.6 m, a curb height of 56.4 mm and curb inlets that had various characteristics and geometric configurations. The sidewalk was designed to accommodate various modifications to the curb inlet presented in Table 3.4.

The gutter section and the chute directing intercepted flow into the yellow flume were fabricated with galvanized sheets. As discussed previously, the geometric configuration of each curb inlet was dependent on the dimensions of the upstream, downstream transition sections and the inlet opening, and these resulted in the construction of six depressed and six undepressed curb inlets. Detailed drawings of the curb inlets are available in Appendix B.

The gutter sections were prepared by cutting and bending galvanized sheets into the required shapes and sizes and then roughened by sandpaper to achieve adhesion between the galvanized sheet and fiberglass resin. The surface roughness of the gutter was then prepared to be the same as the fiber cement boards.

Upon completion of all the model components, they were assembled in the flume. All the components were kept in place and glued together with silicone adhesive that was allowed to dry for at least 24 hours. The adhesive also prevented undesirable water leakages which would negatively impact the experimental data and results. The model was taken through several test runs to ensure that it was water-proof and that the flow on the roadway and through the inlet correctly reflected reality.

3.7 Tests Carried Out

3.7.1 Combination of curb inlets

The investigations of the discharge capacity of the Pretoria type curb inlets were conducted on six model inlets that are referred to as curb inlets A, B, C, D, E, and F, with each being geometrically unique. Each curb inlet model had a specific combination of upstream transition and inlet lengths that are presented in Table 3.4.

The main feature of the Pretoria type curb inlet is the downstream transition section which is kept constant at 1 m (L_m=0.4 m) and as such the downstream transition length was expected to have little to no influence on the performance of the inlet (Grobler, 1994). For this research, the downstream transition section was also kept at 0.4 m. The gutter cross-sectional slope was later adjusted to 29.4% to simulate flow in depressed curb inlets.

Table 3.4 Combinations of model curb inlet dimensions

Curb inlet	Upstream transition length (m)	Inlet length (m)	Downstream transition length (m)	Total curb opening length (m)
A	0.4	0.8	0.4	1.6
B	0.8	0.8	0.4	2
C	0.4	1.2	0.4	2
D	1.2	0.8	0.4	2.4
E	0.8	1.2	0.4	2.4
F	0.4	1.6	0.4	2.4

3.7.2 Test procedure

A total of 2880 test were conducted on undepressed and depressed curb inlets A, B, C, D, E and F. The tests were set up in four groups as shown below.

Group 1 –Undepressed curb inlets A, B, C, D, E and F on a cross-sectional slope of 2%.

Group 2 –Depressed curb inlets A, B, C, D, E and F on a cross-sectional slope of 2%.

Group 3 –Undepressed curb inlets A, B, C, D, E and F on a cross-sectional slope of 3%.

Group 4 –Depressed curb inlets A, B, C, D, E and F on a cross-sectional slope of 3%.

For each group of tests, the variables were: clog height, longitudinal slope and flow-rate. Various combinations of four clog heights and three longitudinal slopes, shown in Table 3.5, were tested on each curb inlet in each group. For every combination of conditions, the street flow was adjusted 10 times, from 2 l/s to 13 l/s.

Table 3.5 Combination of conditions tested on each curb inlet

	Combination of conditions
1.	Clog height = 0 mm, Longitudinal slope= 0.25%
2.	Clog height = 0 mm, Longitudinal slope = 0.5%
3.	Clog height = 0 mm, Longitudinal slope = 0.75%
4.	Clog height = 8 mm, Longitudinal slope = 0.25%
5.	Clog height = 8 mm, Longitudinal slope = 0.5%
6.	Clog height = 8 mm, Longitudinal slope = 0.75%
7.	Clog height = 18 mm, Longitudinal slope = 0.25%
8.	Clog height = 18 mm, Longitudinal slope = 0.5%
9.	Clog height = 18 mm, Longitudinal slope = 0.75%
10.	Clog height = 28 mm, Longitudinal slope = 0.25%
11.	Clog height = 28 mm, Longitudinal slope = 0.5%
12.	Clog height = 28 mm, Longitudinal slope = 0.75%

4 DISCUSSION OF TEST RESULTS

The results from the tests carried out address a wide variety of issues related to the hydraulic behavior of the Pretoria-type curb inlet. These include when the inlet opening is partially clogged and its interception capacities other than the 80% value investigated by Grobler (1994). The chapter concludes with the production of new design curves that offer greater flexibility on interception efficiencies when the inlet is on the grade of a roadway. The subject of inlet clogging, often overlooked in previous studies, is addressed in the current work.

4.1 Comparison between Experimental Results and Literature Based Results

4.1.1 Experimental Results vs. The Izzard Method vs. The HEC-22 Method

The HEC-22 (Equations 2.5, 2.6 and 2.7) and Izzard (Equations 2.12 and 2.13) methods, discussed in the literature review, are commonly used to design or predict the discharge capacity of curb inlets particularly in the USA. Following the extensive research conducted on these two methods, it was assumed that the HEC-22 and Izzard methods could be utilized to predict the discharge capacity, Q_{pi}, of the Pretoria type curb inlet. This assumption was evaluated by comparing the experimental discharge capacities with those predicted by the HEC-22 and Izzard methods.

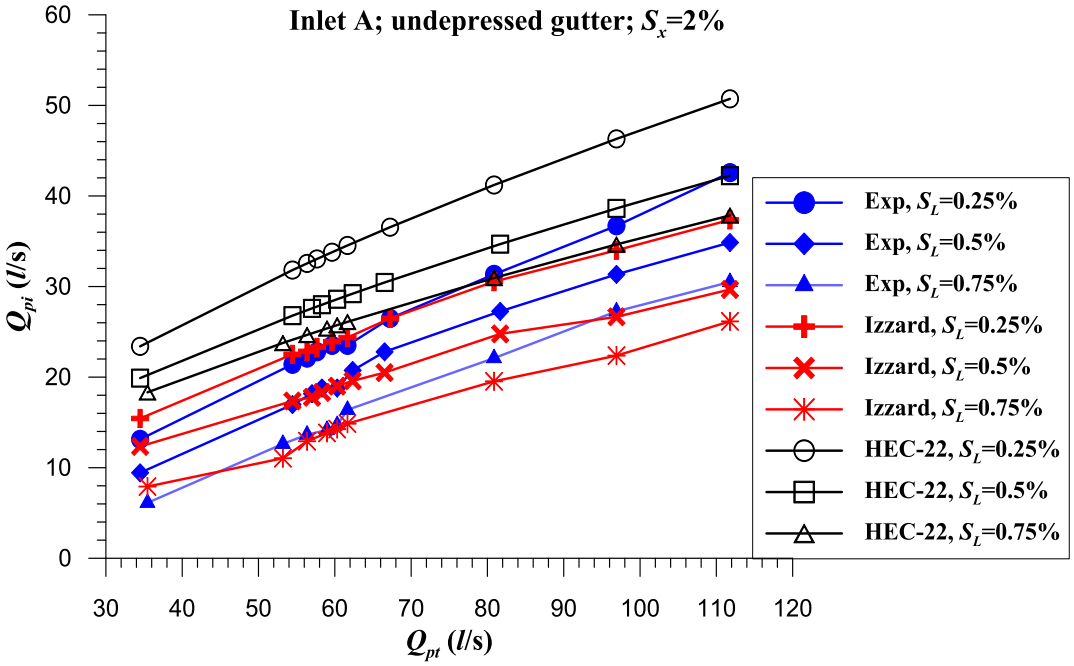


Figure 4.1 Q_{pi} *vs* Q_{pt} for undepressed curb inlet A on S_x= 2%

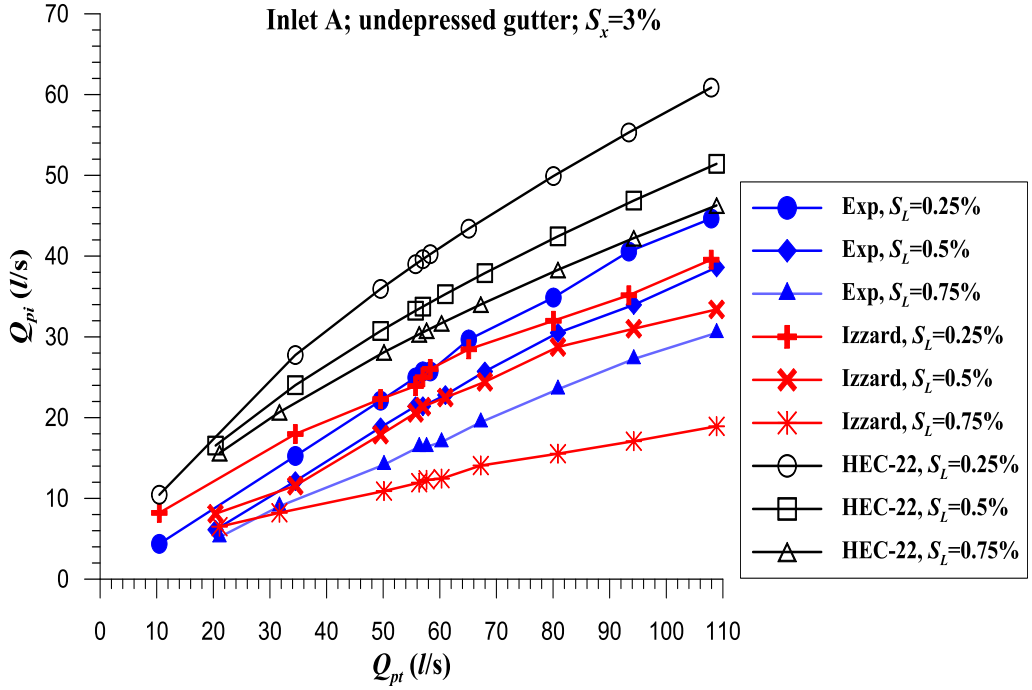


Figure 4.4.2 Q_{pi} *vs* Q_{pt} for undepressed curb inlet A on S_x= 3%

The observed and predicted intercepted flow Q_{pi} for undepressed curb inlet A with total street flow of Q_{pt} are presented in Figures 4.1 and 4.2 for cross-sectional slopes of 2% and 3%. The trend that the intercepted flow decreases with increased longitudinal slope is captured by the experimental data, and the Izzard and HEC-22

methods. There is also a slight increase in intercepted flow with an increase in the cross-sectional slope from 2% to 3%. Furthermore, most of the experimental data for S_L = 0.25%, 0.5% and 0.75% lie within the envelope that has an upper bound of the HEC-22 method with S_L = 0.75%, and a lower bound of the Izzard method with S_L = 0.75% (Figures 4.1 and 4.2). Essentially the HEC-22 method gives higher estimates of the intercepted flows than those of the experimental data, while the Izzard method better predicts the experimental data with only a low level of agreement for the case when S_x = 2%.

The differences in average inlet interception efficiency (= $Q_{pi}/Q_{pt}\times 100$) over the range of Q_{pt} between the observed (experimental) data and predicted intercepted flows are presented in Table 4.1, and they indicate that HEC-22 method overestimates the experimental data at a significantly higher level than the under prediction by the Izzard method.

Table 4.1 Difference between the observed and predicted average *E* (the negative values indicate underestimation while positive ones indicate overestimation)

Undepressed curb inlet A, S_x =2%		
S_L	**Observed-Izzard (%)**	**Observed-HEC-22 (%)**
0.25%	0.45	16.47
0.5%	-0.99	14.52
0.75%	-1.67	17.02
Undepressed curb inlet A, S_x=3%		
0.25%	2.64	26.75
0.5%	-0.78	23.12
0.75%	-6.46	25.85

The variations of the interception flow Q_{pi} and the total street flow Q_{pt} observed experimentally are compared with Izzard and HEC-22 predictive methods and presented in Figures 4.3 and 4.4 for the depressed gutter of curb inlet A with S_x = 2% and 3%, respectively.

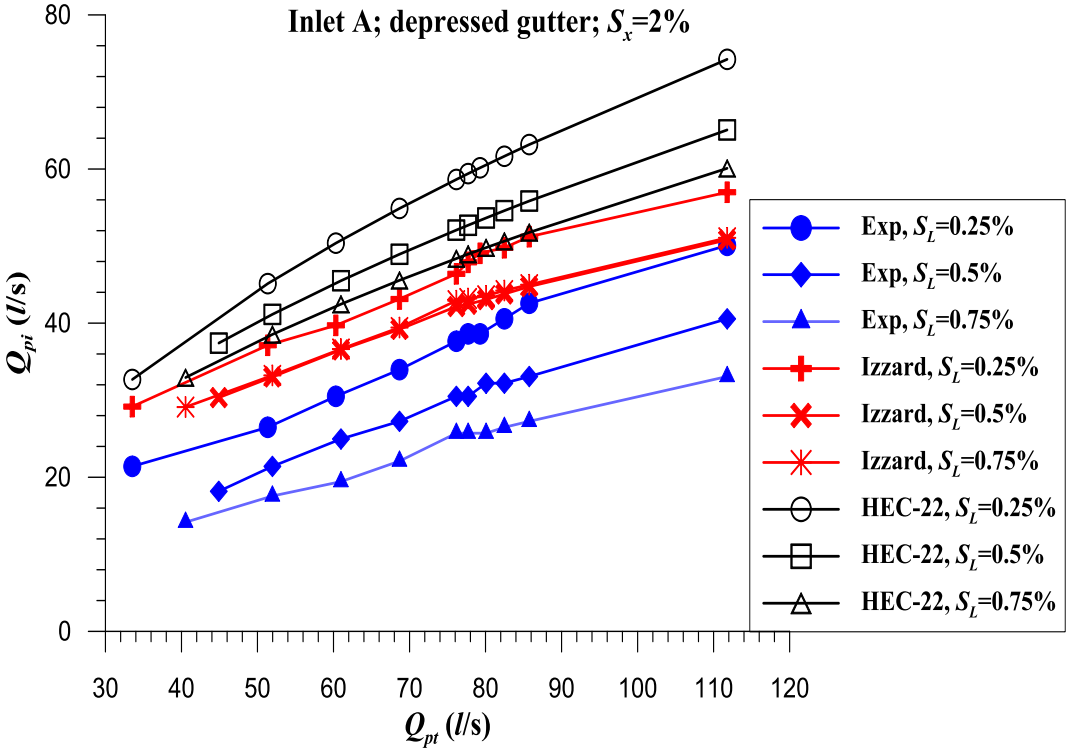


Figure 4.3 Q_{pi} *vs* Q_{pt} for depressed curb inlet A on S_x= 2%

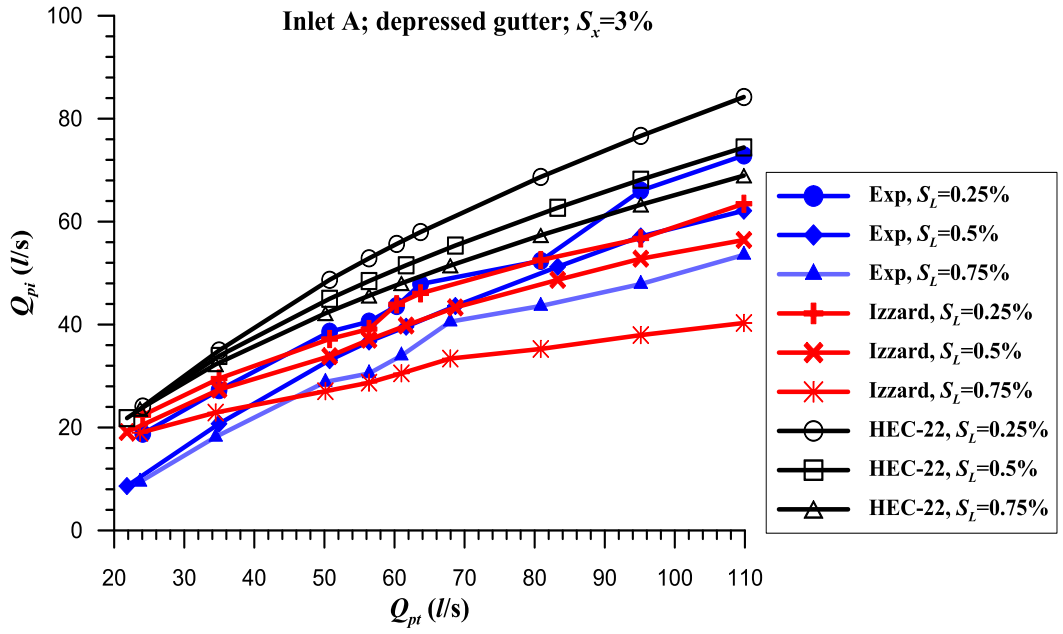


Figure 4.4 Q_{pi} *vs* Q_{pt} for depressed curb inlet A on S_x= 3%

In Figure 4.3, the HEC-22 and Izzard methods overestimate the observed intercepted flow Q_{pi} for S_x=2%. On S_x=3%, the HEC-22 method overestimates the

intercepted flows for the three longitudinal slopes, while the Izzard method underestimates the experimental intercepted flows. The differences in the average interception efficiencies between the experimental data and the Izzard and HEC-22 methods presented in Table 4.2 are high with the exception of depressed inlet A on S_x=3% when comparing the Izzard method to the experimental data.

Table 4.2 Difference between observed and predicted average *E* (the negative values indicate underestimation while positive ones indicate overestimation)

Depressed curb inlet A, S_x=2%		
S_L	**Experimental-Izzard (%)**	**Experimental-HEC-22 (%)**
0.25%	13.66	28.61
0.5%	16.68	30.54
0.75%	24.61	33.04
Depressed curb inlet A, S_x=3%		
0.25%	-0.48	18.14
0.5%	6.27	23.94
0.75%	-0.20	26.71

The differences in interception efficiencies between Izzard and HEC-22 methods and experimental data are plotted in Figures 4.5a and 4.5b for S_x=2% and S_x=3%, respectively for the inlet A in a depressed gutter. Most of the points are higher than 0%, indicating that both methods overestimate the interception flow. The few exceptions are points from the Izzard method which are below 0% and represent underestimation of the interception flows.

The observed differences between the predicted and observed data of depressed and undepressed curb inlet A are most likely due to the distinct differences in the type of curb inlets that underpin the Izzard and HEC-22 methods and the Pretoria type curb inlet. Unlike the Pretoria type curb inlet, the curb inlet models used in Izzard (1950) research and the HEC-22 (FHWA, 2009) are without transition sections and

offset from the curb. Thus, the differences observed nullified the need to assess the performance of the Izzard and HEC-22 methods on the other five curb inlet models.

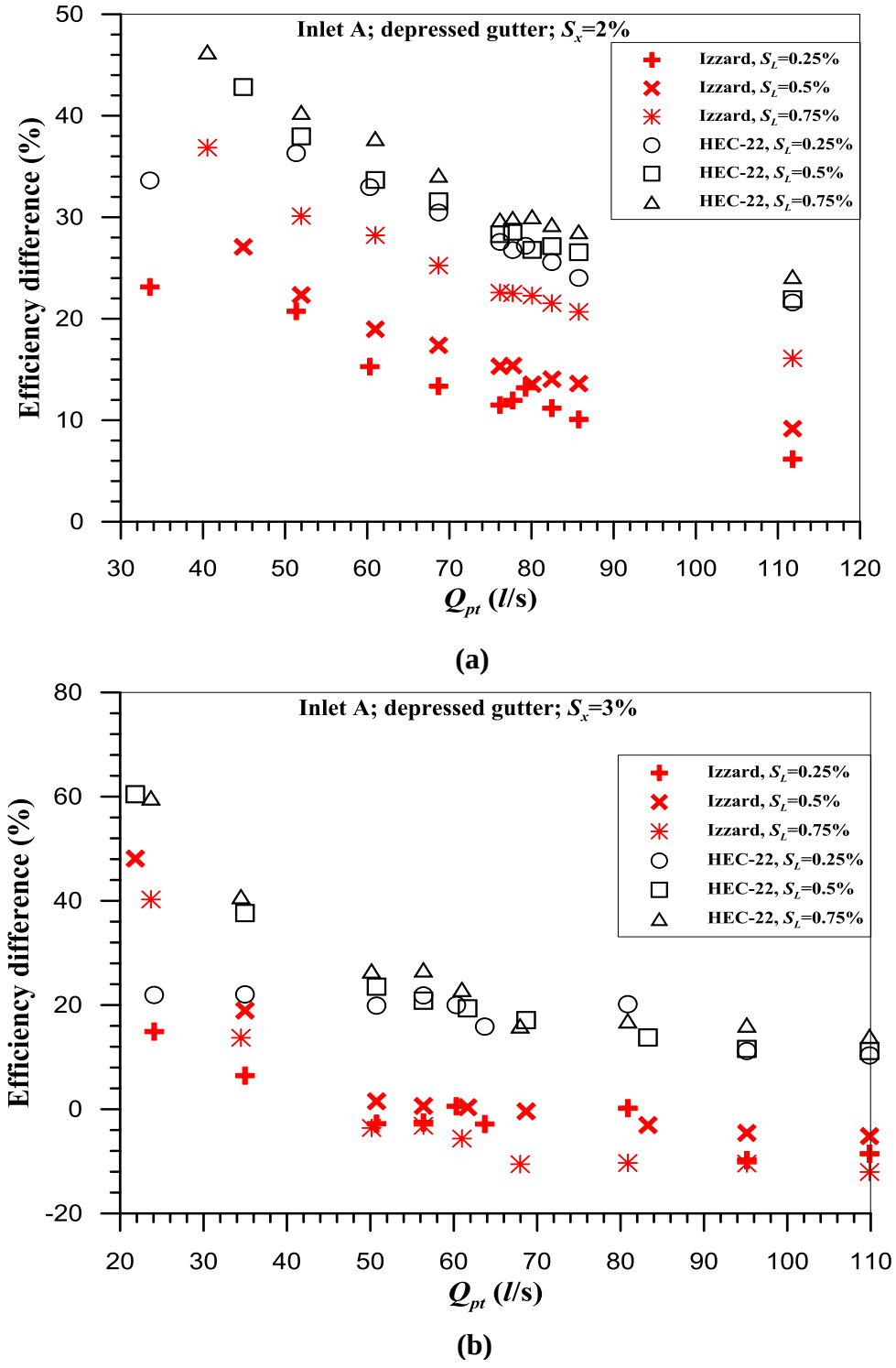


Figure 4.5 Differences in interception efficiency between the observed and Izzard and HEC-22 methods: (a) S_x=2% and (b) S_x=3% for depressed inlet A

4.1.2 Efficiency from The Grobler Method

The Pretoria type curb inlet, studied by Grobler (1994), is similar to the inlets studied in this research except for a few geometric differences noted in Table 4.3. In addition to the geometric differences, the testing conditions were significantly different. Due to the similarities in curb inlets, Grobler's method was expected to accurately predict the experimental results produced in this study, however, Grobler's tests were conducted in a manner that strictly allowed 80% of the streetflow to be intercepted. This was reflected in Grobler's design curves (see Figure 2.12). In this research, however, the efficiency of each curb inlet was not controlled, thus each curb inlet exhibited different efficiencies under varying conditions. Therefore, Grobler's curves could not be used in predicting the actual interception capacities.

Other limitations to the use of the Grobler's curves include, the differences in the gutter cross-sectional slopes, although quite small (1.6 p.p.) difference), impact the prediction capabilities of Grobler's curves. An additional limitation exhibited by Grobler's curves for this research, is the omission of undepressed curb inlets because, in its original design, the Pretoria type curb inlet is depressed.

Table 4.3 Differences between Grobler's Pretoria type curb inlet and the Pretoria type curb inlet studied in this research

Description of curb inlets	**Pretoria type curb inlet (for this research)**	**Pretoria type curb inlet (Grobler,1994)**
Gutter section cross-sectional slope	0%, 29.4	27.8%
Cross-sectional slope	2% and 3%	2%
Longitudinal Slope	0.25% - 0.75	4%
Upstream transition length	3 m – 6 m	1 m – 3 m
Inlet Length	1 m – 3 m	2 m – 4 m
Downstream transition length	1 m	1 m

4.2 Influence of Upstream Transition Section on Inlet Efficiency

The influence of the upstream transition section on the efficiency of the Pretoria type curb inlet was assessed by analyzing the average efficiencies of curb inlets A, B and D on both cross-sectional slopes of 2% and 3% and longitudinal slopes of 0.25%, 0.5% and 0.75%. Inlets A, B and D have inlet lengths of 2 m and upstream transition lengths of 1 m, 2 m and 3 m respectively. The average efficiencies of the three inlets are presented in Figure 4.6 (with undepressed gutter) and Figure 4.7 (with depressed gutter).

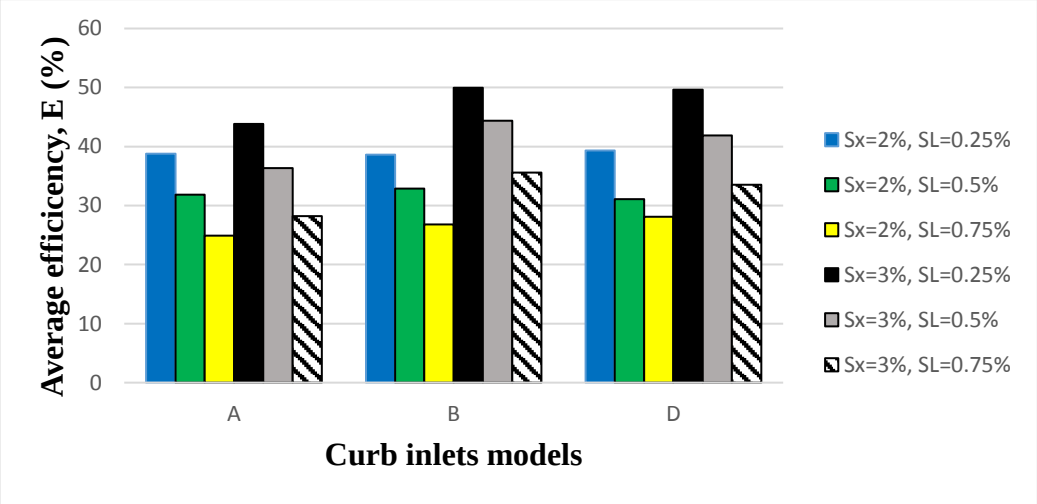


Figure 4.6 Assessment of upstream transition lengths with average efficiencies of undepressed inlets A, B and D without clog material

Inlets A, B and D have similar efficiencies on S_x=2%, thus indicating that adjusting the upstream transition section has minimal influence on the performance of undepressed inlets on S_x=2%. On S_x=3%, inlet B is the most efficient, followed by D and then A. On the three longitudinal slopes, B has approximately 7 p.p. higher interception efficiency than A which is 1 m shorter in transition length. Inlet D, which is 1 m longer in transition length than B, has a lower efficiency by 0.31 p.p., 2.48 p.p. and 2.07 p.p. on S_L=0.25%, S_L=0.5% and S_L=0.75% respectively.

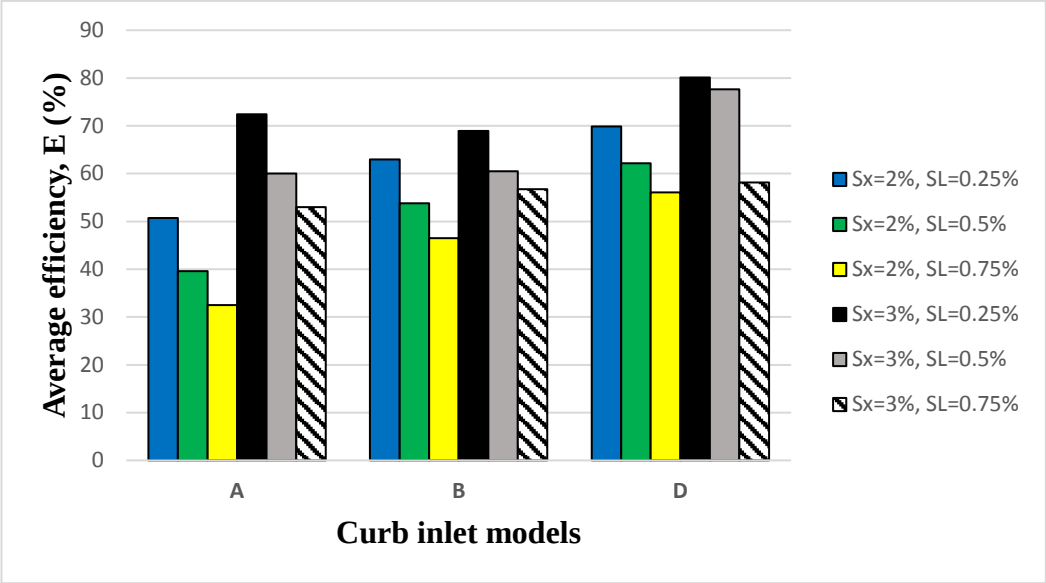


Figure 4.7 Assessment of upstream transition lengths with average efficiencies of depressed inlets A, B and D without clog material

Figure 4.7 shows an upward trend in efficiency as the upstream transition section increases from 1 m to 3 m on S_x=2% and S_x=3%, with the exception of inlet A on S_x=3% which gave an abnormally high interception when S_L=0.25%. This was due to difficulties in measuring the water depth in the flume as turbulence increased with increasing intercepted flow, thereby compromising the accuracy of the measurements. Discountenancing this anomalous result, inlet B had a higher efficiency of approximately 13.49 p.p. and 2.10 p.p. on S_x=2% and S_x=3%, respectively, compared to inlet A. Similarly, D had higher efficiency than A by approximately 21.76 p.p. and 10.17 p.p. on S_x=2% and S_x=3%, respectively, as a result of a 2 m increase in the upstream transition length.

The interception efficiency consistently improved with increased upstream transition length as the cross-sectional slope increased from 2% to 3%. This is due to a combination of three factors which include the diversion of flow transversely due to increased cross-sectional slope, the increased supercritical flow regime around the inlet opening due to the increased upstream transition length, and the damming effect by the downstream transition section as shown in Figure 4.8 (Li, 1956). These two factors have given rise to the concept of the effective inlet length by Grobler (1994).

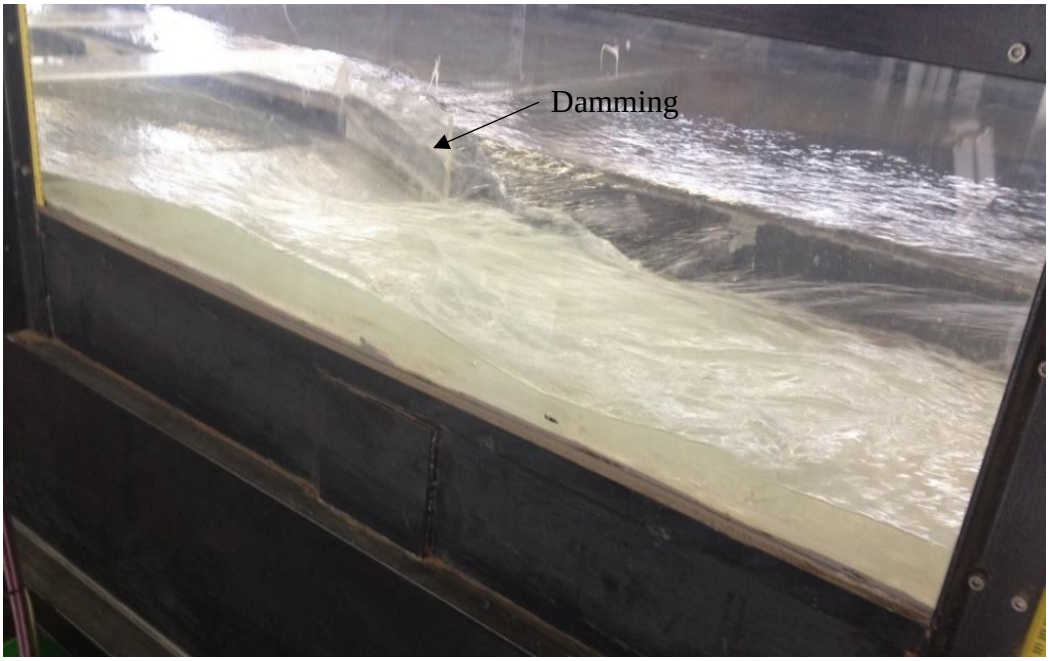


Figure 4.8 Photo of curb inlet showing damming effect from downstream transition section

In Figures 4.6 and 4.7, the average efficiency of each inlet improved as the cross-sectional slope increased and as the longitudinal slope decreased. Tables 4.4 and 4.5 respectively show the influence of the longitudinal slope on the interception efficiency for S_x=2% and S_x=3%, and the influence of the cross-sectional slope on the Pretoria type curb inlets.

Increasing the longitudinal slope by 0.25% and 0.5% reduced the performance of inlets A, B and D on S_x =2% and S_x =3% because, during testing, as the longitudinal slope was increased, the spread of water and the water depth reduced resulting in low interception capacity. Also, it was observed that at steeper longitudinal slopes, more water flowed past the inlet thus reducing the curb inlet's interception capacity. The observation made is in agreement with literature studies such as the HEC-22 (FHWA, 2009) which states that an increase in longitudinal slope leads to an increase in velocity, causing a reduction of water spread and water depth.

Table 4.4 The influence of the longitudinal slope on average interception efficiencies of inlets A, B and D on S_x=2% and S_x=3%

Inlet		S_x (%)	Decrease in efficiency when S_L increases by 0.25% (p. p.)	Decrease in efficiency when S_L increases by 0.5% (p.p.)
Undepressed	Inlet A	2	7	14
		3	8	16
	Inlet B	2	6	12
		3	7	14
	Inlet D	2	6	11
		3	8	16
Depressed	Inlet A	2	11	18
		3	12	19
	Inlet B	2	9	16
		3	8	12
	Inlet D	2	8	14
		3	3	22

Table 4.5 Influence of cross-sectional slope on undepressed and depressed curb inlets when the cross-sectional slope is increased by 1%

	S_L (%)	Increase in inlet A efficiency (p.p.)	Increase in inlet B efficiency (p. p.)	Increase in inlet D efficiency (p.p.)
Undepressed	0.25	5.07	11.31	10.30
	0.5	4.53	11.5	10.80
	0.75	3.29	8.79	5.44
Depressed	0.25	21.71	6	10.27
	0.5	20.45	6.66	15.48
	0.75	20.47	10.24	2.11

The results in Table 4.5, show that increasing the cross-sectional slope improves a curb inlet's efficiency. Test data and observations demonstrated that at a steeper cross-sectional slope (S_x=3%), the water depth increased and the spread of water reduced. The increase in water depth at the curb, allowed more water to be captured, thus improving its interception capacity and efficiency (Jens, 1979). Furthermore, the poor performance of the curb inlets at S_x=2% may also be attributed to higher friction caused by a large spread of water over the road (Zwamborn 1966). However, according to Zwamborn (1966), frictional effects are greater on small-scale models compared to large-scale models.

4.3 Influence of Inlet Opening on Inlet Efficiency

The influence of the inlet opening length on the performance of a curb inlet was assessed by comparing the average efficiencies of curb inlets A, C and F on S_L=0.25%, 0.5% and 0.75%, and S_x=2% and S_x=3% for undepressed gutter (Figure 4.9) and depressed gutter (Figure 4.10). Inlets A, C and F have the same upstream transition lengths and opening lengths of 2 m, 3 m and 4 m respectively.

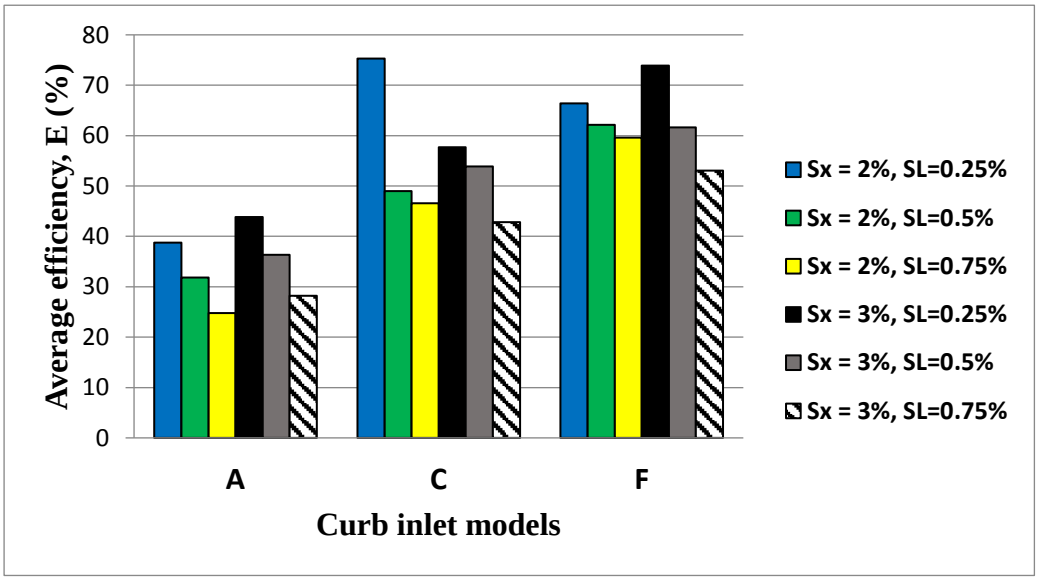


Figure 4.9 Influence of inlet opening on average interception efficiencies of undepressed inlets A, C and F without clog material

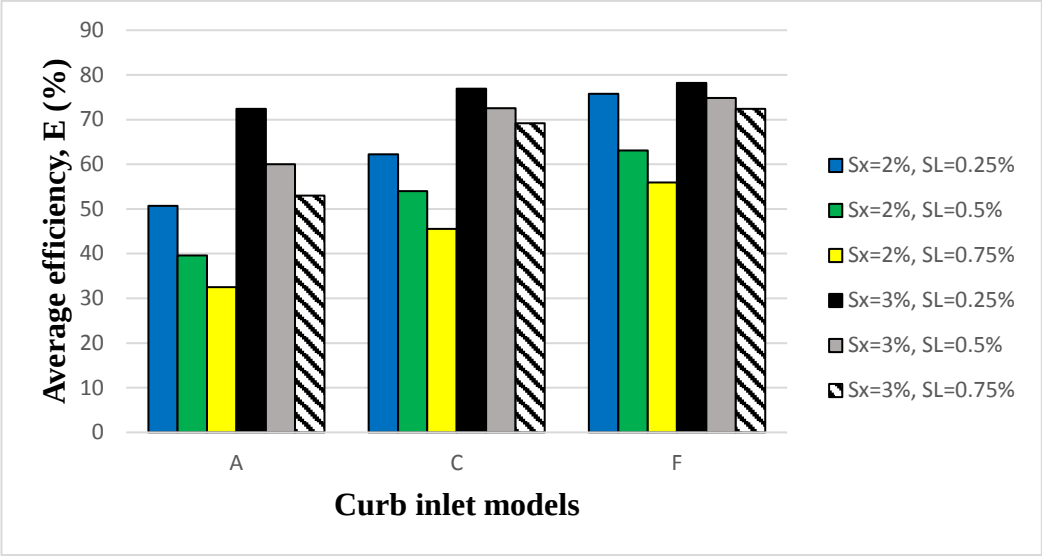


Figure 4.10 Influence of inlet opening on average interception efficiencies of depressed inlets A, C and F without without clog material

In Figures 4.9 and 4.10, inlet A has the lowest efficiency and inlet F has the highest efficiency, thus indicating that there is improved inlet efficiency with increased inlet opening length. The observed results are consistent with studies done by Izzard (1950), Izzard (1977) and Muhammed (2019) that indicate that the flow depth decreases along the inlet opening. This suggests that increasing the inlet length improves the inlet's interception capacity to a maximum of 100% interception. At 100% interception, the inlet length would be excessively long such that the downstream transition and a segment of the inlet opening would cease to contribute to inlet interception (Izzard, 1977).

Some anomalies with inlets C and F were observed for the undepressed gutter, namely (Figure 4.9):

- On S_x=2% and S_L=0.25%, inlet C had the highest efficiency of the three inlets. This anomaly resulted from a malfunctioned measuring instrument used to measure the water level upstream of the tail-box V-notch weir (Figure 3.6).
- On S_L=0.75%, inlet C had a lower efficiency on S_x=3% than on S_x=2%, and similarly for F.

Discountenancing the above mentioned anomalies, increasing the opening length of depressed inlet A by 1 m (inlet C) improved its efficiency by 13 p.p. and 11 p.p. on S_x=2% and S_x=3%, respectively, while the efficiency of undepressed inlet A improved by approximately 19 p.p. and 15 p.p. on S_x=2% and S_x=3%, respectively. Increasing the opening length of depressed inlet A by 2 m (inlet F) improved its efficiency by approximately 24 p.p. and 13 p.p. on S_x=2% and S_x=3%, respectively while the efficiency of undepressed curb inlet A is increased by approximately 31 p.p. and 27 p.p. on S_x=2% and S_x=3%, respectively.

4.4 Influence of Depressed Gutter on Inlet Efficiency

The average interception efficiencies are presented for the six configurations (inlets A, B, C, D, E, and F) of the Pretoria type curb inlet in Figure 4.11 for the cross-sectional slope of 2% and Figure 4.12 for the cross-sectional slope of 3%. The plots provide the means to assess the influence of the gutter depression on the inlet efficiency.

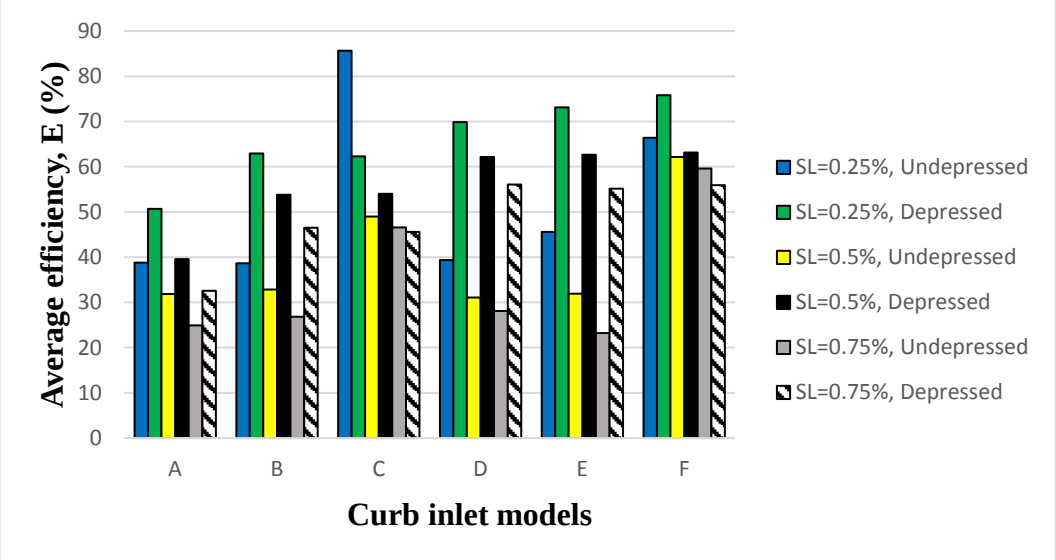


Figure 4.11 Influence of depressed gutter on average efficiencies of inlets A, B, C, D, E and F on S_x=2% without clog material

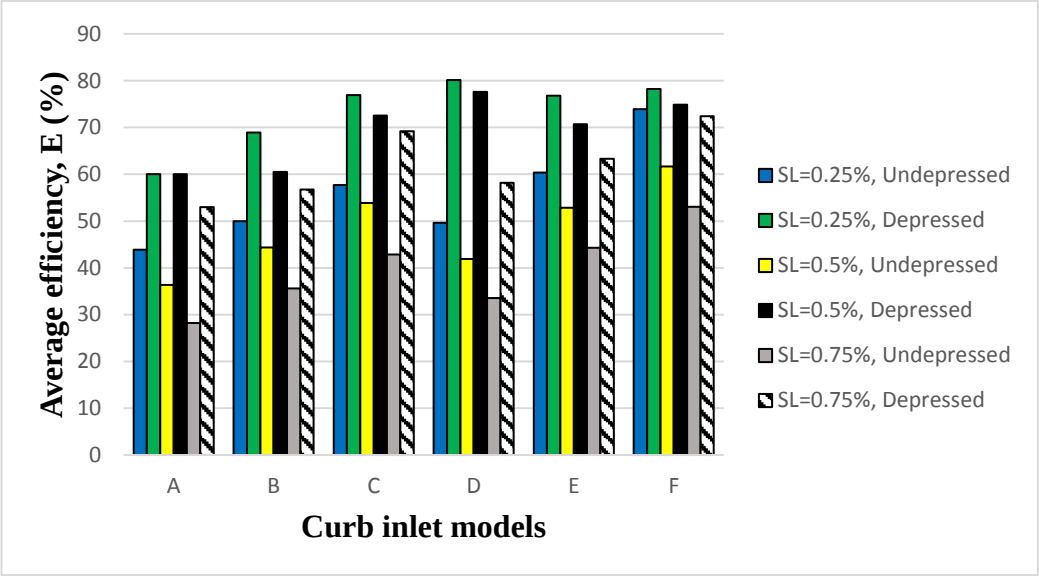


Figure 4.12 Influence of depressed gutter on average efficiencies of inlets A, B, C, D, E and F on S_x=3% without clog material

Figures 4.11 and 4.12 demonstrate that by increasing the gutter cross-sectional slope the average efficiency of a curb inlet is significantly improved. This is because the presence of depressed gutters provides greater water conveyance capacity into the inlet, thus improving the inlet's interception capacity (Hodgens, 2018). Zwamborn's research also concluded that, to some extent, the interception capacity improved when the gutter cross-sectional slope increased (Zwamborn, 1966). For a cross-sectional slope of 2.5%, Zwamborn discovered that increasing the gutter cross-sectional slope from 20% to 30% had negligible effects on the inlet interception capacity, and therefore suggested an optimum gutter cross-sectional slope of 20% (Zwamborn, 1966). This means that a lower gutter cross-sectional slope of 20% should be favored over a slope of 29.4%, as a lower gutter slope is easier and cheaper to construct. It should be noted, however, that Zwamborn's curb inlets did not have transition sections.

Although the overall trend is increased interception with the provision of the depressed gutter, there are a few anomalies to this trend with inlets C and F for S_x=2% (Figure 4.11) as indicated below:

- On S_L=0.25%, undepressed inlet C had a greater efficiency than depressed inlet C.

- On S_L=0.75%, undepressed inlet C had greater efficiency than depressed inlet C by 1%.
- On S_L=0.75%, undepressed inlet F had greater efficiency than depressed inlet F by 3.67%.

Tables 4.4 and 4.5 show the increment in average efficiency of a Pretoria type curb inlet as a result of having a depressed gutter. According to the results presented in Table 4.6, inlets D and E show the greatest improvement in efficiency while inlet F is the least influenced by the depression of a gutter. On S_x=3%, in Table 4.7, inlet D is the most influenced by gutter depression and inlet F is the least influenced. The influence of a depressed gutter on inlets D and F is likely due to their contrasting geometric properties. Inlet D has the longest upstream transition section of 3 m and the shortest opening length of 1 m while inlet F has the longest inlet opening length of 4 m and the shortest upstream transition section of 1 m. This indicates that a depressed curb inlet has optimal performance when it has a long upstream transition section in comparison to its opening length.

Table 4.6 Increment of efficiency of inlets A, B, D, C, E and F when the gutter is depressed on S_x=2%

S_x=2%						
	Inlet A	**Inlet B**	**Inlet C**	**Inlet D**	**Inlet E**	**Inlet F**
S_L=0.25%	11.91	24.31	-23.38	30.53	25.51	9.37
S_L=0.5%	7.75	20.96	5.02	31.06	30.70	0.99
S_L=0.75%	7.62	19.68	-1.01	27.98	31.96	-3.67
Average	9.09	21.65	-6.46	29.86	30.05	2.23

Table 4.7 Increment of efficiency of inlets A, B, D, C, E and F when the gutter is depressed on S_x=3%

S_x=3%						
	Inlet A	**Inlet B**	**Inlet C**	**Inlet D**	**Inlet E**	**Inlet F**
S_L=0.25%	16.17	18.96	19.19	30.50	16.42	4.29
S_L=0.5%	23.66	16.13	18.65	35.73	17.88	13.19

S_L=0.75%	24.80	21.13	26.37	24.65	19.03	19.38
Average	21.54	18.74	21.40	30.29	17.78	12.28

4.5 Influence of Clogging on Inlet Efficiency

The assessment of the performance of a clogged curb inlet was achieved by placing a green sack filled with stones (see Figure 3.4) at the mouth of the inlet. Three different sacks with heights equal to 14.3%, 32.1% and 50% of the curb height were used. The average interception efficiencies for inlets A, B and D are presented in Figures 4.13 ,4.14, 4.15 and 4.16 for S_x=2% and S_x=3%.

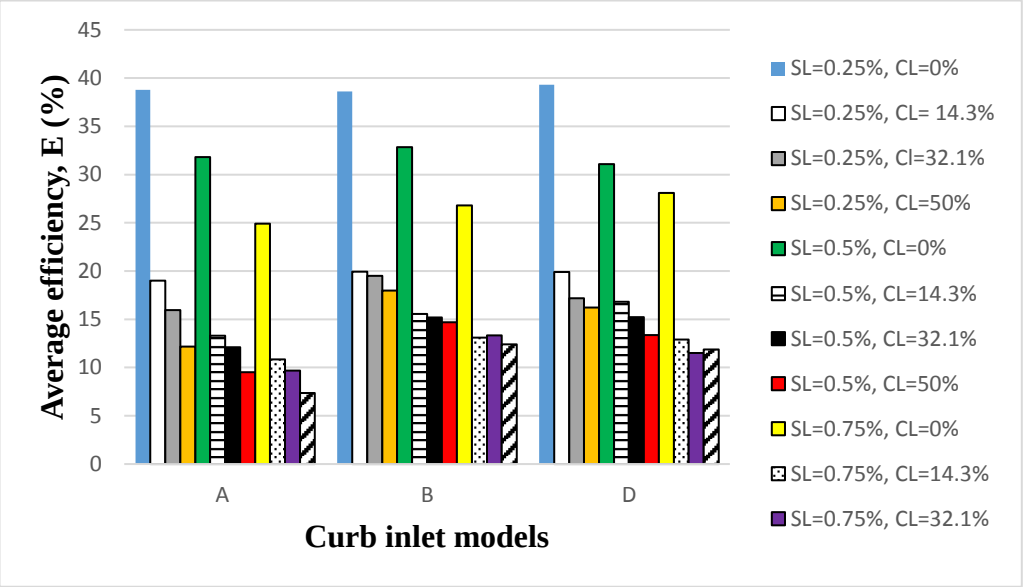


Figure 4.13 Influence of clogging on average efficiencies of undepressed inlets A, B and D on S_x=2%

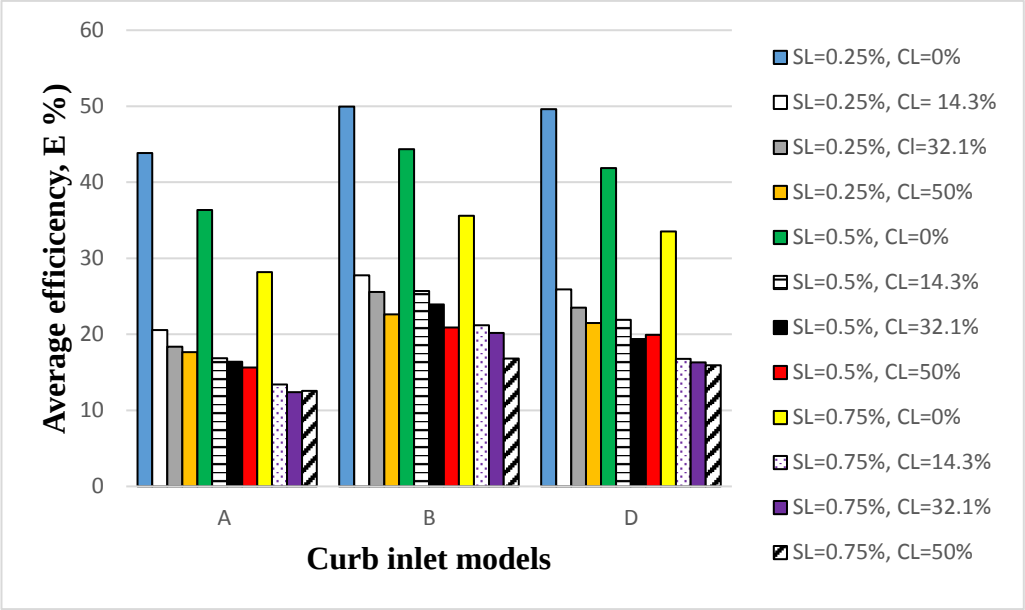


Figure 4.14 Influence of clogging on average efficiencies of undepressed inlets A, B and D on S_x=3%

Figures 4.13 and 4.14 show that the efficiencies of unclogged inlets A, B and D are much higher than those of clogged inlets.

- With C_L= 14.3% on S_x=2%, inlets A, B and D efficiencies are reduced by 19.30 p.p., 16.69 p.p. and 14.32 p.p. when S_L=0.25%, S_L =0.5% and S_L =0.75% respectively.
- With C_L=14.3% on S_x=3%, inlets A, B and D efficiencies are reduced on S_L =0.25%, S_L=0.5% and S_L =0.75% by 23.07 p.p., 19.38 p.p. and 15.32 p.p. respectively.

Additionally, it can be seen in Figures 4.13 and 4.14 that increasing the clog height from 14.3% to 50% had a marginal influence on the efficiency of inlets A, B and D (less than 4 p.p.) in comparison to the difference in efficiency between no clogging, C_L=0%, and C_L=14.3%.

During the experimental investigations, it was observed that the presence of clog material caused backup of water onto the road (Figure 4.15) and this is known as the backwater effect. This reduces a curb inlet's discharge capacity and increases the spread of water on a road, thus causing a street to flood (Hammonds and Holley, 1995).

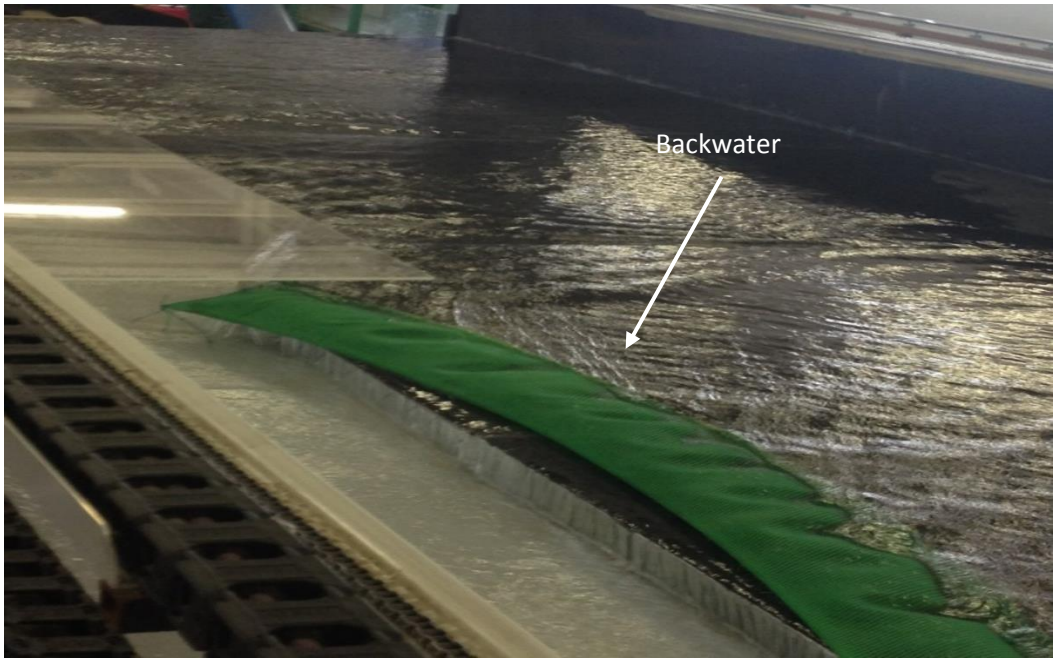


Figure 4.15 Photo of street flow when a curb inlet is clogged

The average interception efficiencies for inlets A, B and D with depressed gutters are presented in Figures 4.16 and 4.17 on S_x=2% and S_x=3%, respectively.

It was observed that with a depressed gutter, the increased flow velocity around the mouth of the inlet due to the depressed gutter caused the clog material to be carried along downstream with the intercepted flow. In practice, the clog material would eventually cause a blockage of stormwater conduits, thereby causing the catch basin to flood and in turn flooding the street.

It was later decided to anchor the sacks in place with 2 bricks, each brick on one end of the curb inlet (within the catch basin), to assess the influence of clogging a depressed curb inlet. The results are presented in Figures 4.16 and 4.17. With C_L=14.3%, the efficiencies for inlets A, B and D were reduced by 4.63 p.p., 3.82 p.p. and 9.13 p.p., respectively on S_x=2%, and 6.49 p.p., 2.62 p.p. and 6.73 p.p., respectively on S_x=3%. Both Figures 4.16 and 4.17 show a number of unexpected results particularly at C_L= 32.1% for which the interception efficiencies are higher than at C_L=14.3%.

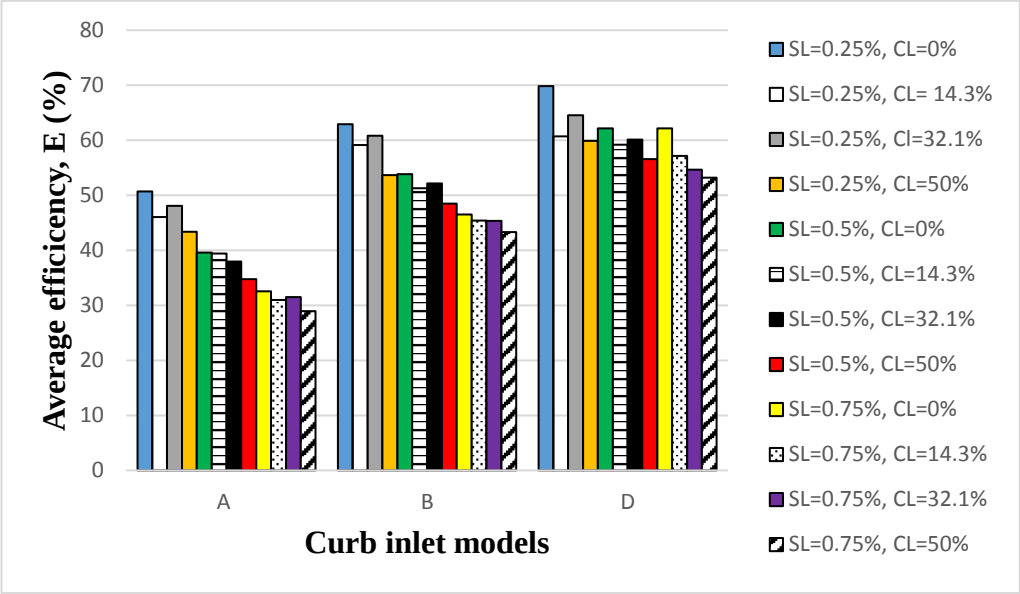


Figure 4.16 Influence of clogging on average efficiencies of depressed inlets A, B and D on S_x=2%

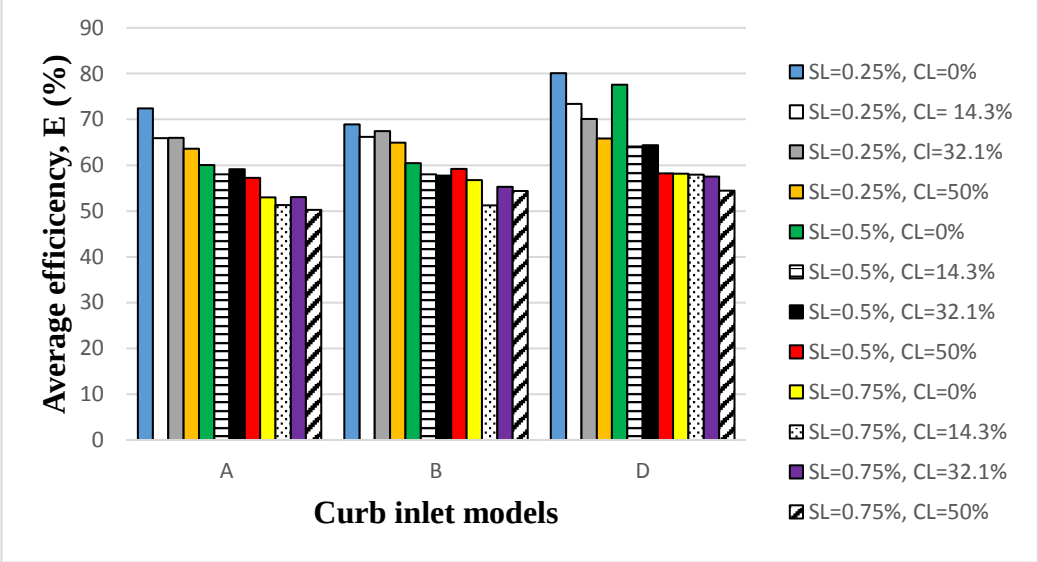


Figure 4.17 Influence of clogging on average efficiencies of depressed inlets A, B and D on S_x=3%

The average reduction in efficiency of each curb inlet presented in Table 4.8 can be used as indicative values in design when the impact of clogging is taken into consideration. It should however be noted that these values are limited to the three longitudinal and two cross-sectional slopes used in the experimental investigations. The average reduction of efficiency of each curb inlet presented in Figure 4.16 and

4.17 should not be used as indicative values in design when the impact of clogging on depressed curb inlets is taken into consideration as the clogging material would be washed into the catch basin.

Table 4.8 The average reduction in efficiency of undepressed curb inlets A, B and D with C_L=14.3%, C_L=32.1% and C_L=50%

	S_x=2%			**S_x=3%**		
	Curb inlet A (p.p.)	**Curb inlet B (p. p.)**	**Curb inlet D (p.p.)**	**Curb inlet A (p.p.)**	**Curb inlet B (p.p.)**	**Curb inlet D (p.p.)**
S_L =0.25%, C_L= 14.3%	19.78	18.71	19.42	23.31	22.18	23.71
S_L =0.25%, C_L=32.1%	22.84	19.12	22.14	25.46	24.35	26.13
S_L =0.25%, C_L=50%	26.59	20.67	23.10	26.20	27.32	28.15
S_L =0.5%, C_L= 14.3%	18.52	17.31	14.24	19.50	18.67	19.95
S_L =0.5%, C_L= 32.1%	19.71	17.67	15.85	19.94	20.41	22.50
S_L =0.5%, C_L = 50%	22.32	18.16	17.69	20.71	23.45	21.93
S_L =0.75%, C_L =14.3%	14.04	13.71	15.20	14.79	14.41	16.76
S_L =0.75%, C_L = 32.1%	15.21	13.47	16.57	15.81	15.43	17.21
S_L =0.75%, C_L = 50%	17.54	14.42	16.23	15.62	18.78	17.61

The intercepted flow of a clogged curb inlet ($Q_{i\,(e)}$) is presented as:

$$Q_{i_{(e)}} = (1 - C_o)Q_i \quad \text{(Guo, 2006)} \qquad 4.1$$

Where Q_i is the intercepted flow without clogging. During testing, the total flow rate could not be accurately set by the digital flowmeter due to technical difficulties that could not be fixed during testing, therefore the total street flow was measured using the 90^o V-notch (Figure 3.6). This caused the total flow rates for each set of experiments to vary inconsistently, hence the analysis of results in this chapter was presented as efficiencies. As a result, Equation 4.1 cannot be used to compute the single unit clogging factor. Gomez at al. (2013) suggest that the clogging factor should be presented in terms of efficiency instead and expressed as:

$$E_{(e)} = (1 - C_o)E \quad \text{(Gómez et al., 2013)} \qquad 4.2$$

Where E_e is the efficiency of a clogged inlet and E is the efficiency of an unclogged inlet. Using Equation 4.2, the actual single unit coefficient was computed from experimental results and presented in Table 4.7.

Designing a curb inlet susceptible to clogging will require determining the effective unclogged length using the single unit clogging factor and Equation 2.3. For example, curb inlet A at S_x=2%, S_L =0.25% with C_L= 14.3% has a full-scale inlet length of 2 m and an effective unclogged length of 0.98 m. This seems to contradict the model set-up as the total inlet length was clogged. This is because the clog material was porous and water seeped through it. If the clog material or debris were an impervious solid block, 0.98 m of the inlet opening would be blocked and only 1.02 m would be intercepting flow.

Given the observations made on depressed curb inlets that clog materials were washed into the inlet because of the high flow velocity, the single unit clogging factor for depressed inlets is expected to be approximately 1.

Table 4.9 Single unit clogging factors for each inlet under varying conditions

	S_x=2%			S_x=3%		
	Inlet A	**Inlet B**	**Inlet D**	**Inlet A**	**Inlet B**	**Inlet D**
S_L =0.25%, C_L= 14.3%	0.510	0.483	0.494	0.531	0.444	0.475
S_L =0.25%, C_L=32.1%	0.589	0.493	0.562	0.580	0.487	0.527
S_L =0.25%, C_L=50%	0.689	0.534	0.587	0.600	0.547	0.566
S_L =0.5%, C_L= 14.3%	0.583	0.527	0.458	0.532	0.421	0.474
S_L =0.5%, C_L= 32.1%	0.619	0.537	0.510	0.544	0.461	0.535
S_L =0.5%, C_L = 50%	0.701	0.551	0.569	0.564	0.529	0.522
S_L =0.75%, C_L =14.3%	0.565	0.509	0.540	0.523	0.404	0.500
S_L =0.75%, C_L = 32.1%	0.607	0.498	0.589	0.558	0.432	0.513
S_L =0.75%, C_L = 50%	0.701	0.539	0.577	0.551	0.526	0.525

4.5 Design Curves

Design curves were derived from the experimental data for the six models of curb inlets with a depressed gutter which is a common feature of the Pretoria type inlet. They are derived using multiple linear regression analysis on the experimental data, and the design curves are presented in terms of the efficiency versus the ratio of depth of water upstream of the curb to the actual length of the inlet. The derived

empirical equations are obtained for the cross-sectional slopes of 2% and 3% on various longitudinal slopes.

4.5.1 Derivation of Design Curves

For each cross-sectional slope of the roadway, the efficiency, *E*, is expressed in terms of three dimensionless quantities as:

$$\mathrm{E} = f(Fr, \frac{d}{L}, S_L) \qquad 4.3$$

Where

Fr is the Froude number of the triangular prism of flow upstream of the inlet ($F_r = v\sqrt{2}/\sqrt{gd}$),

L is the length of the opening of the inlet, and

d is the water depth at the curb upstream of the inlet.

The functional relationship employed is given by

$$E = A \cdot Fr^{\alpha} \cdot d/L^{\beta} \cdot {S_L}^{\gamma} \qquad 4.4$$

Equation 4.5 is linearized using logarithms to

$$\log E = \log A + \alpha \log Fr + \beta \log d/L + \gamma \log SL \qquad 4.5$$

Using multiple regression, the parameters A, α, β and γ are obtained. The range of values for the experimental data for Fr, d/L and S_L are specified for each of the empirical equations so that it is understood that their reliability diminishes farther from these ranges. In order to present these equations as design curves of E versus d/L, the average value of the Froude number is used in the equations. The empirical equations are presented in Table 4.7. It was decided to only present empirical equations for depressed curb inlets as the original design of the Pretoria type curb inlet is depressed.

Table 4.10 Empirical equations for depressed curb inlets on S_x=2% and S_x=3%

Inlet	S_x = 2%	S_x = 3%
Curb inlet A	$E\% = 52.1Fr^{-0.191}\left(\frac{d}{L}\right)^{-0.452} S_L^{-0.388}$ $0.9 < Fr < 1.8,\ \ Fr_{average} = 1.3,$ $2.2\% < \frac{d}{L} < 4.3\%,\ \ 0.25\% \le S_L \le 0.75\%$	$E\% = 53.6Fr^{-0.077}\left(\frac{d}{L}\right)^{0.032} S_L^{-0.197}$ $1.0 < Fr < 6.7,\ \ Fr_{average} = 2.8,$ $1.2\% < \frac{d}{L} < 4.9\%,\ \ 0.25\% \le S_L \le 0.75\%$
Curb inlet B	$E\% = 42.0Fr^{0.152}\left(\frac{d}{L}\right)^{-0.063} S_L^{-0.353}$ $0.8 < Fr < 2.0,\ \ Fr_{average} = 1.3,$ $2.2\% < \frac{d}{L} < 4.5\%,\ \ 0.25\% \le S_L \le 0.75\%$	$E\% = 29.2Fr^{0.121}\left(\frac{d}{L}\right)^{0.587} S_L^{-0.060}$ $1.0 < Fr < 12.0,\ \ Fr_{average} = 2.7,$ $0.9\% < \frac{d}{L} < 4.9\%,\ \ 0.25\% \le S_L \le 0.75\%$
Curb inlet C	$E\% = 81.6Fr^{-0.580}\left(\frac{d}{L}\right)^{-0.515} S_L^{-0.124}$ $0.9 < Fr < 1.6,\ \ Fr_{average} = 1.3,$ $1.6\% < \frac{d}{L} < 2.9\%,\ \ 0.25\% \le S_L \le 0.75\%$	$E\% = 91.7Fr^{-0.183}\left(\frac{d}{L}\right)^{-0.077} S_L^{0.066}$ $1.0 < Fr < 8.0,\ \ Fr_{average} = 2.9,$ $0.7\% < \frac{d}{L} < 3.0\%,\ \ 0.25\% \le S_L \le 0.75\%$
Curb inlet D	$E\% = 112.2Fr^{-0.332}\left(\frac{d}{L}\right)^{-0.540} S_L^{-0.140}$ $0.9 < Fr < 2.3,\ \ Fr_{average} = 1.3,$ $2.0\% < \frac{d}{L} < 4.2\%,\ \ 0.25\% \le S_L \le 0.75\%$	$E\% = 41.4Fr^{0.112}\left(\frac{d}{L}\right)^{0.259} S_L^{-0.167}$ $0.9 < Fr < 3.4,\ \ Fr_{average} = 1.9,$ $2.0\% < \frac{d}{L} < 4.8\%,\ \ 0.25\% \le S_L \le 0.75\%$
Curb inlet E	$E\% = 41F_r^{0.012}\frac{d}{L}^{-0.309} S_L^{-0.314}$ $0.9 < F_r < 2.4,\ \ F_{r\,average} = 1.4$ $1.3\% < \frac{d}{L} < 2.9\%,\ 0.25\% \le S_L \le 0.75\%$	$E\% = 41.0Fr^{0.125}\left(\frac{d}{L}\right)^{0.525} S_L^{-0.064}$ $0.9 < Fr < 8.1,\ \ Fr_{average} = 2.7,$ $0.8\% < \frac{d}{L} < 3.3\%,\ \ 0.25\% \le S_L \le 0.75\%$

Curb inlet F	$E\% = 3.7Fr^{2.168}\left(\frac{d}{L}\right)^{1.336} S_L^{-1.746}$ $0.9 < Fr < 2.2, \quad Fr_{average} = 1.4,$ $1.1\% < \frac{d}{L} < 2.2\%, \quad 0.25\% \le S_L \le 0.75\%$	$E\% = 72.8Fr^{-0.019}\left(\frac{d}{L}\right)^{0.158} S_L^{0.010}$ $1.1 < Fr < 7.4, \quad Fr_{average} = 2.9,$ $0.6\% < \frac{d}{L} < 2.4\%, \quad 0.25\% \le S_L \le 0.75\%$

4.5.2 Froude Number Sensitivity Analysis

The average Froude number for each empirical equation presented in Table 4.10 was computed from the experimental results. The average Froude number is expected to be applied when using the empirical equations. However, it is important to assess how variations about the average Froude number influence the inlet's efficiency for varying longitudinal slopes and *d/L*, hence the assessment of the sensitivity of the equations to the Froude number.

The exponent on the Froude number in each empirical equation provides a good indicator of its sensitivity to the Froude number. On the cross-section slope S_x=2%, the empirical equation for curb inlet E is least sensitive to changes to the Froude number while the empirical equation for curb inlet F is the most sensitive. On S_x=3%, curb inlet F is the least sensitive to changes to the Froude number and curb inlet C empirical equation exhibits the highest sensitivity (Table 4.10). It is worth noting that Inlet F which is most sensitive to the Froude number with S_x=2% is least sensitive at the higher cross-sectional slope of 3%.

4.5.3 Predicted vs. observed efficiency for inlets on SL=0.25% from the empirical equations

The predicted efficiencies were calculated from the empirical equations presented in Table 4.10 and compared to the actual (experimental) efficiencies and presented in Figures 4.18, 4.19, 4.20 and 4.21.The figures presented show the best and worst-performing empirical equations. The performance of the remaining empirical equations and the corresponding R^2 are presented in Appendix D and Appendix C respectively.

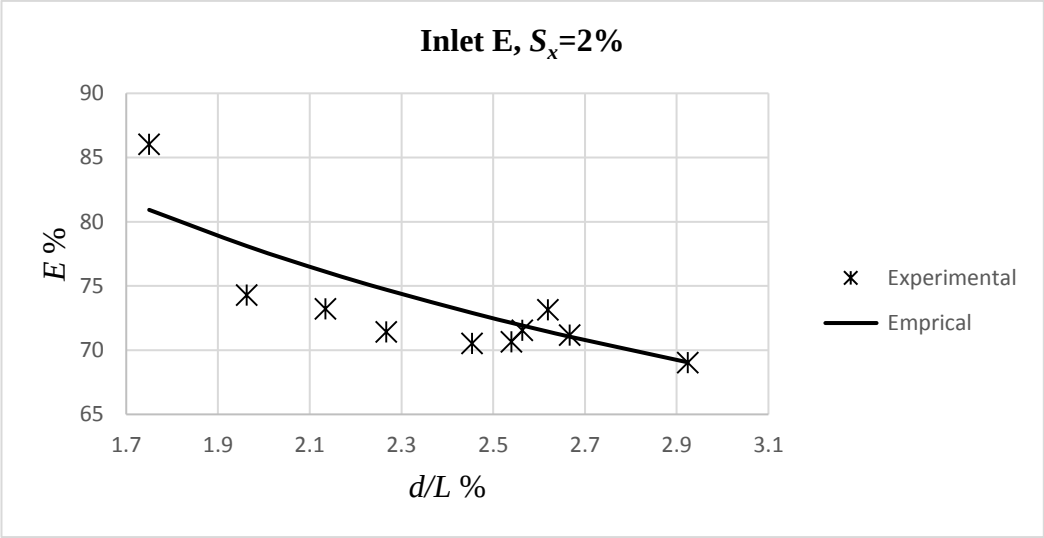


Figure 4.18 Comparison between inlet E empirical equation and experimental results

- Average difference = 0.737 p.p.
- Average Percentage difference = -1.016%
- R^2 (empirical equation) = 0.930

The empirical equation fits the experimental results well, producing small differences. There is good agreement at lower efficiencies. On S_x=2%, curb inlet E empirical equation has the highest accuracy of the six empirical equations.

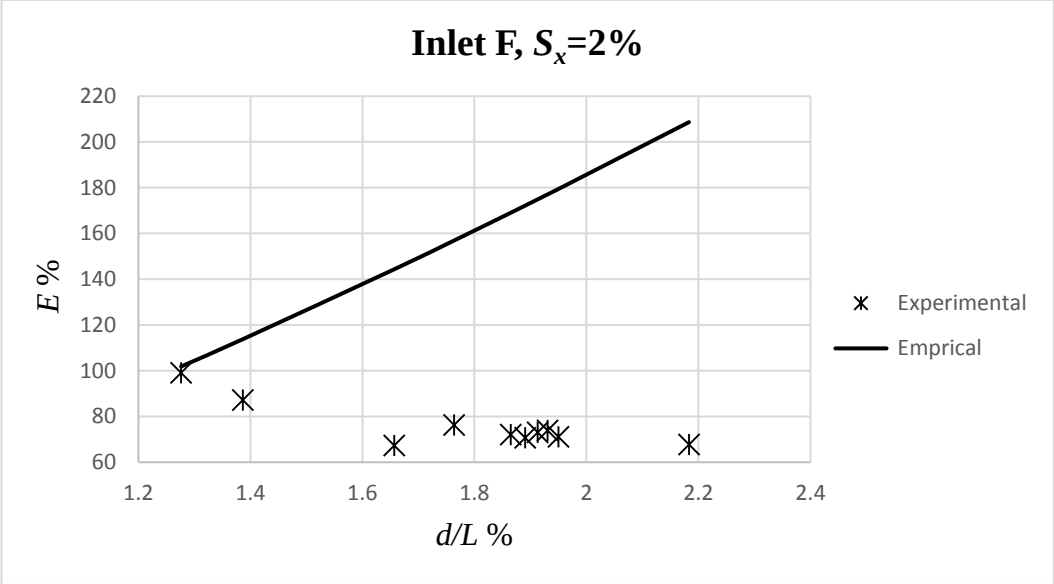


Figure 4.19 Comparison between inlet F empirical equation and experimental results

- Average difference = 84.031 p.p.
- Average Percentage difference = -49.195%
- R^2 (empirical equation) = 0.772

The curb inlet F empirical equation on S_x=2% had a moderately low R^2 and poorly fits the experimental results as shown in Figure 4.19 thus causing extremely large errors. Regression analysis is computed from the experimental results as discussed previously. Observing the experimental results on S_L=0.75%, the average efficiency was extremely low in comparison to the average efficiency of curb inlet F on S_L=0.50%. This was likely due to the malfunctioning of the V-notch weir (see Figure 3.6) during testing. The unexpected experimental results have produced a flawed empirical equation for curb Inlet F which also affected the sensitivity of the equation to the Froude number discussed previously.

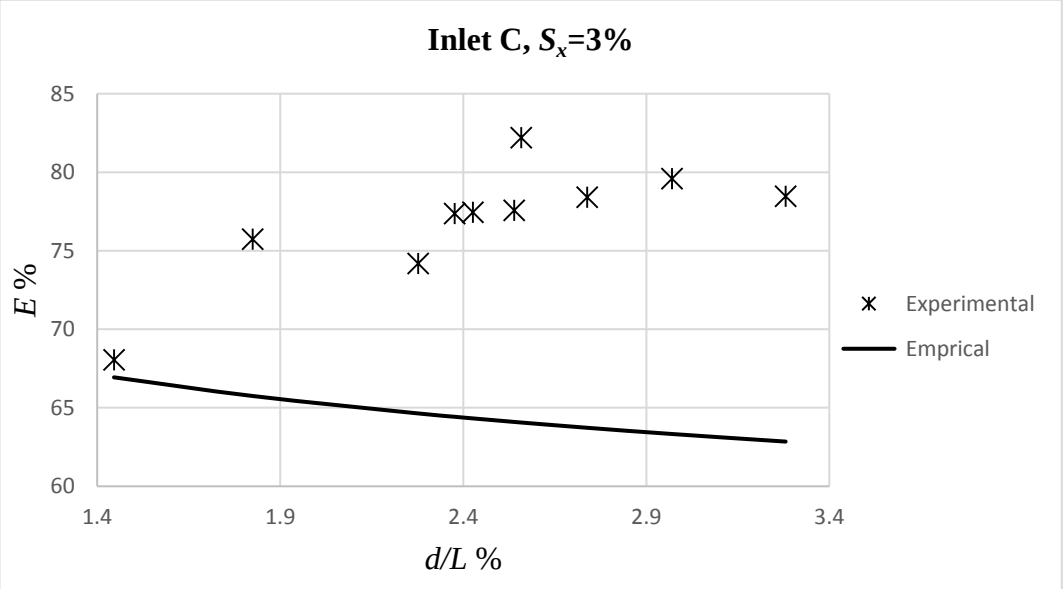


Figure 4.20 Comparison between inlet C empirical equation and experimental results

- Average difference = 12.483 p.p.
- Average Percentage difference = 19.492%
- R^2 (Empirical equation) = 0.579

Agreement between curb inlet C empirical equation and experimental results is very low and produced the largest errors of the six empirical equations on S_x=3%. The

deviation of experimental results from the empirical equation slightly increased as *d/L*% and efficiency increased.

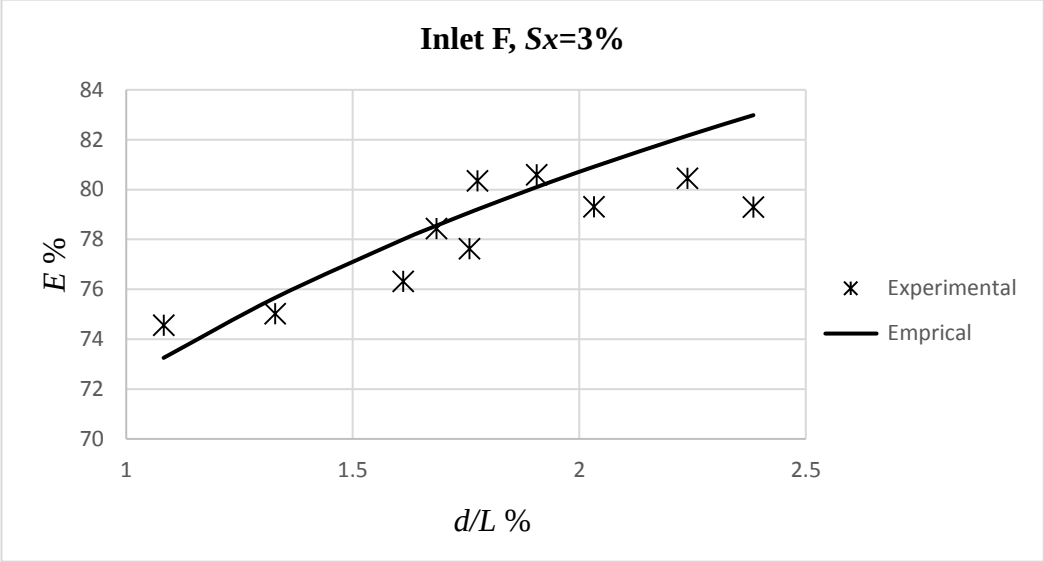


Figure 4.21 Comparison between inlet E empirical equation and experimental results

- Average difference = 0.79 p.p.
- Average Percentage difference = -0.959%
- R^2 (Empirical equation) = 0.9156

The curb inlet F empirical equation on S_x=3% has a high R^2 value and there is good agreement between curb inlet F empirical equation and the experimental results thus producing very low percentage errors.

4.5.4 Demonstration of Use of Design Curves to Estimate Curb Inlet Length

Table 4.10 and 4.11 can be used to design a curb inlet which requires estimates for the upstream transition and inlet lengths. Table 4.9 gives the ratios of upstream transition length/inlet opening length (r_{UP}/L) and downstream length/inlet opening length (r_D/L) for inlet types A through F.

Table 4.11 Ratio of dimensions of a curb inlet

Curb inlet	$r_{UP/L}$	$r_{D/L}$
A	0.5	0.5
B	1.0	0.5

C	0.33	0.33
D	1.5	0.5
E	0.67	0.3
F	0.25	0.25

It is only the design curves for inlet A that are presented in Figure 4.22 on a cross-sectional slope of 2% as an example of how the design equations are expected to be illustrated.

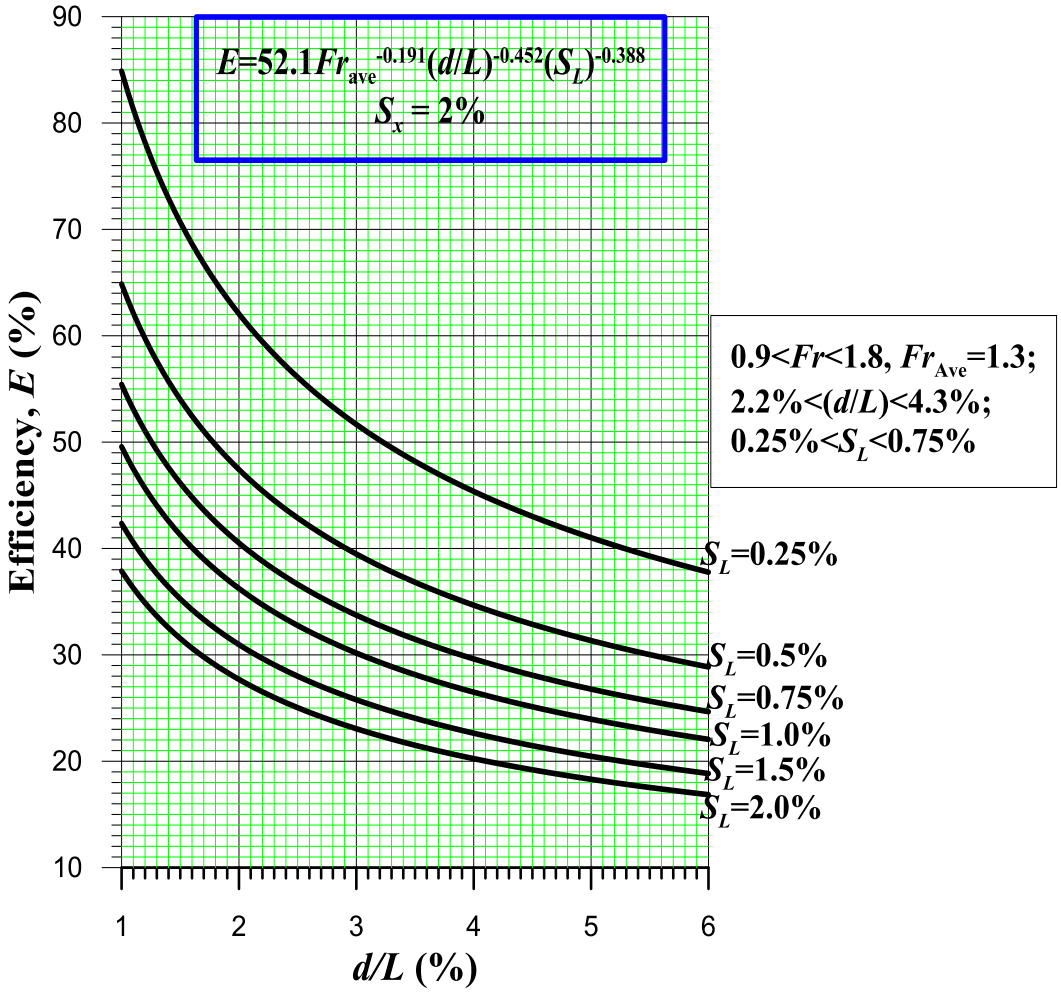


Figure 4.22 Design curves for depressed curb inlet A on S_x= 2%

Example

For a curb inlet A type with a longitudinal slope S_L = 1% and cross-sectional slope S_x = 2% for a roadway where the spread should not exceed 2.5 m and 30% of the roadway flow should be captured by the inlet, calculate the inlet length and the upstream and downstream transition lengths.

Solution:

Allowable spread, T = 2.5 m; depth of water upstream of the inlet, $d = T \times S_x$

$d = 2.5 \times 0.02 = 0.05$ m

Using Figure 4.17:

d/L = 3.0 % = 0.03

L = 0.05/0.03 m = 1.7 m

Inlet length = 1.7 m

To determine the length of upstream and downstream transition length, Table 5.2 is used.

r_{UP}/L = 0.5 and r_D/L = 0.5

$r_{UP} = r_D/L = 0.5 \times 1.7 = 0.85$ m

Therefore,

The upstream transition length = the downstream transition length = 0.85 m

Froude number check:

For E% = 30%, d/L% = 3% and S_L = 1%,

F_r=1.3.

5 CONCLUSION AND RECOMENDATIONS

5.1 Conclusions

The objectives of this study were to investigate the influences of the inlet opening, the upstream transition, depressed gutter, clogging, cross-sectional slope and longitudinal slope on the performance of the Pretoria type curb inlet that is predominantly used in the Gauteng Province of South Africa. It also aimed to formulate the design equations for six configurations of the inlet from data collected from experimental investigations using regression analysis. Furthermore, a comparison of the experimental data was carried out with two methods widely used in predicting the discharge capacities of curb inlets in the USA. The analyses of experimental data were conducted to fulfill the objectives of this research and the following conclusions were arrived at:

(i) The HEC-22 and Izzard methods were identified from the literature review to be commonly used, particularly in the USA, in predicting the capacities of curb inlets. They were formulated for a curb inlet whose opening is aligned with the curb, but the Pretoria type inlet is offset from the curb and has upstream and downstream transition sections. The comparisons of the HEC-22 and Izzard methods with the experimental data were only carried out for inlet A which has an opening length of 2 m, upstream transition length of 1 m and a downstream transition length of 1 m. The comparisons were done when the inlet has an undepressed and a depressed gutter.

The HEC-22 method generally overestimated the experimental intercepted flow, while the Izzard method underestimated the observed intercepted flow for the undepressed inlet A. While, the predictions of the intercepted flow by both methods are considered to be poor, the Izzard method gives a slightly better prediction than the HEC-22. For the depressed gutter, both methods were found to generally overestimate the experimental interception flow, indicating that the Izzard and the HEC-22 methods are not appropriate tools for predicting the interception flows of the Pretoria type curb inlet. The only agreement between the HEC-22, Izzard and experimental data is that the intercepted flows were higher with lower longitudinal slopes and higher cross-sectional slopes. The observed differences between the predicted and

actual results were assumed to be a result of the differences in the type of curb inlets studied by Izzard (1950) and the HEC-22 (FHWA, 2009) and the Pretoria type curb inlet.

(ii) Increasing the length of the upstream transition section by 1 m improves the efficiency of the undepressed Pretoria type curb inlet by approximately 1 p.p and 7 p.p. on S_x=2% and S_x=3% respectively. However, maximum performance was observed when the upstream transition section was 2 m.

Increasing the upstream transition length of a depressed Pretoria type curb inlet by 1 m improves the inlet's efficiency by approximately 14 p.p. and 2 p.p. on S_x=2% and S_x=3% respectively, and increasing the upstream transition length by 2 m improves the inlet's efficiency by approximately 8 p.p. and 10 p.p. on S_x=2% and S_x=3% respectively.

(iii) The performance of the Pretoria Type curb inlet is dependent on the length of the inlet opening. Increasing the opening length of depressed curb inlet A by 1 m improves the inlet's efficiency by approximately 13 p.p. and 11 p.p. on S_x=2% and S_x=3% respectively while undepressed curb inlet A is improved by approximately 19 p.p. and 15 p.p. on S_x=2% and S_x=3% respectively when the opening length is increased by 1 m..

Increasing the opening length of depressed curb inlet A by 2 m improves the inlet's efficiency by approximately 24 p.p. and 13 p.p. on S_x=2% and S_x=3% respectively, while undepressed curb inlet A is increased by approximately 31 p.p. and 27 p.p. on S_x=2% and S_x=3% respectively.

The influence of the inlet opening was found to be greatest on undepressed curb inlets and on S_x=2%. There are however higher cost implications with longer inlets, and this means that an optimum design should be the best compromise between inlet length, depression of inlet and its cost.

(iv) The experimental data analyzed for cross-sectional slopes of 2% and 3%, and longitudinal slopes of 0.25%, 0.5% and 0.75% revealed that the efficiency of the inlets favors steep cross-sectional slopes and gentle longitudinal slopes. This is very much in line with the hydraulics of flow into inlets which accommodate flows transverse to the longitudinal direction of the roadway. The evaluation of the test results concluded that:

- On S_x=2%, increasing the longitudinal slope by 0.25% increases the efficiency by 7 p.p. for undepressed inlet A and 6 p.p. for undepressed inlets B and D. For depressed curb inlets A, B, and D on S_x=2%, increasing the longitudinal slope by 0.25% increases the efficiency by 11 p.p., 9 p.p. and 8 p.p. respectively.
- On S_L=0.25%, an increment of cross-sectional slope by 1 p.p. increases the efficiency of undepressed curb inlets A, B, and D by approximately 5 p.p., 11 p.p. and 10 p.p. respectively while for depressed curb inlets on S_L=0.25% efficiency increases by 22 p.p., 6 p.p. and 10 p.p. respectively.

(v) Depressed curb inlets are more efficient than the undepressed curb inlets and also favor steep cross-sectional slopes and gentle longitudinal slopes. On S_L=0.25% and S_x=3%, the increase in efficiency due to gutter depression for curb inlets A, B, C, D, E, and F is 16.17 p.p., 18.96 p.p., 19.19 p.p., 30.50 p.p., 16.42 p.p. and 4.29 p.p. respectively and on S_L=0.75% and S_x=2% the efficiency increases by 7.62 p.p., 19.68 p.p., -1 p.p., 27.98 p.p, 31.96 p.p. and -3.67 p.p. for curb inlets A, B, C, D, E, and F respectively.

(vi) Clogging of curb inlets greatly reduces their performance and increases the spread of water on a road thus contributing to street flooding. This is, particularly noticeable on undepressed curb inlets. The efficiencies of undepressed inlets when C_L= 14.3 p.p. are reduced by 19.78 p.p., 18.71 p.p. and 19.42 p.p. for curb inlets A, B, and D respectively on S_x=2% and S_L=0.25%. On S_x=3% and S_L=0.75%, the efficiency is reduced by 14.79 p.p.,

14.41 p.p. and 16.76 p.p. for undepressed curb inlets A, B, and D respectively.

Depressed inlets promote high flow velocities at the entrance to the inlet, particularly on steep longitudinal slopes, which destabilize the clog materials and cause them to be carried downstream into the drainage channel. Over a long period, materials build up in the stormwater drainage conduit until it gets to be completely clogged. During the experimental investigations, the clog material was anchored by placing two bricks, each on one end inside the curb inlet. The efficiencies of curb inlets A, B, and D at C_L=14.3% are reduced by 4.63 p.p., 3.82 p.p. and 9.13 p.p., respectively on S_x=2%, and by 6.49 p.p., 2.62 p.p. and 6.73 p.p., respectively on S_x=3%.

(vii) The multiple linear regression analysis was utilized to produce design equations and curves for inlets on 2% and 3% cross-sectional slopes. These two cross-sectional slopes are typically those used in South Africa. However, noting that the regressed data was for longitudinal slopes of 0.25%, 0.5%, and 0.75%, the confidence of the design curves or design equations is higher for gentle longitudinal slopes and steep cross-sectional slopes.

5.2 Recommendations

This research project faced some constraints that prevented the production of more comprehensive design equations and curves. The biggest constraint was the available time. To improve or build on this research project, it is suggested that experiments be carried out on steeper longitudinal slopes (greater than 0.75%) and more curb inlets of varying geometric properties (inlet opening, upstream and downstream transition sections).

It is recommended that a full-scale model be adopted to avoid the possibility of scaling errors. As most streets have depressed gutters along the edge of the road and the walkway, it would be advisable to include it in a street model to obtain the best street replica. By widening the scope of the study, the design curves would be more refined and more accurate.

6 REFERENCES

Allison, R.A., Walker, T.A., Chiew, F.H.S., O'Neil, I.C.O. and McMahon, T.A. (1998) From roads to rivers: gross pollutant removal from urban waterways, Cooperative Research Center for Catchment Hydrology, Report no. 98/6, Department of Civil Engineering, Monash University, Clayton, Australia.

Arcement, G.J. and Schneider, V.R. (1989) Guide for selecting Manning's roughness coefficients for natural channels and flood plains, United States Geological Survey Water Supply Paper 2339, US Government Printing Office, Washington, USA.

Butler, D. and Davies, J.W. (2004) Urban drainage, Second Edition, Spon Press, London, UK

Chadwick, A. J., Morfett, J. C. and Borthwick, M. (2004) Hydraulics in civil and environmental engineering, Fourth Edition, Spon Press, London, UK.

City of Lubbock Texas Storm Water Management (1997) Drainage Criteria Manual. [Online] Available at: https://www.ci.lubbock.tx.us/departmental-websites/departments/storm-water-management/top-navigation-menu/drainage/drainage-criteria-manual [Accessed: 2016, March 26].

City of Tshwane Roads and Transport Department (2013) Catchpit details: Isometric view and cross sections, [Online] Available at: http://www.tshwane.gov.za/sites/residents/Services/Documents/STD003_sh1of2.pdf [Accessed: 2019, October 17]

Comport, B. C., Thornton, C. I. and Cox, A. L. (2009) Hydraulic efficiency of grate and curb inlets for urban storm drainage, The Urban Drainage and Flood Control District, Fort Collins, USA.

Federal Highway Administration (2009) Urban Drainage Design Manual, Report no. FHWA-NHI-10-009, Hydraulic Engineering Circular No. 22, Third Edition, Washington, USA.

Gilau, A. (2008) An integrated approach for the estimation of litter loads in urban areas of South Africa, Proceedings of the 11th International Conference on Urban drainage, Edinburg, Scotland, pp 1-10. [Online] Available at: https://www.ajol.info/index.php/wsa/article/view/5100 [Accessed: 2016, March 10].

Government of Western Australia Department of Water (2011) Sensitive urban design - litter and sediment traps. [Online] Available at: http://www.water.wa.gov.au/_data/assets/pdf_file/0018/1575/99301.pdf. [Accessed: 2016, March 24]

Grobler, P. (1994) Verification of the inlet capacities of modified stormwater kerb inlets and the development of new design curves, Thesis, Stellenbosch University, Stellenbosch, South Africa.

Gómez, M., Rabasseda, G.H. and Russo, B. (2013) Experimental campaign to determine grated inlet clogging factors in an urban catchment of Barcelona. Urban Water Journal, vol .10, no. 1, pp.50-61.

Guo, J.C.Y. (2000) Design of grate inlets with a clogging factor, Advances in Environmental Research, vol. 4, no. 3, pp. 181-186

Guo, J.C.Y. (2006) Design of street curb opening inlets using a decay-based clogging factor, Journal of Hydraulic Engineering, vol.132, no. 11, pp.1237-1241.

Guo, J.C.Y and MacKenzie, K. (2012) Hydraulic efficiency of grate and curb-opening inlets under clogging effect, Report no. CDOT-2012-3, University of Colorado and Urban Drainage and Flood Control District, Denver, USA.

Guo, J.C.Y. (2017) Urban flood mitigation and stormwater management, CRC Press, USA.

Hammonds, M.A. and Holley, E. (1995) Hydraulic characteristics of flush depressed curb inlets and bridge deck drains, Report no. FHWA/TX-96/1409-1, Center for Transportation Research, The University of Texas, Austin, USA.

Henderson, F. M. (1966) Open Channel Hydraulics, Macmillan, New York, USA.

Hodgens, B.R., Barrett, M.E., Ashraf, M., Engineer, H. and Schalla, F.E. (2018) Interception capacity of conventional depressed curb inlets and inlets with channel extension, Report no. FHWA/TX-18/0-6842-1, Center for Transportation Research, The University of Texas, Austin, USA.

Izzard, C.F. (1950) Tentative Results on capacity of curb opening Inlets, Report no. 11B, Highway Research Board, pp. 36-53.

Izzard, C.F. (1977) Simplified method for design of curb-opening inlets, Report no. 631, Transportation Research Record, pp.39-46.

Jens, S.W. (1979) Design of Urban Highway Drainage: The State of the Art, Report no. FHWA-TS-79-225, Federal Highway Administration, Washington, USA.

Johannesburg Roads Agency (2015) Stormwater kerb inlet detail (precast type). [Online] Available at: http://www.jra.org.za/documents/standarddrawings/JRA-SD-S006.pdf [Accessed: 2019, October 17]

Johannesburg Roads Agency roads and stormwater manual (2015) Code of procedure. [Online] Available at: https://www.jra.org.za/documents/standarddrawings/Code_of_Procedure.pdf [Accessed: 2017, February 11].

The Southern Sydney Regional Organisation of Councils and the Natural Heritage Trust (2010) Do it right on site: Protection of gutter and street stormwater drains, Australia. [Online] Available at: https://www.woollahra.nsw.gov.au/building_and_development/building/environmental_protection_tips#doitright [Accessed: 2019, September 20].

Li, W. H. (1956) Design of storm-water inlets, The Johns Hopkins University, Baltimore, USA.

McEnroe, B.M., Wade, R.P. and Smith, A.K. (1999) Hydraulic performance of curb and gutter inlets, Report no. K-TRAN: KU-99-1, The University of Kansas, Lawrence, USA.

Muhammad, M.A. (2018) Interception capacity of curb opening inlets, Doctoral dissertation, The University of Texas, Austin, USA.

PACE Advanced water engineering (2011) East Garden Grove: Wintersburg channel-physical model study I-405. [Online] Available at: http://30zz0j1ewgra3qf6cz317ytj.wpengine.netdna-cdn.com/wp-content/uploads/2011/11/ASCE-EGGWC-Model-Study.pdf [Accessed: 2016, October 14].

Piketh, S.J., Vogel, C., Dunsmore, S., Culwick, C., Engelbrecht, F. and Akoon, I. (2014) Climate change and urban development in southern Africa: The case of Ekurhuleni Municipality (EMM) in South Africa, Water SA, vol. 40, no. 4, pp. 749–758.

The South African National Roads Agency Limited (2007) Drainage Manual, Pretoria, South Africa.

Urban Drainage and Flood Control District (2008) Urban Storm Drainage Criteria Manual, vol. 1, Denver, USA.

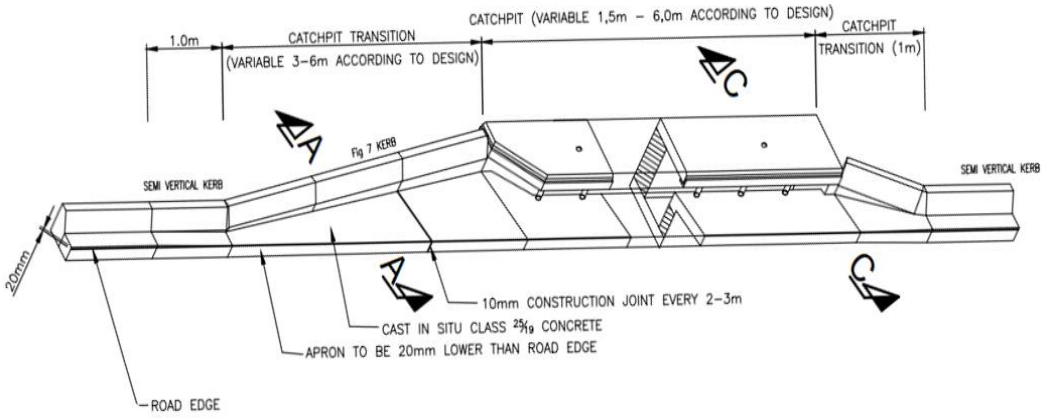
Urban Drainage and Flood Control District (2016) Urban Storm Drainage Criteria Manual, vol. 1 and 2, Denver, USA.

Uyumaz, A. (1992) Discharge capacity for curb-opening inlets, Journal of Hydraulic Engineering, vol. 118, no 7, pp.1048-1051.

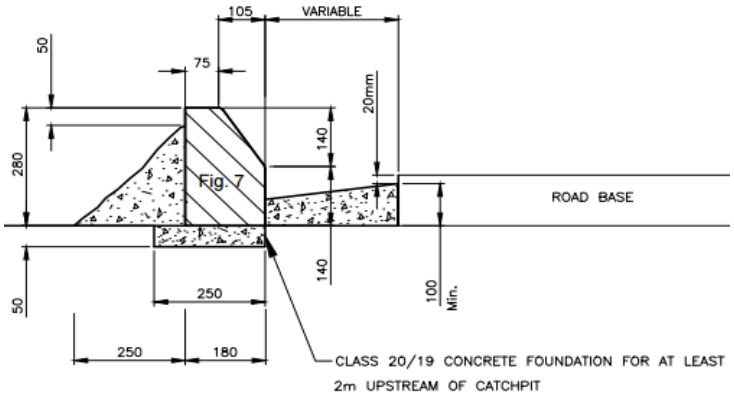
Zwamborn, J.A. (1966) Stormwater Inlet Design, The Institution of Municipal Engineers of Southern Africa Annual Journal, Vol. 1, no 4, pp. 61-70.

7 APPENDICES

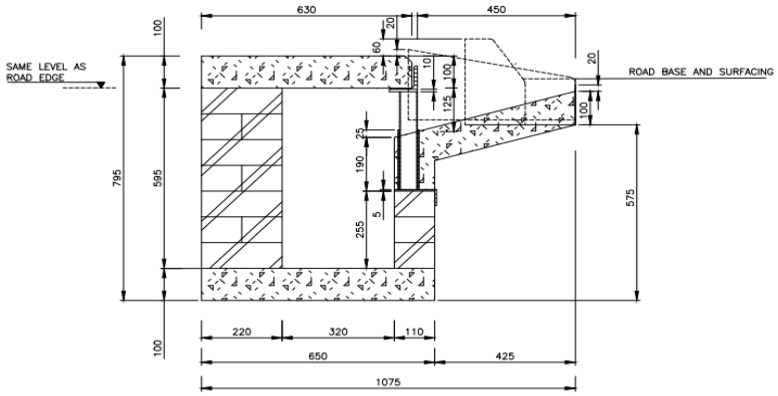
7.1 Appendix A – Detailed Drawings of The Pretoria Type Curb Inlet



DETAIL OF CATCHPIT (Semi-Vertical kerb both sides)



SECTION A-A



SECTION C-C

Figure 7.1 Pretoria type curb inlet isometric view and cross-sections (City of Tshwane Roads and Transport Department, 2013)

7.2 Appendix B - Model Schematics

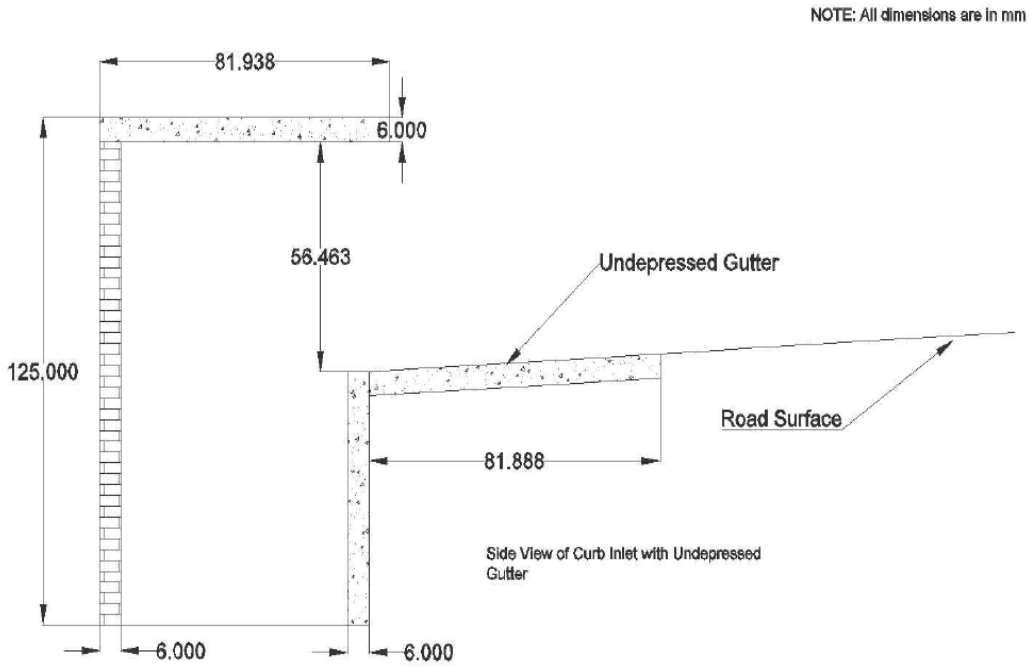


Figure 7.2 Side view of a curb inlet with an undepresed gutter

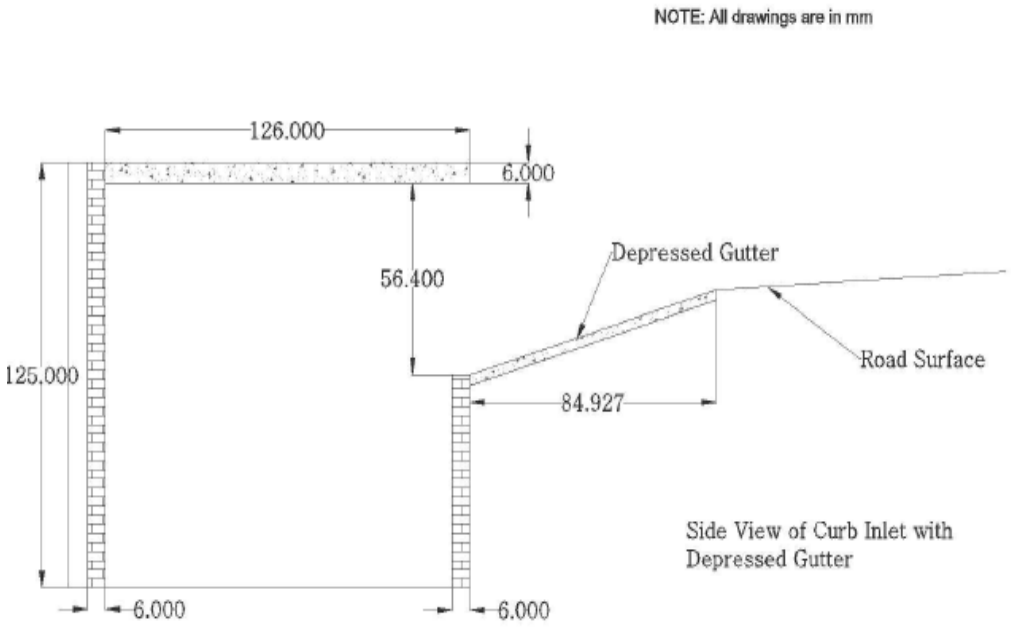


Figure 7.3 Side view of a curb inlet with a depressed gutter

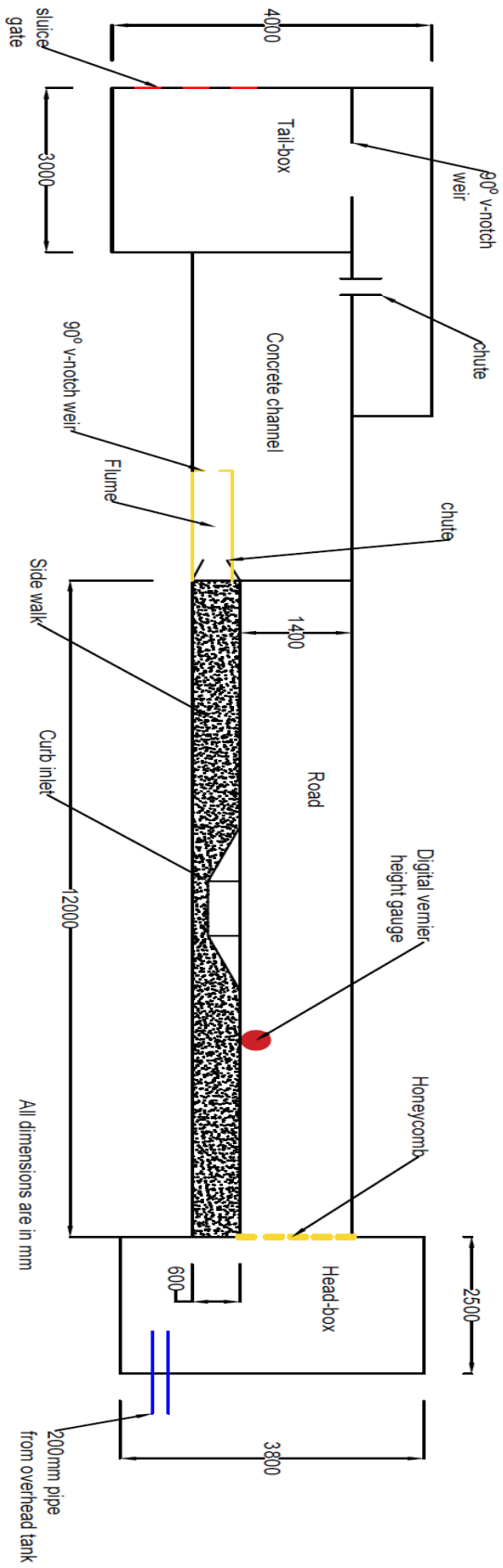


Figure 7.4 Plan view of the model set-up in the flume



Figure 7.5 Honeycomb used to stabilise the flow-rate

7.3 Appendix C - Regression Analysis Statistics

Table 7.1 Regression analysis statistics for depressed curb inlets on S_x=2%

Curb Inlet A	**Regression Statistics**	
	Multiple R	0.982
	R^2	0.965
Curb Inlet B		
	Multiple R	0.984
	R^2	0.968
Curb Inlet C		
	Multiple R	0.972
	R^2	0.945
Curb Inlet D		
	Multiple R	0.963
	R^2	0.927
Curb Inlet E		
	Multiple R	0.964
	R^2	0.931
Curb Inlet F		
	Multiple R	0.879
	R^2	0.772

Table 7.2 Regression analysis statistics for depressed curb inlets on S_x=3%

Inlet	Regression Statistics	
Curb Inlet A		
	Multiple R	0.792
	R^2	0.627
Curb Inlet B		
	Multiple R	0.883
	R^2	0.779
Curb Inlet C		
	Multiple R	0.761
	R^2	0.579
Curb Inlet D		
	Multiple R	0.509
	R^2	0.259
Curb Inlet E		
	Multiple R	0.921
	R^2	0.848
Curb Inlet F		
	Multiple R	0.957
	R^2	0.916

7.4 Appendix D – Predicted Vs. Experimental Efficiency (S_L=0.25%)

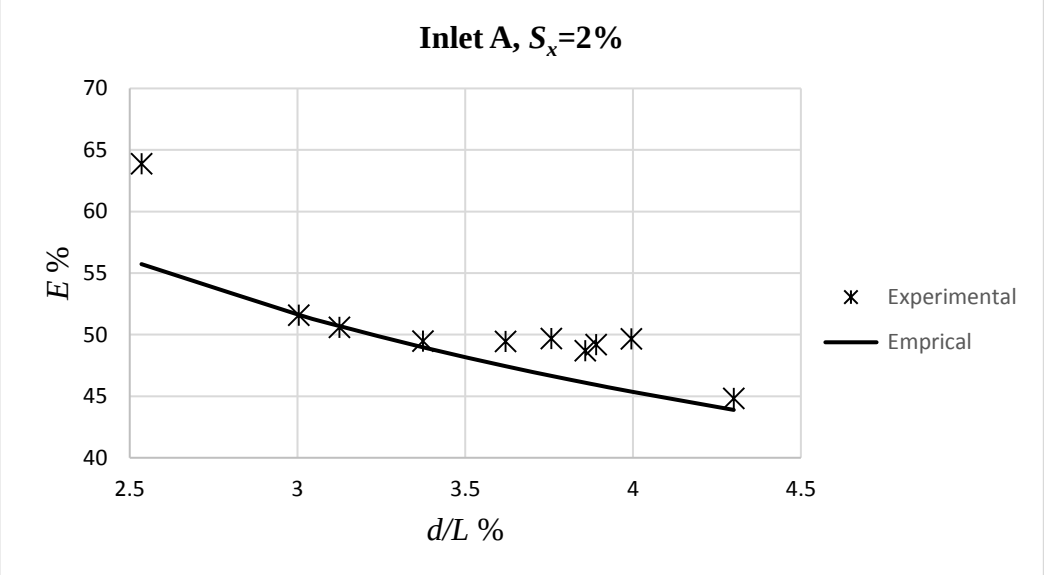


Figure 7.6 Predicted vs. Experimental Efficiency for inlet A on S_x=2% and S_L=0.25%.

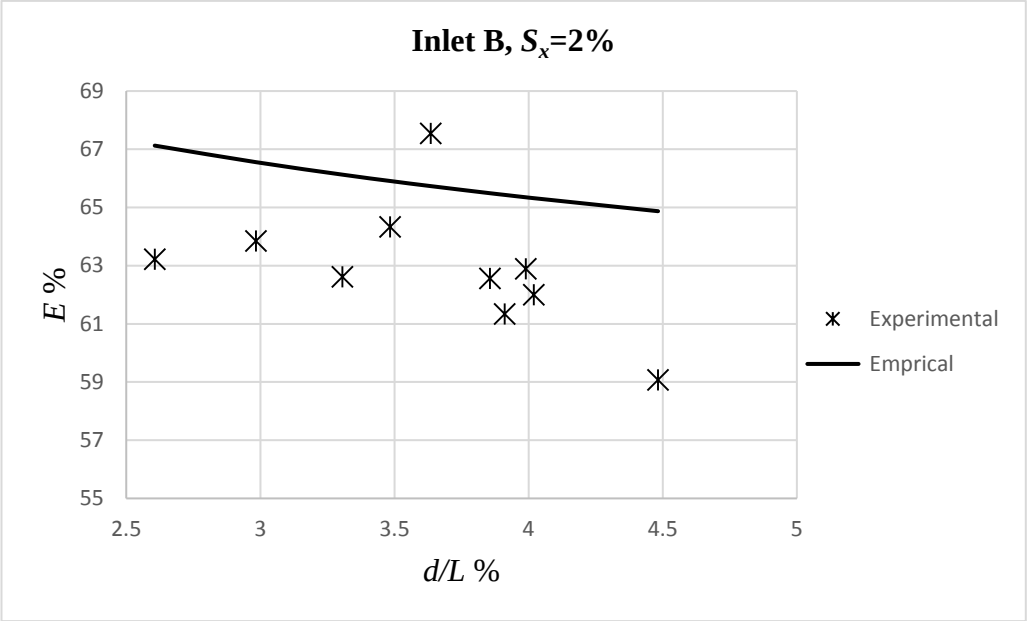


Figure 7.7 Predicted vs. Experimental Efficiency for inlet B on S_x=2% and S_L=0.25%.

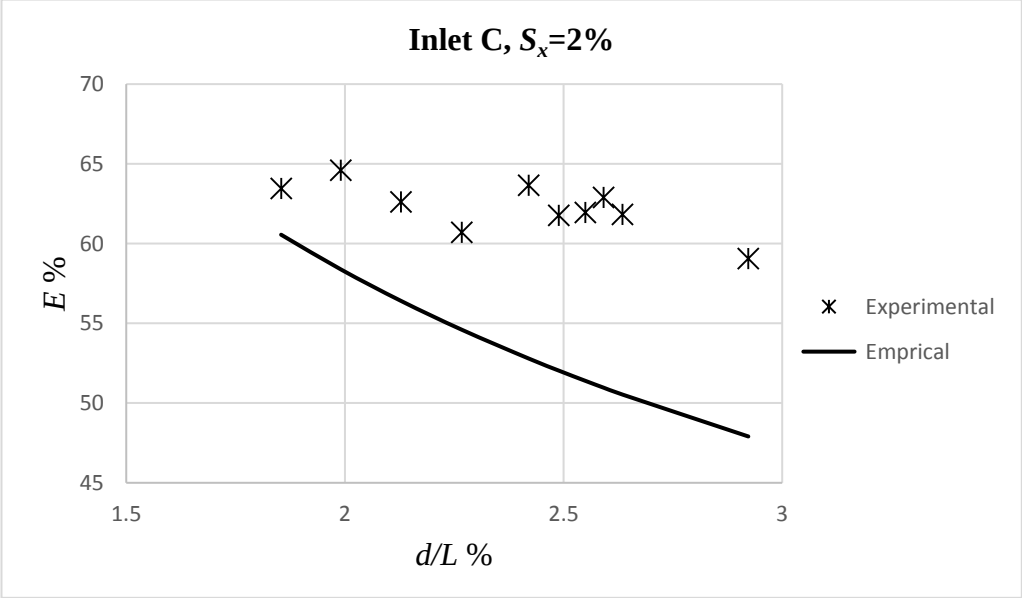


Figure 7.8 Predicted vs. Experimental Efficiency for inlet C on S_x=2% and S_L=0.25%.

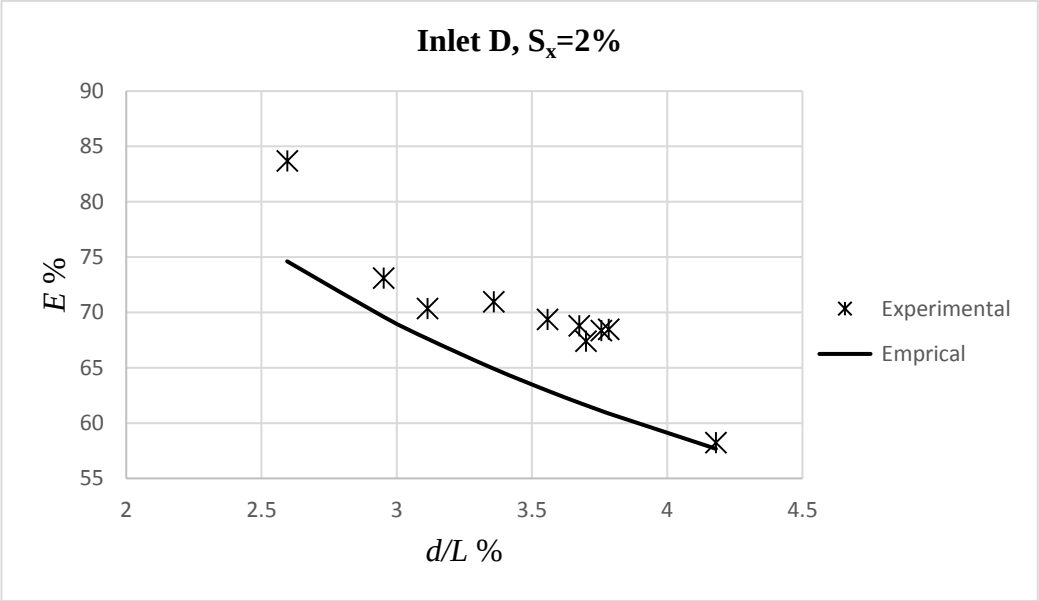


Figure 7.9 Predicted vs. Experimental Efficiency for inlet D on S_x=2% and S_L=0.25%.

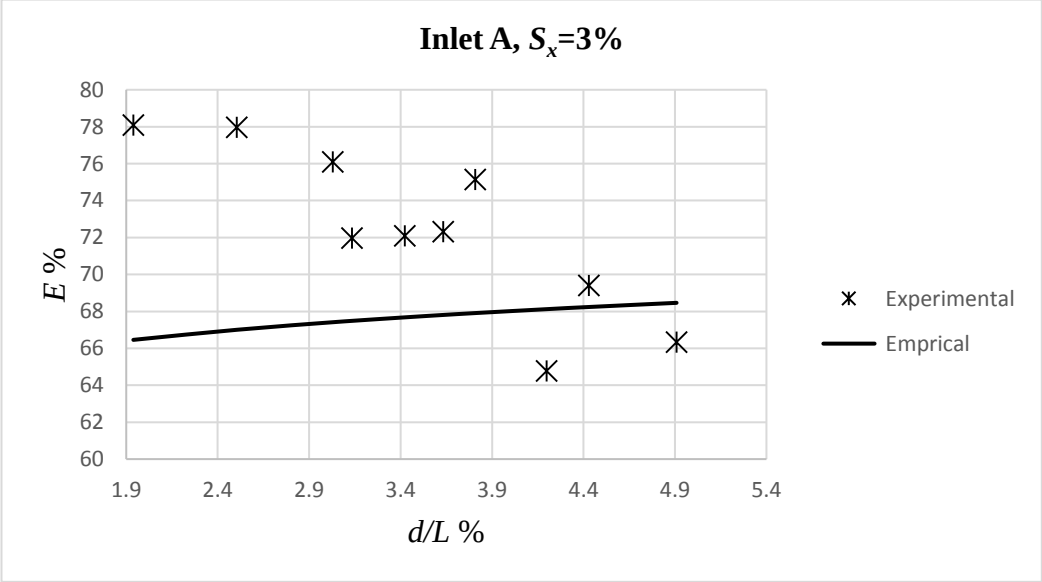


Figure 7.10 Predicted vs. Experimental Efficiency for inlet A on S_x=3% and S_L=0.25%.

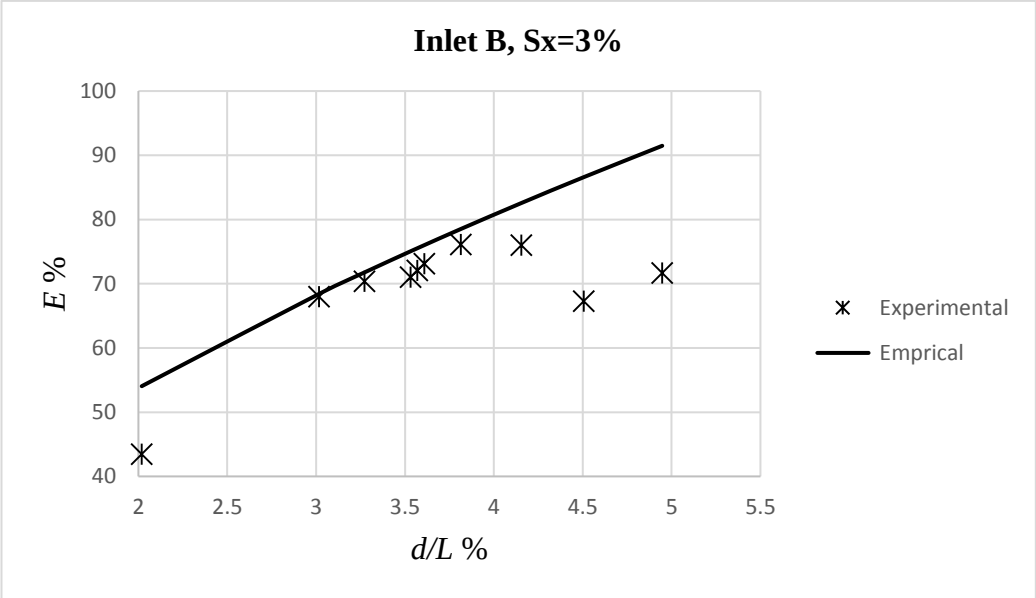


Figure 7.11 Predicted vs. Experimental Efficiency for inlet B on S_x=3% and S_L=0.25%.

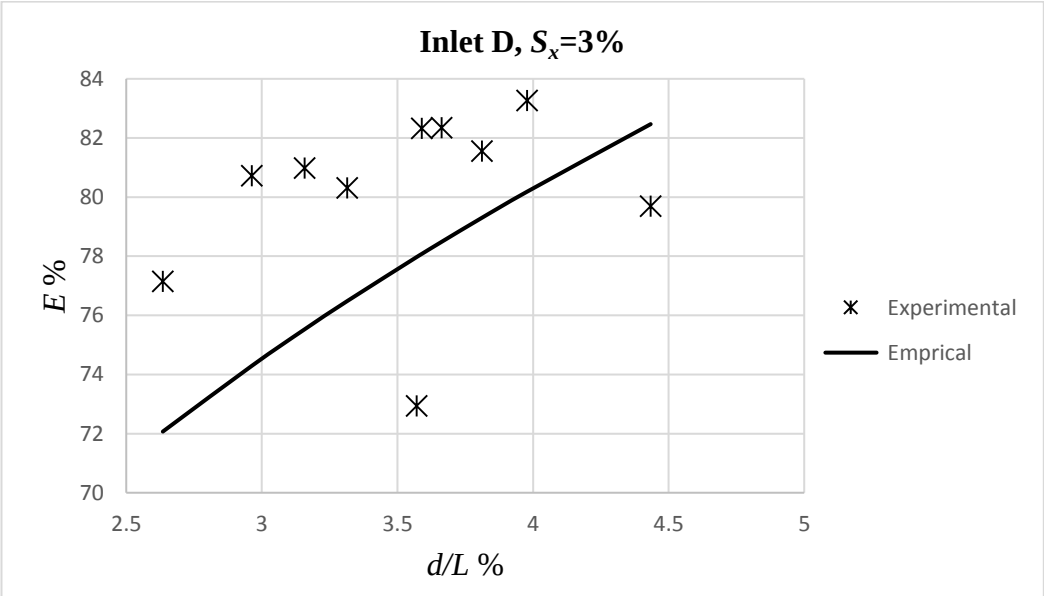


Figure 7.12 Predicted vs. Experimental Efficiency for inlet D on S_x=3% and S_L=0.25%.

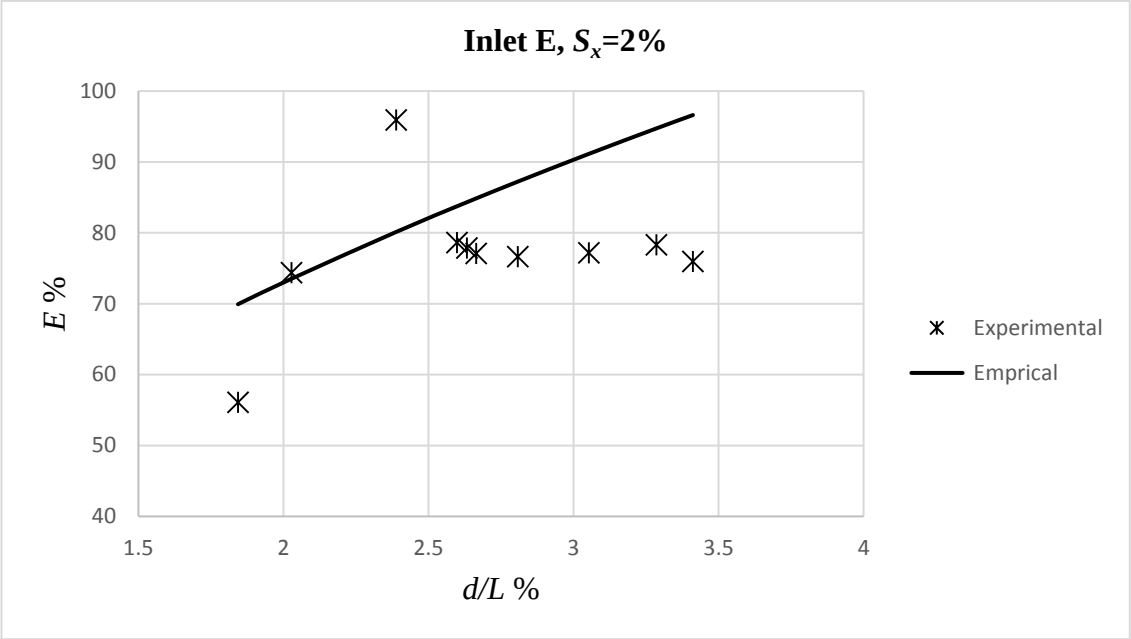


Figure 7.13 Predicted vs. Experimental Efficiency for inlet E on S_x=3% And S_L=0.25%.